UNIVERSIDAD DE LAS PALMAS
DE GRAN CANARIA

Tesis doctoral

Programa de Doctorado en Oceanografía y Cambio Global

Observaciones de la estructura geomorfológica de los paisajes costeros macaronésicos.

Implicaciones para el conocimiento de su evolución en amplias escalas espacio-temporales

Nicolás Ferrer Valero

Diciembre de 2018

Las Palmas de Gran Canaria

UNIVERSIDAD DE LAS PALMAS
DE GRAN CANARIA

D. SANTIAGO HERNÁNDEZ LEÓN, COORDINADOR DEL PROGRAMA DE DOCTORADO DE OCEANOGRAFÍA Y CAMBIO GLOBAL DE LA UNIVERSIDAD DE LAS PALMAS DE GRAN CANARIA,

INFORMA,

Que la Comisión Académica del Programa de Doctorado, en su sesión de fecha 6 de diciembre de dos mil dieciocho tomó el acuerdo de dar el consentimiento para su tramitación, a la tesis doctoral titulada "Observaciones de la estructura geomorfológica de los paisajes costeros macaronésicos. Implicaciones para el conocimiento de su evolución en amplias escalas espacio-temporales" presentada por el doctorando D. Nicolás Ferrer Valero y dirigida por los Doctores Luis Hernández Calvento y Antonio I. Hernández Cordero. Asimismo, se acordó el informar favorablemente la solicitud para optar a la Mención Internacional del Título de Doctor, por cumplir los requisitos reglamentarios. Y para que así conste y a efectos de lo previsto en el Artº 11 del reglamento de Estudios de Doctorado (BOULPGC 7/10/2016) de la Universidad de Las Palmas de Gran Canaria, firmo la presente en Las Palmas de Gran Canaria, a 6 de diciembre de dos mil dieciocho.

UNIVERSIDAD DE LAS PALMAS DE GRAN CANARIA

Programa de Doctorado en Oceanografía y Cambio Global

Escuela de Doctorado de la Universidad de Las Palmas de Gran Canaria

Observaciones de la estructura geomorfológica de los paisajes costeros macaronésicos.

Implicaciones para el conocimiento de su evolución en amplias escalas espacio-temporales

Presentada por D. Nicolás Ferrer Valero

Dirigida por Dr. Luis Hernández Calvento

Codirigida por Dr. Antonio I. Hernández Cordero

El Director El Codirector El Doctorando

En Las Palmas de Gran Canaria, a 5 de diciembre de 2018

Contenidos

Presentación

En este documento se muestran los resultados de 4 años de investigación como miembro del Grupo de Investigación en Geografía Física y Medioambiente (GFyMA), del Instituto de Oceanografía y Cambio Global (IOCAG) de la Universidad de Las Palmas de Gran Canaria (ULPGC), y estudiante del programa de doctorado en Oceanografía y Cambio Global (IOCAG, ULPGC). Durante este tiempo, todo el esfuerzo y entusiasmo ha estado dirigido a la búsqueda de una perspectiva distinta desde la que explorar y examinar las características de las costas volcánicas de dos archipiélagos de la región macaronésica (Canarias y Cabo Verde), que aportase una visión original de su evolución a lo largo del tiempo. Como resultado, se presenta esta tesis doctoral cuyo núcleo esta condensado en forma de tres artículos publicados en revistas internacionales con impacto JCR (Q1), más los resultados de un cuarto artículo en proceso de envío para revisión por pares.

Durante este periodo he sido beneficiario de un contrato como Personal Investigador en Formación (PIF), de 4 años de duración, por la ULPGC (cód. E-35-2014-0231941). Para la consecución de la investigación, he contado con la supervisión de Luis F. Hernández Calvento, como director de tesis y responsable de la ayuda, y de Antonio I. Hernández Cordero, como codirector. Asimismo, los resultados de estas investigaciones suponen una contribución al proyecto de investigación *Análisis de procesos naturales y humanos asociados a los sistemas playa-duna de Canarias* (cód. CSO2016-79673-R), financiado por el Plan Estatal de I+D+i (Ministerio de Economía y Competitividad, MINECO, Gobierno de España), cuyo investigador principal es Luis F. Hernández Calvento.

Agradecimientos

Le debo a mi familia haber llegado hasta aquí, a mis padres, hermano, tíos y primas. En especial, se lo agradezco a mi madre y a mi pareja, por su apoyo permanente e incondicional.

Asimismo, tengo que agradecer la inmejorable acogida que he recibido durante este tiempo por parte de todos los miembros del grupo de Geografía Física y Medioambiente. En especial a Luis Hernández Calvento, por la oportunidad al inicio y el gran apoyo y la confianza durante toda la investigación.

Por último, agradecer a la maravillosa y singular tierra canaria, fuente de fascinación e inspiración de esta tesis doctoral.

Introducción

Como se desprende del título de la tesis, la investigación pivota sobre tres grandes ejes temáticos: (i) la geomorfología costera, (ii) las islas volcánicas de punto caliente y (iii) las medidas estructurales de paisaje (*landscape metrics*), con especial atención a la aplicación del concepto de diversidad. Podríamos situar las coordenadas de este trabajo en la intersección de estos tres campos (Figura I). Las islas volcánicas ofrecen la coordenada espacial del estudio, la geomorfología costera, la coordenada temática, y las métricas del paisaje, la aproximación analítica. A su vez, los tres campos están puestos en común en el eje temporal, dando lugar a un estudio sobre la *evolución geomorfológica de costas de islas oceánicas analizadas por medio de métricas de paisaje* (en especial, de la diversidad). Por sus características, este trabajo se sitúa, espacialmente, en la escala paisajística (de decenas a cientos de kilómetros de costa), y temporalmente, en la escala geológica (de cientos de miles a millones de años). Tratamos, por lo tanto, de grandes escalas que rara vez aparecen representadas en los estudios de geomorfología costera actuales.

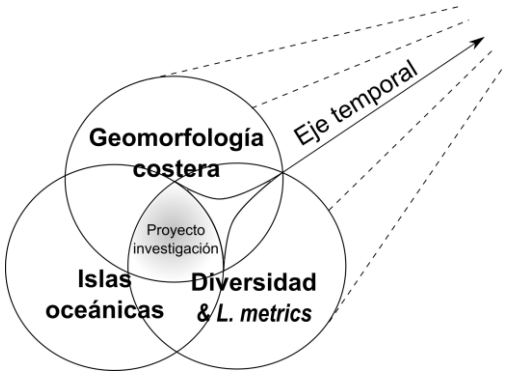

Figura I. Campos temáticos de la investigación.

A continuación, se amplían algunos antecedentes relevantes en los respectivos campos temáticos que son transversales a esta investigación (Figura I).

Geomorfología, clasificación y evolución de costas

La costa constituye la zona de transición o de interfaz entre la tierra y el mar (Woodfroffe, 2002), donde los ambientes terrestres influyen en los ambientes marinos, y viceversa (Carter, 1988), y

donde se encuentran e interactúan la hidrosfera, litosfera, atmósfera y biosfera (Bird, 2008). La dualidad ambiental marino-terrestre y la interacción de esta variedad de medios constituyen, desde el punto de vista físico-natural, el concepto de medio costero. En la práctica esta delimitación es, sin embargo, compleja, puesto que la zona costera constituye una franja marcada por gradientes cambiantes en el espacio y en el tiempo (Carter, 1988). Además, la interacción del factor humano añade complejidad a las áreas costeras, puesto que son la fuente principal de recursos a nivel global, albergando actualmente entre el 50% y el 70% de la población y la mayor parte de la actividad económica mundial (Mimura et al., 2007).

La delimitación de la costa puede hacerse desde la misma multiplicidad de esferas que la definen, con resultados no siempre coincidentes (Carter, 1988). La clásica zonificación de la costa en *offshore*, *nearshore*, *foreshore* y *backshore* (Davidson-Arnott, 2010), emplea un criterio hidrodinámico según el cual la costa comienza donde el oleaje se ve modificado por el fondo (asomeramiento), hasta el límite de la penetración de las aguas marinas por interacción con el relieve, la atmósfera y las comunidades de seres vivos. Desde un punto de vista biológico, el medio costero queda definido por la presencia de seres vivos, marinos y terrestres, adaptados a vivir en las condiciones de salinidad, humedad, dinámica sedimentaria y viento, propias de esta interfaz ambiental. De igual forma, se pueden adoptar otros criterios, como climáticos, humanos o geomorfológicos.

El criterio geomorfológico surge de la observación de la impronta erosiva y sedimentaria producida por los agentes atmosféricos, biológicos y (sobre todo) marinos, sobre relieve superficial costero. La interacción de procesos marinos y subaéreos genera formas superficiales (geoformas) características de estos ambientes que, en gran parte, son comunes a todas las líneas de costa del mundo (acantilados, plataformas, farallones, playas, dunas, marismas, etc.). Así, la zona costera puede verse en sus formas de modelado características. Un acantilado, un campo de dunas o un estuario, pueden marcar el límite terrestre, mientras la plataforma continental marca el límite marino (Davidson-Arnott, 2010). El examen de los procesos de transformación de la superficie terrestre en los medios costeros, y su expresión en el modelado superficial de una gran variedad de geoformas (Gray, 2004), es lo que se conoce por geomorfología costera.

Aunque existe una relativa abundancia de cartografías locales y regionales (e.g. Alexander, 1966; Owens, 1994; Isola et al., 2011; De Muro et al., 2015; Biolchi et al., 2016) no existe otro estudio a escala global que el mapa mundial de geoformas costeras de McGill (1958). A pesar de ello, desde que Emery y Kuhn (1982) estimaran que el 80% de la costa mundial es rocosa, se acepta que estos ambientes son predominantes frente a los sedimentarios. No obstante, la distinción entre costa rocosa y sedimentaria es ambigua: bajo condiciones erosivas, geoformas típicas de las "costas rocosas", como acantilados y plataformas, se desarrollan también en rocas

blandas y sedimentos, y las geoformas sedimentarias pueden experimentar también procesos de consolidación (e.g. eolianitas, *beachrocks*) (Naylor et al., 2010). Los términos costa erosiva *versus* costa acumulativa (Davies, 1980), podrían ser geomorfológicamente más precisos y útiles para una distinción general. Al margen de esto, lo más común en cualquier localización costera es encontrar una geomorfología mixta, donde existe una variedad de geoformas dentro de un gradiente que fluctúa desde la deposición hasta la erosión. Captar esta variedad dentro de un esquema funcional y evolutivo es un reto más importante que simplemente establecer tipologías cerradas y estáticas.

El "ciclo geográfico" de Davis (1899) es quizás el primer modelo de evolución geomorfológica en el que se planteó el tiempo como un factor primordial, irreversible y ordenado (Woodroffe, 2002). Dentro de su teoría, Davis trató de extrapolar el "ciclo erosivo" de los paisajes terrestres, a la evolución de las costas. Así, el proceso de erosión y arrasamiento de los perfiles de las montañas, tenía su análogo en el desarrollo temporal de las costas hacia una forma en planta menos irregular con el tiempo, a medida que se erosionan los promontorios y se rellenan las bahías.

Las ideas de Davis fueron recogidas y desarrolladas por Douglas Johnson, quien formuló un marco para analizar secuencialmente la evolución costera (Johnson, 1919). Para Johnson, al igual que para Davis, la complejidad costera disminuye con el tiempo y se minimiza en etapas maduras, tanto en planta como en perfil. Estas teorías, que dominaron durante al menos la primera mitad del siglo XX, atribuían a la acción marina el objetivo último de regularizar la costa. Según esto, cualquiera que fuese el relieve inicial, las costas tenderían en su fase última a simplificarse en un proceso de evolución convergente. King (1961) describe el 'ciclo marino' (*marine cicle*) en costas de 'emersión' (*emergence coasts*), como sigue: el estadio inicial (*initial stage*) se caracteriza por la inundación de valles fluviales, lo que genera un trazado costero típicamente irregular sin modelado marino, donde las pendientes inhiben la deposición de sedimento y la dinámica del oleaje está condicionada por la topografía preexistente. En la segunda fase, o estado temprano de modificación (*early stage of modification*), comienzan a reflejarse los efectos de i) la erosión diferencial debido a los contrastes de resistencia litoestructural, que puede resultar en una forma todavía más dentada que la original (*crenulate coastline*), y ii) la proliferación de una gran variedad de formas sedimentarias (barreras, tómbolos, flechas, playas encajadas, pequeños deltas, cordones de tormenta), que tienden a compensar las irregularidades y linearizar la costa prolongando las direcciones del margen terrestre. La madurez (*maturity*) se plasma finalmente en la rectilinearización costera, una vez los promontorios se retranquean y las bahías progradan por sedimentación, dando lugar a playas de transporte libre a lo largo de una costa acantilada de trazado suavemente ondulado. La etapa final del ciclo marino (*old stage*) no es observable en

ningún lugar debido al elevado dinamismo del nivel del mar, por lo que es solo una fase teórica. Se alcanzaría al cabo del ciclo con el arrasamiento total del margen continental (*marine planation*), en virtud de un proceso simultáneo en el que la disipación gradual de la energía por el ensanchamiento de la plataforma litoral favorece la degradación subaérea de los relieves costeros.

Recogiendo las ideas anteriores, surgen a mediados del siglo XX las primeras clasificaciones de costas en torno a los conceptos de etapa de desarrollo, dinamismo iso-eustático y procesos de retroceso y progradación. Valentin (1952; en Finkl, 2004) propuso una clasificación basada en el desplazamiento de la línea de costa hacia mar o hacia tierra. Distingue, en un primer nivel, costas de avance y costas de retroceso; y en un segundo, costas de emersión *versus* inmersión, si se debe a cambios relativos en el nivel del mar, o costas de progradación *versus* retrogradación, si se debe a procesos de acreción o erosión. Shepard (1937, 1976) introduce un sencillo sistema de clasificación basado en los conceptos de (i) costas primarias o juveniles, donde la morfología dominante se relaciona con procesos no-marinos (fluviales, glaciales volcánicos, tectónicos, etc.), y ii) costas secundarias o maduras, donde el modelado dominante obedece a la actividad, erosiva o sedimentaria, del oleaje, mareas, corrientes y organismos marino-costeros.

La tectónica de placas (Wegener, 1966) proporcionó sentido a la distinción estructural entre costas pacíficas, o concordantes, y costas atlánticas, o discordantes. Es Cotton (1954) quien, observando la influencia de la tectónica a escala continental en la configuración geomorfológica de las costas, determina la diferenciación clásica entre costas de borde convergente y de borde pasivo (Mitchell y Reading, 1969; Inman y Nordstrom, 1971). Inman y Nordstrom (1971) proponen clasificarlas en: (i) costas de colisión (*collision coasts*), típicas de las fachadas pacíficas de América y Asia, donde se encuentras grandes cadenas montañosas, acantilados, terrazas marinas, estrechas plataformas continentales y fosas marinas, así como ríos cortos y energéticos que aportan mayoritariamente sedimento grueso; y (ii) costas de borde pasivo (*trailing-edge coasts*), típicas de las fachadas atlánticas de América, Europa y África, donde la estabilidad tectónica permite la formación de planicies litorales y amplias plataformas continentales favorables a la acumulación de sedimentos. A su vez, la subdivisión en: (a) *neo-trailing-edge coasts,* (b) *afro-coasts* y (c) *amero-coasts*, implica una evolución morfológica desde estados juveniles a maduros, con la progresiva reducción de la actividad sísmica y volcánica. Esta origina relieves costeros menos elevados, un aumento de la sedimentación y un creciente desarrollo de plataformas continentales y redes de drenaje.

Estas teorías evolutivas y sistemas de clasificación forman parte de la geomorfología costera clásica, descriptiva y, en gran parte, atravesada por las ideas davisianas (Woodroffe, 2002). En las últimas décadas, la geomorfología costera se ha interesado más por los procesos costeros en el

campo de acción del oleaje, las mareas o los vientos, a distintas escalas. Aunque hay ejemplos de nuevas propuestas globales de clasificación (Finkl, 2004; Brocx y Semeniuk, 2010), éstas han perdido interés en el conjunto de la materia. Los avances en la instrumentación para medir con precisión los fluidos, el transporte y los cambios morfológicos a corto plazo, han favorecido el desarrollo de estudios de morfo-dinámica (de segundos, horas y días) y de modelización de los procesos costeros a través de modelos proceso-respuesta (e.g. Storms et al., 2002; Castedo et al., 2012) o autómatas celulares (Dearing et al., 2006). Conceptos como, retroalimentación (Zarnetske et al., 2012), auto-organización (Baas, 2002; Werner, 2003), fractales (Tanner, 2006), equilibrio dinámico (Fagherazzi et al., 2007), umbrales (Phillips, 2006; Limber et al., 2008) o herencias (Trenhaile et al., 1999), han pasado a formar parte del cuerpo actual de la geomorfología costera. Asimismo, la disponibilidad cada vez mayor de información geográfica sobre amplias superficies (fotografías aéreas, imágenes de satélite y modelos digitales de elevaciones), ha impulsado el desarrollo de estudios de procesos históricos (de años, décadas y siglos), a nivel de paisajes y sistemas geomorfológicos (Anthony et al., 2014; Hernández-Cordero et al., 2018). También los avances en las técnicas de datación radiométrica han contribuido a la reconstrucción de paleoambientes costeros y al estudio de la evolución costera a escala geológica (de miles a millones de años), en la cual cobran especial relevancia los procesos tectónicos y los cambios climáticos y del nivel del mar durante el Cuaternario.

La pretensión de extrapolar los modelos morfodinámicos de pequeña escala a la predicción de la evolución de los sistemas costeros a mayor escala se ha demostrado ineficaz (Davidson-Arnott, 2010), por lo que uno de los retos más importantes de la geomorfología actual es establecer conexiones entre la dinámica de los procesos a pequeña escala y los controles a largo plazo (Spedding, 1997; Walker et al., 2017).

Las islas oceánicas de punto caliente

Muchos de los grupos y cadenas de islas que salpican los océanos, como Hawái, Islas Sociedad, Canarias, Cabo Verde o Reunión, se consideran "puntos calientes" (*hot-spots*). En el conjunto de las masas emergidas del planeta, suponen apenas el 0,04%, por lo que constituyen contextos geográficos muy singulares que han atraído el interés científico desde muy temprano. Forman un conjunto numeroso de pequeñas islas nacidas desde las profundidades oceánicas y formadas por rocas semejantes, donde es relativamente fácil aislar los efectos de las variables naturales (Menard, 1986).

El modelo de punto caliente explica la aparición los archipiélagos intraplaca a partir de la actividad eruptiva de una pluma mantélica en la base de una placa listosférica en movimiento. El magma proveniente del manto inferior se eleva en forma de estrechas plumas que atraviesan la litosfera formando volcanes en el suelo oceánico. Como resultado de la generación de nuevas islas sobre el área activa (punto caliente), se crea una cadena lineal de islas (*hot-spot track*), progresivamente más viejas en el sentido del movimiento de la placa (Wilson, 1963; McDougall, 1971; Langenheim y Clague, 1987; Moore, 1987). Este fenómeno geofísico tiende a crear cadenas insulares (*island chains*), a veces tan perfectas como Hawái, y en otras ocasiones grupos menos ordenados de islas (*clustered islands*), como Galápagos, o islas solitarias (*isolated islands*), como Bermudas o Santa Helena.

Su origen y configuración convierte a estos archipiélagos en contextos geográficos singulares a escala global, especialmente interesantes en el estudio de la evolución de los relieves terrestres y marinos, y también de la evolución costera (Woodroffe, 2014). La teoría de Darwin acerca de la evolución de los anillos de coral y su relación con los procesos de subsidencia tectónica en islas oceánicas del Pacífico, puede considerarse uno de los ejemplos más prematuros de un modelo conceptual de evolución costera, que todavía hoy sigue vigente (Woodroffe, 2002). De la observación de la estructura de las costas a lo largo de las cadenas de islas, Darwin dedujo que los anillos de coral evolucionaban a barreras y después a atolones, como resultado combinado del hundimiento tectónico gradual de las islas y el crecimiento vertical de los arrecifes (Darwin, 1842). Posteriormente, fue Dana (1890) quien propuso definitivamente la existencia de la progresión de edades observando la secuencia erosiva de los relieves terrestres en el archipiélago de Hawái. Además, ya dedujo la posibilidad de un vulcanismo minoritario y local posterior a la vasta actividad inicial que forma el núcleo de los escudos volcánicos (Menard, 1986). No fue, sin embargo, hasta un siglo después, cuando Wilson (1963) propuso por primera vez que la corteza oceánica se movía empujada por células convectivas en el manto, y cuando McDougall (1964) corroboró, mediante dataciones isotópicas, la progresión de edades de Dana.

Los volcanes oceánicos surgen del fondo marino, y algunos consiguen emerger a la superficie y convertirse en islas, para después experimentar largos periodos de erosión, subsidencia y reactivaciones volcánicas hasta finalmente desaparecer bajo las aguas. En este proceso, pasan por varias etapas de desarrollo. La evolución de los sistemas de islas oceánicas es algo diferente según las configuraciones geodinámicas/geográficas donde los puntos calientes se localicen, pero frecuentemente siguen un mismo patrón (Ramalho et al., 2013). En general, se puede decir que su crecimiento es rápido, pues experimentan un gran impulso constructivo al inicio, que decrece con rapidez en el tiempo. La mayoría de los volcanes del Pacífico tardan menos de un millón de años en alcanzar su máximo volumen antes de abandonar el punto caliente (Menard, 1986). En

las islas Canarias, los escudos volcánicos antiguos suelen tener edades comprendidas en intervalos de pocos millones de años (Carracedo et al., 1998). Durante esta fase de rápido crecimiento, primero submarino y después subaéreo, los volcanes oceánicos experimentan típicamente procesos de inestabilidad gravitacional que desembocan en deslizamientos gigantes (*giant slumps, flank collapse*s) que a menudo afectan a flancos enteros de los edificios volcánicos (Moore y Normark, 1994; Carracedo et al., 1999).

En la transición de monte submarino a volcán subaéreo, las erupciones cerca de la superficie del mar producen potentes explosiones, al entrar la lava en contacto con el agua. Estas explosiones pulverizan el material, que se acumula en forma de conos hialoclastíticos muy fácilmente erosionables por el oleaje. A medida que la emisión de lava continúa, va formándose un medio sólido de transición que permite la solidificación de la lava en forma de coladas basálticas (Menard, 1986). Si tal proceso persiste, la acumulación supera la acción destructiva del oleaje y tiene lugar el nacimiento definitivo de una isla. Durante su desarrollo subaéreo, las islas oceánicas experimentan, según el modelo establecido en la cadena de volcanes de Hawái, tres etapas volcánicas principales (Menard, 1986; Ramalho et al., 2013). La primera es la etapa de escudo (*shield stage*), durante la cual el volcán emite la mayor parte de su volumen final en un intervalo a menudo inferior a 1 ma., dando lugar a un típico edificio de base amplia y pendiente tendida, compuesto por apilamientos de lavas basálticas. La siguiente etapa, o etapa de madurez (*old stage*), está marcada por la diferenciación del magma y la emisión de volúmenes comparativamente menores de lavas más acidas y viscosas que culminan la cima del escudo. A esta etapa le sigue un periodo de erosión caracterizado por una falta de actividad volcánica que puede prolongarse varios millones de años. Finalmente, la tercera y última etapa se ha denominado post-erosiva o de rejuvenecimiento (*posterosive*, *rejuvenation)*. Se caracteriza por una actividad eruptiva residual, puntual y anecdótica en volumen, aunque puede tener llegar a tener una impronta muy significativa en el paisaje. Tras esta etapa, las islas oceánicas entran en un prolongado proceso erosivo, que acaba formando *guyots*, montes submarinos de cima plana, coronados por plataformas.

Diversidad, geodiversidad y diversidad geomorfológica

Entre las medidas estructurales de paisaje (*landscape metrics*), la diversidad es tal vez la de mayor desarrollo teórico. La diversidad es una idea general que envuelve conceptos como variedad o heterogeneidad, y que se relaciona con la idea de complejidad. Debido a su carácter general, cualquier conjunto de elementos clasificables y cuantificables puede ser objeto de un análisis de

diversidad. Ha sido, por ello, transversal a las ciencias naturales y humanas (McDonald y Dimmick, 2003). En ecología, especialmente, la diversidad de especies ha sido un problema central desde hace décadas (Magurran, 1988).

La diversidad es un concepto complejo y dual, con al menos dos parámetros. El primero, al que se puede denominar "riqueza" (*richness*), se refiere al número distinto de clases que componen la población que se analiza, de tal forma que la diversidad es mayor en las poblaciones donde existe un mayor número o variedad de clases. El segundo parámetro, denominado "equidad" o "equi-abundancia" (*evenness*), se refiere a la frecuencia con que aparecen representadas cada una de las clases y la proporción que ocupan dentro del conjunto de la población, es decir, a la horizontalidad de la distribución (Pielou, 1975). Una población será tanto más diversa cuanto más homogénea sea la cantidad en la que aparece representada cada clase. En el campo de la biología (Clarke y Warwick, 1998; Owens y Bennet, 2000; Faith, 2002), se ha trabajado lo que puede considerarse un tercer parámetro de la diversidad: la "distancia taxonómica" (*taxonomic distance*) o "disimilitud" (*dissimilarity*). Este concepto parte del hecho de que, dentro de cualquier sistema de clasificación jerárquico (e.g. un árbol filogenético) donde existan varios niveles de organización, las clases de un mismo orden sobre las que se quiere conocer la diversidad, no guardarán el mismo grado de parentesco o proximidad entre todas ellas, puesto que se encuentran agrupadas. Dos clases del mismo grupo tendrán características más similares que dos clases de grupos distintos, aunque pertenezcan al mismo orden. Teniendo esto en cuenta, la diversidad general de la población es tanto mayor cuanto más repartidas se encuentren las clases por el espectro de la clasificación, y menor cuanto más concentradas.

La complejidad del concepto de diversidad no termina en el hecho "multiparamétrico". En ecología, se han dado además tres "dimensiones" a la diversidad. Cuando el interés es conocer la diversidad interna de una población estadística o conjunto, o de varias poblaciones o conjuntos, por separado, se habla de "diversidad alfa" (α-*diversity*). En estos casos se trata de conocer, normalmente a través de algún índice de cálculo, cual es la riqueza, equi-abundancia o, incluso, disimilitud, de cada población estadística. Cuando lo que se quiere conocer es, sin embargo, la diversidad inter-poblacional, es decir, el grado o tasa de cambio que se produce al pasar de una población o comunidad a otra, se habla de "diversidad beta" (β-*diversity*). En este caso se busca conocer la diversidad como intensidad de un gradiente de cambio. La diversidad beta será alta cuando dos comunidades presentan contrastes fuertes en cualquiera de los parámetros de diversidad. En este sentido, un simple cálculo de variación proporcional puede considerarse ya una estimación de diversidad beta. Existen, no obstante, una amplia propuesta de índices para estimarla (e.g. Whittaker, 1960; Cody, 1975; Routledge, 1977). Dos poblaciones pueden tener una baja diversidad alfa (riqueza, equiabundancia o distancia taxonómica), y, sin embargo, una

elevada "disimilitud beta" si presentan una baja correspondencia de clases. Finalmente, se denomina "diversidad gamma" (γ-*diversity*), también llamada "diversidad regional", al resultado de integrar las diversidades alfa y beta de varias poblaciones, con el fin de obtener una estimación global de la diversidad en una región, teniendo en cuenta la diversidad intrínseca de cada población, así como el grado de cambio entre ellas.

La geodiversidad es la aplicación del concepto general de diversidad al estudio de los elementos abióticos de la naturaleza. Se puede definir, por analogía y complementariedad con la bio-diversidad, como el estudio de la parte abiótica (geología, geomorfología, suelos, hidrología, topografía, etc.) de la diversidad natural (Serrano y Ruiz-Flaño, 2007; Gray, 2008). Como concepto, surge en la década de 1990, en Australia (Sharples, 1993; Kiernan, 1994; Dixon, 1995), y como campo de investigación, experimenta su impulso definitivo en la década de 2000 a raíz de una serie de trabajos que actualmente enmarcan la materia (Gray, 2004; Gordon et al., 2012; Thomas, 2012). La relativa juventud de este campo permite identificar en él una serie de rasgos característicos.

Gray (2004), en la definición quizás más citada del concepto, lo define como "*el rango natural (diversidad) de los elementos geológicos (rocas, minerales, fósiles), geomorfológicos (geoformas, procesos) y edafológicos, incluyendo sus asociaciones, relaciones, propiedades, interpretaciones y sistemas*". En ese mismo tratado, Gray otorga un peso preponderante a la vinculación de la geodiversidad con la geoconservación (*geoconservation*) y el geopatrimonio (*geoheritage*). A ello han contribuido otros autores estableciendo la importancia de los elementos abióticos de la naturaleza como recurso económico y cultural para las sociedades humanas, y como fundamento de la sostenibilidad de ecosistemas, hábitats y paisajes (e.g. Gray, 2005, 2008; Serrano y Ruiz-Flaño, 2007; Gordon et al., 2012; Thomas, 2012; Hjort et al., 2015). Estas conceptualizaciones originales han introducido en el campo de la geodiversidad una fuerte impronta conservacionista, orientándolo al estudio y conservación del patrimonio natural. Así pues, se han multiplicado los trabajos, metodológicos y aplicados, sobre identificación, catalogación y valoración de espacios de interés geopatrimonial (*geosites*) con base en procedimientos multicriterio, escalas de valor y listas de indicadores (e.g. Bruschi y Cendrero, 2005; Panizza y Piacente, 2009; Feuillet y Sourp, 2011; Brilha, 2015; Çetiner et al., 2018). La fusión ocasional de los conceptos geopatrimonio-geodiversidad ha conducido a cierta confusión terminológica, así como al empleo del término geodiversidad de una forma un tanto inespecífica, en referencia a una totalidad o conjunto que se prefigura implícitamente como diverso y de alto valor.

Los trabajos de investigación que tratan la geodiversidad en sentido estricto (estimación de la heterogeneidad o variabilidad de los elementos abióticos en el espacio), han adoptado un enfoque holístico o totalizador, también acorde con las líneas 'fundacionales' que han atravesado

la materia y guiado las investigaciones desde hace por lo menos una década. En el enfoque holístico, el objetivo es estimar la geodiversidad total, combinando para ello un número variable, heterogéneo y representativo de componentes de la geodiversidad (litología, geomorfología, topografía, edafología, hidrología, etc.) (Benito-Calvo et al., 2009; Argyrioua et al., 2016; Serrano et al, 2009; Hjort y Luoto, 2010; Ruban, 2010; Pellitero et al., 2011; Pereira et al., 2013; Ilić et al., 2016; Melelli et al., 2017; Özşahin, 2017; Stepišnik y Trenchovska, 2018). En esta línea, Zwoliński et al. (2018) llegan a calificar los estudios específicos, de un solo componente (por ejemplo, diversidad litológica), de "enfoque arbitrario".

Por otro lado, la mayoría de las investigaciones han tratado la geodiversidad como un caso especial de diversidad en la naturaleza, ignorarando los abundantes antecedentes teóricos que ya existían en materia de diversidad, tanto a nivel conceptual como matemático. Salvo excepciones (Benito-Calvo et al., 2009; Argyrioua et al., 2016), se ha recurrido a la elaboración de formas de cálculos especiales, denominadas índices de geodiversidad (*geodiversity indices*). Estos son producto generalmente de operaciones cartográfico-algebraicas con base en la superposición de mapas en sistemas de información geográfica (SIG), donde el parámetro medido es fundamentalmente la riqueza. De todos ellos, el índice más aplicado ha sido, con diferencia, el propuesto por Serrano y Ruiz-Flaño (2007). En este cálculo, el número de clases distintas (riqueza), multiplicada por un parámetro de rugosidad del terreno, es dividido por el logaritmo de la superficie, lo que remite aparentemente a una adaptación del índice de Margalef (1958) al problema de la geodiversidad.

Como campo específico o sub-campo de la geodiversidad, la diversidad edafológica (*pedodiversity*) constituye una excepción a estas tendencias "holísticas", por un lado, y "particularistas", por otro. Ibáñez et al. (1995) sentaron las bases de un estudio de la diversidad de suelos asentado en los conceptos, modelos e índices desarrollados en ecología matemática. Ello produjo diferentes teorías acerca de la distribución global de la diversidad de suelos (Ibáñez et al., 1998) y las relaciones área-diversidad en islas (Ibáñez et al., 2005; Ibáñez y Effland, 2011). A partir de entonces ha habido un creciente interés por medir la diversidad de suelos a diferentes escalas y en relación a distintas variables mediante índices y modelos clásicos (e.g. Guo et al., 2003; Ibáñez et al., 2005; McBratney y Minasny, 2007; Minasny et al., 2010). A través del diseño de tablas de atributos característicos (*key atributes*), también ha sido abordado el problema de la distancia taxonómica o disimilitud de clases en diversidad de suelos (Minasny et al., 2010; Huyssteen et al., 2014; Smirnova y Gerasimova, 2016).

Los estudios de geodiversidad se han dirigido mayoritariamente al estudio de la distribución espacial de la geodiversidad (e.g. Pellitero et al., 2011; Pereira et al., 2013; Melelli et al., 2017) o al estudio de las relaciones entre geodiversidad y biodiversidad (e.g. Burnett et al., 1998; Parks y

Mulligan, 2010; Brazier et al., 2012; Hjort et al., 2012). En este sentido, el estudio de la evolución temporal de la geodiversidad, o "geodiversidad evolutiva", ha recibido poca atención. Encontramos solo algunos ejemplos de evolución a escala histórica (Ruban, 2010; Rodrigues y Silva, 2012) y o a escala geológica (Ibáñez et al., 1994, Seijmonsbergen et al., 2017). Además, con este predominio de los enfoques integradores, las investigaciones centradas a un solo componente de la geodiversidad ha sido muy escasas. Por ello, la diversidad geomorfológica, en un sentido estricto y exclusivo, ha recibido una escasa atención. Aunque sea la variable protagonista en algunos trabajos, suele combinarse analíticamente con otro tipo de variables de geodiversidad que restan especificidad a la geomorfología (e.g. Kot, 2017; Melelli et al., 2017), o utilizarse variables morfométricas y topográficas en vez de lo que son estrictamente categorías geomorfológicas (e.g. Burnett et al., 1998).

Con esta tesis se desarrolla una línea de investigación novedosa que, como se expuso en los antecedentes, cubre una falta de estudios en la intersección de la geomorfología costera con las islas volcánicas de punto caliente y el empleo de medidas estructurales de paisaje (*landscape metrics*).

Hipótesis y objetivos

Hipótesis de investigación

Según el modelo de punto caliente, el ciclo de vida de una isla se enmarca dentro de los momentos de emersión y sumersión (Ramalho et al., 2013). Una isla emerge desde el suelo oceánico hasta alcanzar la superficie del mar gracias a la actividad eruptiva de una pluma mantélica. Habrá necesariamente, en el punto de emersión, un momento inicial de "cero diversidad y abundancia geomorfológica", en el que no hay todavía transformación geomorfológica por procesos costeros en el nuevo margen terrestre (Figura II). Este momento podría ser casi un instante a juzgar por la velocidad a la que se erosionan algunos volcanes oceánicos en etapas iniciales (Ramalho et al., 2013). Incluso el edificio podría cruzar la superficie del mar en más de una ocasión, producto de un balance extrusión-erosión negativo o determinado por oscilaciones eustáticas. Una vez ha emergido definitivamente, el movimiento de la placa tectónica la alejará del punto caliente, la actividad volcánica decaerá progresivamente y los procesos erosivos dominarán la geodinámica externa a lo largo de millones de años. En muchos casos, se producirá también una dinámica subsidente por enfriamiento cortical. El cualquier caso, el proceso terminará, al cabo de unos cuantos millones de años, con el arrasamiento completo del edificio volcánico y su inmersión total bajo las aguas. Puede considerarse este punto un momento final de "cero diversidad y abundancia geomorfológica".

La hipótesis afirmativa (H_1) consiste en que entre los dos puntos de "cero diversidad y abundancia geomorfológica", correspondientes a los momentos de nacimiento (emersión) y extinción (sumersión) del volcán oceánico, debe existir un patrón parabólico, de crecimiento y caída, con un máximo por definir, en la complejidad geomorfológica (diversidad y abundancia) de las costas (Figura II, izquierda). La alternativa a esta hipótesis, que podríamos llamar hipótesis negativa (H_0), consiste en que la evolución de la diversidad y abundancia geomorfológica en las costas no tiene un patrón o expresión a escala geológica en el marco del nacimiento y extinción de una isla, y que, en todo caso, podría seguir curvas o ciclos de una u otra escala relacionados con procesos diferentes (Figura II, centro). Entre estas dos alternativas cabría, no obstante, una posibilidad combinada (Figura II, derecha).

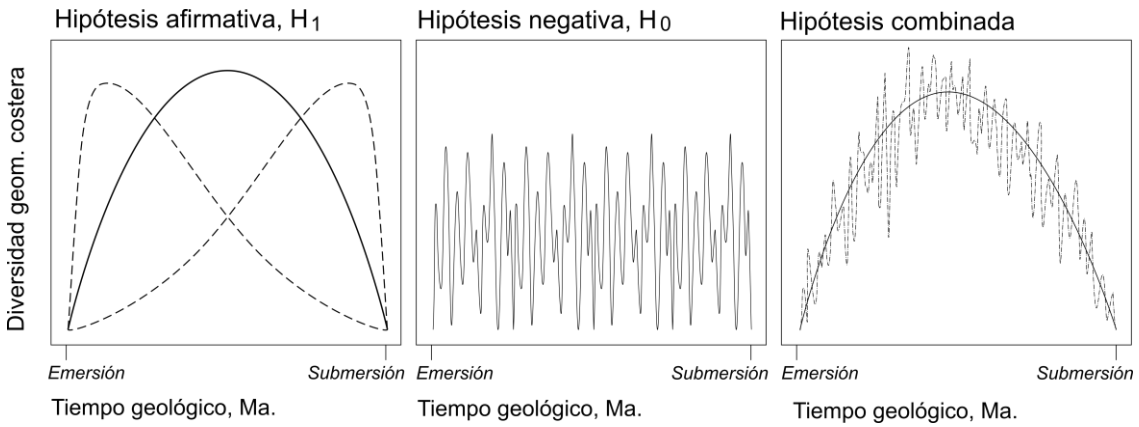

Figura II. Hipótesis de investigación.

Objetivo general

Para contrastar la hipótesis, el objetivo general que se plantea en esta investigación es analizar la evolución costera a escala geológica en islas oceánicas, desde la perspectiva de la composición y configuración geomorfológica, y en especial de la diversidad. Para llevarlo a cabo, se plantea comparar la composición y configuración geomorfológica de un número representativo de costas de islas de diferente edad y estado de desarrollo en archipiélagos volcánicos de punto caliente.

Objetivos específicos

Para la consecución del objetivo general y el contraste de la hipótesis de investigación, se plantean una serie de objetivos específicos, cuya secuencia temporal se enumera a continuación:

1) Seleccionar el conjunto de islas que componen la muestra. Deberá ser representativo en cantidad, en función del número de islas que compongan el archipiélago, y en características, en función de su edad, etapa de desarrollo y tamaño.
2) Reconstruir las características geomorfológicas pre-humanas de las costas en las islas seleccionadas, con el fin de suprimir las transformaciones humanas, como factor de distorsión en la observación de la estructura geomorfológica natural.
3) Diseñar un sistema de clasificación mesoescalar de geoformas costeras, que pueda ser aplicado consistentemente a lo largo grandes distancias (por todo el perímetro costero de las islas seleccionadas), que se adapte a las fuentes disponibles, y que recoja el espectro de variabilidad geomorfológica de estos ambientes, sin redundancias y de forma equilibrada (sin dar mayor o menor peso a procesos y formas de uno u otro tipo).

4) Recopilar las fuentes de información válidas disponibles para el levantamiento geomorfológico conforme a la taxonomía propuesta (fotografías aéreas, imágenes de satélite, modelos digitales del terreno y mapas) y estructurar las mismas dentro de un proyecto cartográfico.
5) Diseñar un protocolo de criterios para la identificación sistemática de las geoformas propuestas en el sistema taxonómico.
6) Diseñar y ejecutar un sistema de representación cartográfica y de almacenamiento de datos espaciales que sea representativo, eficaz y analíticamente válido para contabilizar clases y cuantificar abundancias, que permita así analizar la estructura geomorfológica a partir de la composición de geoformas y su distribución espacial y de frecuencias.
7) Planificar y realizar campañas de trabajo de campo para validar *in situ* el levantamiento geomorfológico.
8) Seleccionar y ensayar métricas de abundancia y diversidad para el conjunto de datos y elaborar análisis comparativos.
9) Analizar los errores e incertidumbres asociadas al método de trabajo.
10) Obtener, interpretar y discutir los resultados en el marco de la hipótesis planteada, ¿se rechaza o se valida, provisionalmente, conforme a los datos disponibles?

Métodos

Los aspectos más importantes de la metodología se encuentran detallados en cada uno de los artículos que componen el núcleo de esta tesis doctoral. En este apartado se realiza un repaso por los puntos comunes o más importantes de la misma (figura III), ampliando información que, por cuestión de espacio, no pudo ser incluida en los artículos.

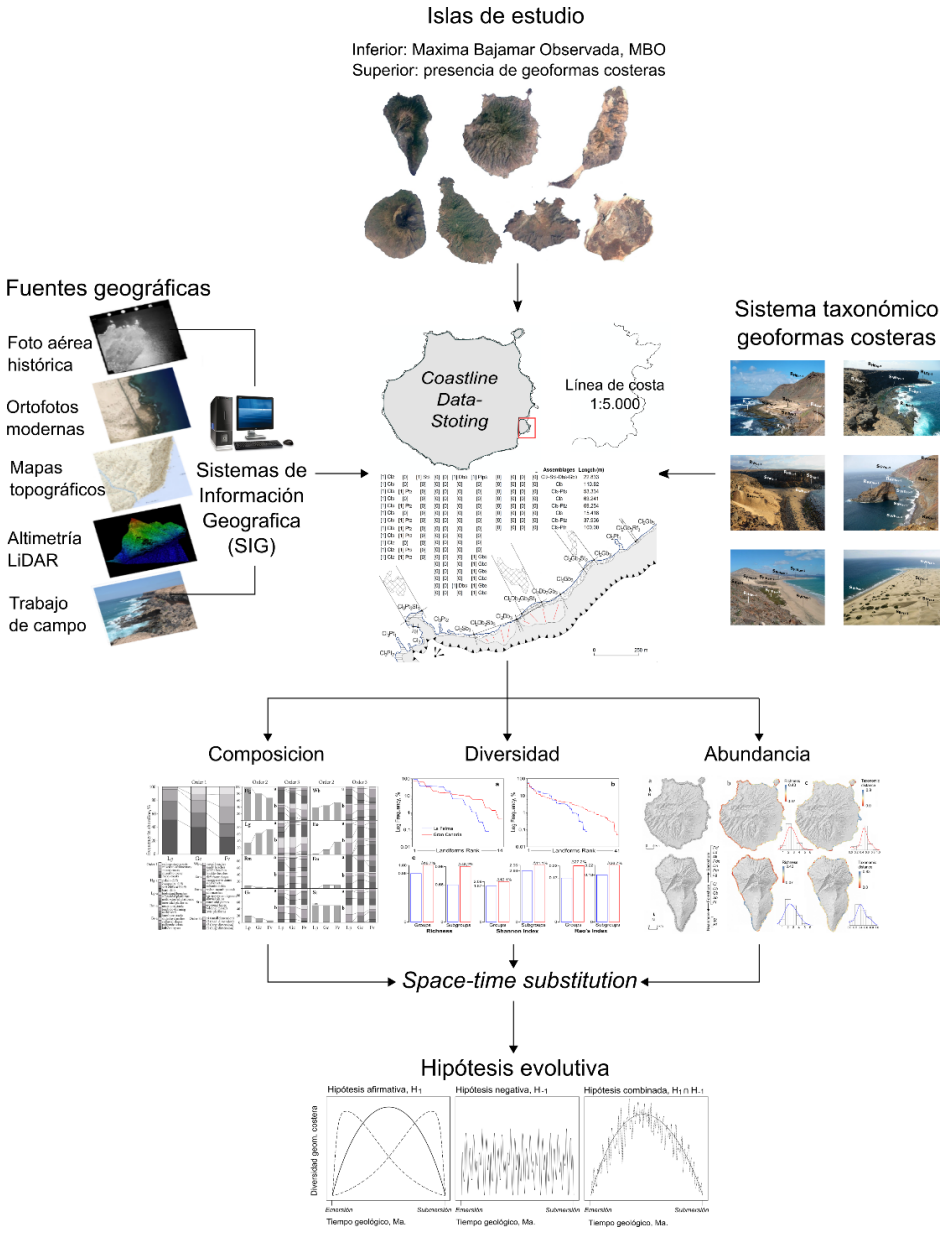

Figura III. Flujo de trabajo y metodológico.

Islas de estudio y razonamiento "espacio por tiempo"

La aplicación del razonamiento "espacio por tiempo" (*space-for-time substitution* o SFT) (Pickett, 1989) constituye la premisa fundamental de esta investigación. En este método, se asume que la variación espacial es equivalente a la variación temporal a la hora de inferir cronosecuencias de largo plazo mediante la comparación de muestras de diferente edad o estado de desarrollo (Pickett, 1989). Mediante observación indirecta, o aproximación estática, se infieren los rasgos de la evolución costera a largo plazo en esta investigación. Picket (1989) apunta a las limitaciones de este método a la hora comprender los mecanismos subyacentes, pero reconoce su potencial en el establecimiento de marcos conceptuales e hipótesis generales para los estudios experimentales y las observaciones directas. La aplicación del enfoque sincrónico ha sido muy recurrente en el estudio de la dinámica de las comunidades vegetales en ecología (e.g. Aber, 1979; Travis y Hester, 2005).

Las cadenas de islas de punto caliente son un laboratorio natural para la aplicación de este enfoque debido a la sucesión natural de edades, y a que las islas son pequeñas, nuevas, aisladas y sujetas a un rango limitado de factores ambientales. Charles Darwin fue uno de los primeros en darse cuenta del potencial de investigación en islas oceánicas (Menard, 1986). Ejemplos mucho más recientes pueden verse en los trabajos de Whitaker et al., (2008), sobre la adaptación de las líneas generales del modelo MacArthur y Wilson (*Theory of Island Biogeography)* a la dinámica evolutiva de especies en los sistemas de islas oceánicas; o en el trabajo de Seijmonsbergen et al. (2017), sobre la evolución de la geodiversidad terrestre a lo largo del punto caliente hawaiano.

Para un aislamiento efectivo de la variable temporal en un método SFT, los elementos que se comparan deben compartir sus "condiciones de contorno" (*boundary conditions*). En evolución costera, estas son principalmente el clima atmosférico, el régimen marítimo y las características tectónicas y litológicas. El papel dominante de las condiciones lito-estructurales en la geomorfología se ha sustanciado en la "teoría del control litológico" (*Rock Control Theory*) (Yatsu, 1962; Benumof et al., 2000; Naylor y Stephenson, 2010; Carpenter et al., 2014).

En esta investigación, la variabilidad ambiental se controla, al menos parcialmente, comparando islas de un mismo archipiélago, en archipiélagos de la misma región. Así, se han analizado dos cadenas de islas de la zona central y sur de la Macaronesia: Canarias y Cabo Verde (Figura IV). Estos archipiélagos constituyen puntos calientes cuya peculiaridad principal reside en los anormalmente largos periodos de pervivencia de las islas, lo cual supone una oportunidad para observar cambios estructurales en periodos excepcionalmente amplios. En Hawái, y en la

mayoría de los archipiélagos del Pacífico, donde juega un papel primordial la subsidencia tectónica, no pasan más de 5 millones de años antes de que las islas se sumerjan convirtiéndose en atolones (Langenheim and Clague, 1987), pero en la Macaronesia existen ejemplos de islas con más de 20 millones de años, como Fuerteventura (20,5 ma.), Maio (18-22 ma.) o Sal (23-28 ma.) (Carracedo et al, 1998; Dyhr y Holm, 2010).

De las 7 islas principales de Canarias, se escogieron 3 (La Palma, Gran Canaria y Fuerteventura), y de las 10 islas principales de Cabo Verde, se escogieron 4 (Fogo, Santiago, São Vicente y Boa Vista). En suma, un total de 7 islas y 1.416 km de costa han sido objeto de esta investigación. El ámbito de estudio ha sido ampliado a nuevas islas a lo largo de la investigación:

>En el primer artículo (Ferrer-Valero et al., 2017), una isla: Gran Canaria (islas Canarias).

>En el segundo (Ferrer-Valero, 2018), dos islas: La Palma y Gran Canaria (islas Canarias).

>En el tercero (Ferrer-Valero et al., 2018), tres islas: La Palma, Gran Canaria y Fuerteventura (islas Canarias).

>En el cuarto (no publicado), cuatro islas: Fogo, Santiago, São Vicente y Boa Vista (Cabo Verde).

En la selección de las islas analizadas ha primado un criterio de edad, de forma que los casos representan estados de desarrollo diferenciados. Este criterio ha estado acompañado de otro, relativo al tamaño de las islas, con el fin de minimizar las diferencias, teniendo en cuenta que no se encuentran islas de igual tamaño que además cumplan la primera condición en esta región.

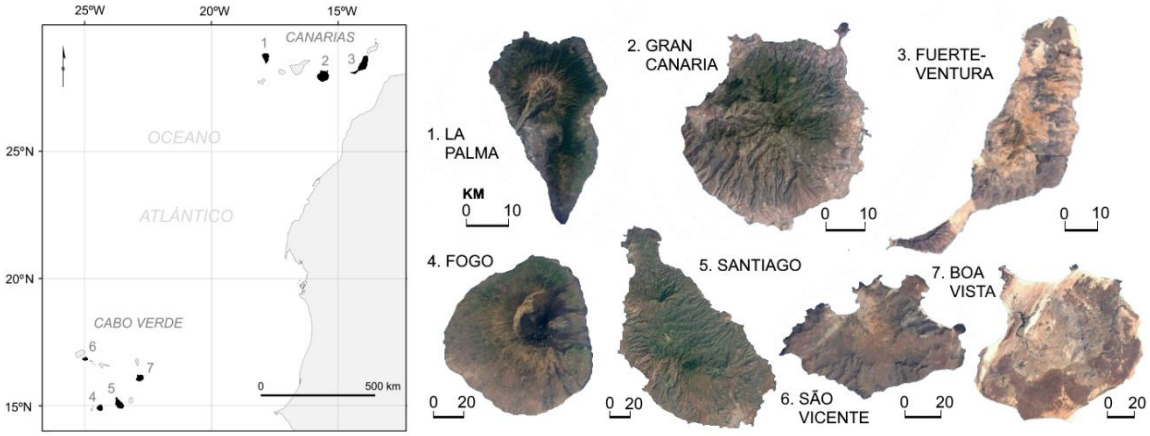

Figura IV. Islas estudiadas en orden creciente de edad.

En el archipiélago Canario, la isla de La Palma (706 km^2, 2.426 msnm., 198 km de costa, 1,8 ma.) representa el estado juvenil de un escudo volcánico activo y en crecimiento; Gran Canaria (1.560 km^2, 1.956 msnm., 256 km de costa, 14,5 ma.) representa una isla madura, en una etapa posterosiva más avanzada; y Fuerteventura (1.660 km^2, 817 msnm., 385 km de costa, 20,6 ma.)

una isla oceánica muy antigua, de las más longevas del planeta. En el archipiélago de Cabo Verde, la isla de Fogo (476 km^2, 2.829 msnm., 105 km de costa, <1 ma.) representa un estado volcánico juvenil todavía anterior a La Palma; Santiago (991 km^2, 1.394 msnm., 244 km de costa, ~3 ma.), una etapa posterosiva temprana; San Vicente (227 km^2, 725 msnm., 98 km de costa, ~7 ma.), una etapa posterosiva avanzada; y Boa Vista (620 km^2, 378 msnm., 130 km de costa, ~17 ma.), una fase última *a priori* semejante a Fuerteventura (Figura IV).

Una taxonomía geomorfológica *ad hoc*

La geomorfología es una ciencia arraigada en el uso de categorías. Como prueba de ello vale examinar los principales tratados de geomorfología costera, estructurados en capítulos como "playas", "marismas", "barreras", "dunas" o "acantilados" (e.g. Woodroffe, 2002; Bird, 2008; Davidson-Arnott, 2010). Además, se pueden ver buenos ejemplos de cartografías geomorfológicas basadas en el reconocimiento de geoformas a escala local (De Muro et al., 2015; Rovere et al., 2015; Sander et al., 2016), regional (Alexander, 1966; Isola et al., 2011; Biolchi et al., 2016), nacional (Owens, 1994) y mundial (McGill, 1958). Algunos trabajos recientes han propuesto nuevos sistemas de clasificación de costas globales y multiescalares (Fairbridge, 2004; Finkl, 2004; Brocx y Semeniuk, 2010).

A pesar de ello, la geomorfología, y en particular la geomorfología costera, carecen de un sistema global de clasificación que garantice un marco común de análisis y comparación, por ejemplo, para la aplicación de métricas de paisaje y estimaciones de diversidad. No existe una taxonomía internacional, estandarizada y multiescalar donde se sistematicen los tipos geomorfológicos y sus relaciones jerárquicas, genéticas y de parentesco. Ante esta carencia, se ha desarrollado, en esta tesis doctoral, una taxonomía *ad hoc* de geoformas costeras, válida para implementar esta investigación. La propuesta se ha construido, progresivamente, en base a la observación directa de las costas de Canarias y Cabo Verde, y con referencia a términos y conceptos recogidos en la literatura (McGill, 1958; Alexander, 1966; Young y Clayton, 1972; Emery y Kuhn, 1982; Pethick, 1984; Sunamura, 1992; Kjerfve, 1994; Owens, 1994; Mattox y Mangan, 1997; Wilkerson, 1997; Carracedo et al., 1999; Zazo, 1999; Brooke, 2001; Jennings y Shulmeister, 2002; Fairbridge, 2004; Finkl, 2004; Hall et al., 2006; Bird, 2008; Shipman, 2008; Brocx y Semeniuk, 2010; Davidson-Arnott, 2010; Isola et al., 2011; Criado et al., 2012; Hesp and Walker, 2013; Kennedy, 2014; De Muro et al., 2015; Rovere et al., 2015; Biolchi et al., 2016; Sander et al., 2016).

La taxonomía fue creciendo y mejorándose con el progreso de la investigación. De esta forma, encontramos:

>En el primer artículo (Ferrer-Valero et al., 2017): 9 clases (un nivel jerárquico).

>En el segundo (Ferrer-Valero, 2018): 14 clases y 42 subclases (dos niveles jerárquicos).

>En el tercero (Ferrer-Valero et al., 2018): 3 clases, 8 subclases y 64 sub-subclases (tres niveles jerárquicos).

>En el cuarto, se retoma la clasificación del segundo, para zonas con baja disponibilidad de fuentes, ampliando de 14 a 21 clases y de 42 a 60 subclases.

La taxonomía es (1) mesoescalar, pues abarca grandes tipos y grupos geomorfológicos, lo que permite el levantamiento de largos tramos de costa; (2) jerárquica y fractal, pues está estructurada en niveles u órdenes taxonómicos con igual número de subdivisiones, para garantizar un equilibrio de procesos y formas; y (3) abierta, pues es ampliable con base en nuevas observaciones. Con esta taxonomía, los levantamientos geomorfológicos se adaptan a las fuentes disponibles, son consistentes a los largo de grandes distancias y son representativos del rango de variabilidad geomorfológica mesoescalar.

En la jerarquía taxonómica se incluyen categorías nominales y subcategorías morfométricas que enriquecen la información estructural del paisaje costero. Definiciones de las categorías y más detalles sobre el sistema de clasificación pueden encontrarse en cada uno de los artículos que conforman el núcleo de esta tesis doctoral.

Identificación multifuente

El reconocimiento se realizó mediante identificación remota, integrando y superponiendo fuentes fotográficas y cartográficas georreferenciadas en SIG, con apoyo de trabajo de campo. A continuación se amplía alguna información que, por cuestión de espacio, no se detalló en los artículos.

Reconstrucción histórica

Por medio de fuentes históricas, se procedió a la reconstrucción del perímetro y las geoformas originales de las áreas transformadas por actividades y ocupaciones humanas. Este trabajo fue especialmente intenso en la isla de Gran Canaria, donde aproximadamente el 42% de la costa está transformada en un grado significativo. Las fuentes utilizadas fueron:

>Fotografías aéreas digitales de 1962, 1977 y 1981, para toda Gran Canaria (fototeca del Cabildo de Gran Canaria), y de los 60, 70, 80 y 90, para todo el archipiélago (fototeca de GRAFCAN, S.A., Gobierno de Canarias), disponibles para descarga y georreferenciación.

>Ortofotos digitales del sur de Gran Canaria (1961), Las Palmas de Gran Canaria (1966), mitad y sur de La Palma (1964) y Fuerteventura (1994), disponibles por *Web Map Service* (WMS) en la infraestructura de datos espaciales de Canarias (GRAFCAN, S.A.-Gobierno de Canarias).

>Fotografías del archivo de fotografía histórica de Canarias (Fundación para la Etnografía y el Desarrollo de la Artesanía Canaria, FEDAC, Cabildo de Gran Canaria).

>Cartografía antigua, principalmente la Carta Náutica de Las Palmas de Gran Canaria (Dirección Hidrográfica, 1879) y el Plano de Santa Cruz de La Palma de Antonio Rivière (1740).

En Cabo Verde, las fuentes histórico-geográficas son muy escasas, pero las intervenciones "duras" en la costa están bastante localizadas en los núcleos urbanos principales (Praia, Mindelo) y generalmente son recientes, por lo que se pueden ver bien las alteraciones en las series modernas de fotografías aéreas o imágenes de satélite.

Ortofotos digitales modernas e imágenes de satélite

La foto-identificación por imágenes aéreas modernas fue un pilar fundamental en el levantamiento geomorfológico. Las islas Canarias cuentan con una serie de 14 ortofotos digitales modernas, con las que se trabajó en línea, vía WMS (IDE-Canarias). Cubren todo el territorio, con resoluciones entre 1 m/px y 25 cm/px, aumentando a 12,5 cm/px en áreas urbanas, y con un error planimétrico medio (RMS) inferior a 1,5 m. En el examen de fechas pudo comprobarse que la toma de imágenes es preferentemente en los meses de invierno para evitar nubosidad, y que las épocas mayoritariamente coindicen entre islas, favoreciendo la homogeneidad de las cartografías resultantes (Tabla I).

En Cabo Verde las fuentes abiertas disminuyen en número y calidad notablemente. Se trabajó en conexión WMS con 4 series de ortofotos (2003-actualidad), para todo el territorio, con resoluciones entre 50 y 12,5 cm/px (IDE-Cabo Verde, Gobierno de Cabo Verde), y con 10 imágenes satelitales (2002-2018) de Landsat/Copernicus, CNES/Airbus y Digital Globe (QuickBird y WorldView), incorporadas en la plataforma 3D de *Google Earth*.

Tabla I. Compendio de ortofotos disponibles en la IDE de Canarias para conexión por WMS. LP, La Palma; GC, Gran Canaria; FV, Fuerteventura.

		Mes de la captura, resolución (m/pixel)											
Fecha	Isla	1	2	3	4	5	6	7	8	9	10	11	12

1998	LP											1,0	
	GC											1,0	
1998/99	FV		1,0									1,0	
2002	LP GC FV	1,0											
2004/05	LP GC	0,4											
2006	LP GC										0,5		
	FV											0,5	
2006 (NIR)	LP GC FV											0,5	
2007	LP			0,5									
	GC											0,4	
	FV			0,5									
2008	LP											0,4	
	GC FV										0,4		
2009	LP											0,4	
	GC FV										0,4		
2011	LP FV	0,4											
	GC									0,4			
2012	LP GC FV				0,25								
2013	LP												0,25
	GC	0,25											
2012/13	FV	0,25											0,25
2014	GC								0,25				
2014/15	LP FV	0,25			0,25								
2015	LP GC			0,25									
	FV											0,25	
2016	LP						0,25						
	GC					0,25							
	FV				0,25								

Mapas topográficos, temáticos y altimetrías LiDAR

Para el reconocimiento del relieve se trabajó con mapas topográficos a escalas 1:1.000, 1:5.000 y 1:10.000, equidistancia de las curvas de nivel de 5 m, y con los mapas de sombras derivados de los modelos digitales de elevaciones (MDE) disponibles en conexión WMS en las IDEs de Canarias y Cabo Verde. Adicionalmente, en Canarias están disponibles en abierto altimetrías de nubes de puntos LiDAR (*Light Detection and Ranging*), con densidad media de 1 pt/m^2 (GRAFCAN, S.A.-Gobierno de Canarias) y de 0,5 pt/m^2 (Instituto Geográfico Nacional, IGN-Gobierno de España).

Para las islas Canarias se contó además con la información de los mapas geológicos 1:50.000 de la serie MAGNA (IGME, Gobierno de España) y del mapa de Vegetación 1:25.000 (del Arco et al., 2006). Para Cabo Verde, se recurrió a cartografías geológicas publicadas de Fogo (Machado y Asunção, 1965), Santiago (Serralheiro, 1976), São Vicente (Ancochea et al., 2010) y Boa Vista (Dyhr y Holm, 2010; Hernández-Calvento et al., 2017).

Trabajos de campo

El trabajo de campo se desarrolló durante los años 2015, 2016 y 2017, estando dirigido al refuerzo y verificación de las observaciones efectuadas por identificación remota en lugares representativos o localizaciones problemáticas que presentasen dudas de clasificación. Siguiendo

la cronología de la investigación, en los años 2015 y 2016 se exploró la isla de Gran Canaria en numerosas campañas por tierra, y en tres campañas a bordo de embarcación ligera que permitieron fotografiar el perímetro completo de la isla a corta distancia. Durante 2016 y 2017, se realizaron dos campañas de 5 días en La Palma, y otras dos en Fuerteventura, durante las cuales se hicieron reconocimientos *in situ* de la cartografía elaborada en puntos de interés previamente seleccionados. Finalmente las campañas de reconocimiento en las islas de Cabo Verde se realizaron durante las tres primeras semanas de noviembre de 2017.

Métodos cartográficos, SIG y bases de datos

Criterios de identificación y clasificación

El levantamiento devino de la observación continua de la costa desde el punto septentrional hasta completar el perímetro de cada isla. A lo largo de cada costa se identificaron las geoformas costeras emergidas, tomando como límite inferior del levantamiento la bajamar máxima observada (BMO) en la serie ortofotográfica, y como el límite superior, la presencia de geoformas de origen costero. No se fijó una unidad mínima cartografiable, o sea que el grado de detalle está limitado por la resolución de las fuentes y la agudeza de identificación, que en esta investigación se sitúa en torno a geoformas de 10 m^2. Cada geoforma se identificó y cartografió de manera sistemática. Aquellas de las que no se tuvo seguridad de un registro preciso y sistemático por medio de identificación remota (por ejemplo, paleo-playas) se excluyeron previamente del estudio.

Si bien se hizo un uso combinado de fuentes, el peso de estas en la identificación varía en función de sus características. En las formas de tipo acantilados, pendientes costeras o plataformas colgadas, tuvieron un papel preferente las fuentes topográficas (mapas, MDEs, LiDAR), mientras que en otras, como playas, plataformas o campos de dunas, el papel prioritario fue de las fuentes fotográficas. En la figura V se puede ver esquematizado el procedimiento general de identificación de algunas de las geoformas principales. La identificación es individual pero las formas pueden coexistir y combinarse en un mismo punto o tramo de la costa.

A pesar de la fijación de criterios objetivos, el proceso no estuvo exento de incertidumbres de clasificación. Vale mencionar como ejemplo el caso de taludes de derrubios (deslizamientos, desprendimientos, coluviones, etc.), que pueden resultar difícilmente diferenciables cuando existen (i) substratos deleznables en la base de un acantilado, con ángulos de reposo más bajos; (ii) pendientes medias de tipo estructural en edificios estrombolianos, o (iii) dunas rampantes en

ocasiones imbricadas con depósitos de ladera. Asimismo, pueden generar dificultades de discernimiento de relieves residuales, cuando un bloque de desprendimiento penetra en la zona de asomeramiento, o de playas de bolos en los frentes de movimientos en masa. En casos de incertidumbre, que no hayan podido resolverse por observación *in situ*, se ha adoptado un "principio conservativo" (*conservative criterion*), contrario al registro positivo.

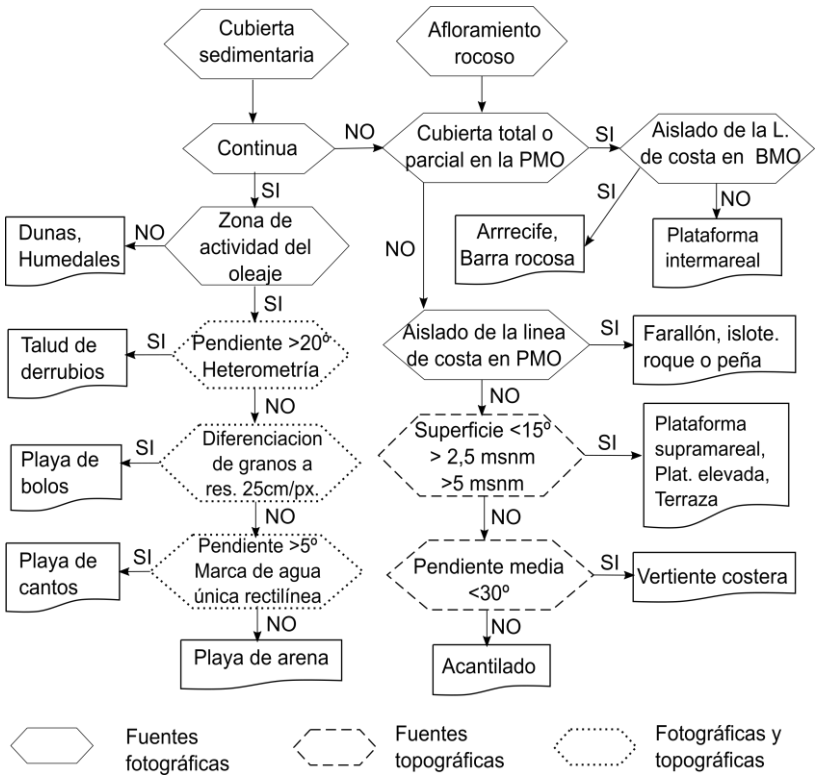

Figura V. Criterios de identificación de geoformas.

Las transformaciones visibles en el intervalo de la serie ortofotográfica moderna (aproximadamente una década) generó incertidumbre temporal en la clasificación de algunas formas sedimentarias, sobre todo en playa arenosas y medios lagunares. La solución adoptada fue capturar e integrar tal variabilidad, registrando su presencia cuando dicha clase apareciese con claridad en alguno de los fotogramas de la serie.

El criterio de delimitación espacial de las geoformas difiere según el tipo geomorfológico. En acantilados, el límite superior se fijó en la ruptura de la pendiente. En plataformas, en la base del acantilado o playa, si los hubiese, en el límite típicamente oscurecido de las algas cianofíceas del intermareal superior (Ramírez et al., 2008), o en la presencia de micromorfologías de erosión marina. Los umbrales de 2,5 y 5 msnm para delimitar diferentes niveles de plataformas, se establecieron según los parámetros medios de oleaje y mareas. Los sistemas sedimentarios eólicos (dunas y mantos eólicos) fueron fácilmente delimitables debido a su composición en

arenas claras carbonatadas, de origen biológico, que contrastan notablemente con los substratos predominantemente basálticos de colores oscuros (Hernández-Cordero et al., 2019). En la delimitación de algunos humedales, se empleó como indicador la presencia de saladares y comunidades de aguas salobres (del Arco et al., 2006).

Cartografía analítica y estructura de datos

Las clases taxonómicas se registraron sobre la línea de costa, en forma de presencia [1] o ausencia [0]. Esto significa que la cartografía de este estudio tiene una estructura vectorial lineal. La línea de costa empleada es la cota 0 del mapa topográfico 1:5.000/1:20.000, para las islas Canarias, y 1:10.000 para las islas de Cabo Verde. El resultado cartográfico es una línea de costa de escala invariante dividida en N segmentos (por ejemplo, 12.817 en Fuerteventura), donde cada segmento representa un tramo de costa definido por una combinación de geoformas distinta a la de los segmentos contiguos. A este método se le ha llamado *Coastline Data-Storing* (CDS) (Ferrer-Valero et al., 2017; Ferrer-Valero, 2018; Ferrer-Valero et al., 2018). Al margen de su mayor sencillez, que permite ahorrar trabajo, la justificación del procedimiento viene dada por dos motivos:

>*El concepto de abundancia*. Surge cuando se requiere conocer no solo la presencia de las clases taxonómicas si no también responder a la pregunta de cuánto existe de cada una. El campo de la biodiversidad cuenta generalmente con la referencia del *individuo* a la hora de establecerlo. En geodiversidad, sin embargo, se trabaja sobre un *continuum*, lo que implica emplear una aproximación espacial. Utilizando la lógica euclidiana, ésta puede ser volumétrica, superficial o lineal. Cuál sea la más adecuada depende de su capacidad para representar la idea y normalizar los valores poblacionales. Respecto a lo primero, debe ser significativa para todo el conjunto taxonómico, representando la "cantidad" en todas las clases. La volumetría y la superficie, si es planimétrica, queda descartada pues no lo cumplen, por ejemplo, en acantilados (no tienen representación volumétrica y pueden no tenerla tampoco planimétrica). Respecto a lo segundo, el hecho de que el desarrollo espacial sea intrínsecamente distinto entre geoformas (por ejemplo entre relieves residuales y campos de dunas) induce un posible sesgo que se acentúa en los cálculos superficiales. Pero la aproximación lineal tiene capacidad normalizadora: dos geoformas son igualmente abundantes cuando ocupan la misma longitud de costa, expresable a su vez en términos relativos como proporción del perímetro. La representatividad y adecuación del método CDS como *proxi de abundancia* queda reflejada en la frecuencia con que se caracterizan las costas

a través de proporciones en ellas de diferentes sistemas (ver, por ejemplo, estadísticas del ISTAC-Gobierno de Canarias).

>*La posibilidad combinatoria*. La proyección de las geoformas y su representación en la línea de costa permite conocer, para cada tramo, las geoformas presentes. Esto abre una posibilidad analítica adicional basada en las estimaciones de riqueza, equidad, disimilitud, abundancia, etc., sobre combinaciones o *coastal morphoassemblages,* a lo que se ha llamado método de cálculo combinatorio (Ferrer-Valero et al., 2018). El número máximo de combinaciones posibles es k^s, donde *k* el rango de sucesos posibles (en este caso=2, presencia o ausencia), y *s* el número de clases combinables en determinado orden taxonómico. Esto da lugar a un número excepcional de combinaciones distintas o *morphoassemblages* (por ejemplo, 918 en Fuerteventura en el tercer orden taxonómico), y se convierten en una medida directa de la diversidad geomorfológica y de la complejidad estructural de las costas.

La estructura cartográfica contiene una base de datos con una nomenclatura específica. Los códigos son cadenas compuestas de siglas, referentes a la clase tipológica en el orden dado. Los subíndices numéricos son la indicación del intervalo de dimensión al que pertenece la geoforma dentro de cada serie paramétrica. Por ejemplo:

"$Ac_3Pl_1Pt_2$", significa un tramo costero con "acantilado bajo (Ac_3), playa larga (Pl_1) y plataforma de anchura media (Pt_2)". Los valores numéricos no son intervalos arbitrarios si no cortes sobre las series de mediciones. El método de cuartiles maximiza la diversidad intramuestral (alfa) y minimiza la intermuestral (beta), mientras que los cortes naturales (Jenks, 1967) maximizan la intermuestral (alfa) y minimizan la intramuestral (beta). Los intervalos geométricos se sitúan en un término medio. En los artículos se pueden ver los datos precisos y el ensayo de diferentes métodos.

Estimaciones e incertidumbres

Métricas

El primer dato derivado es la frecuencia absoluta (km de costa) y relativa (*p*) de las geoformas a lo largo de la línea de costa. Del valor *p* derivan el resto de métricas. Varía entre 0, cuando la clase no se identifica en ningún punto de la línea de costa, y 1, cuando se observa a lo largo de toda ella. Entonces $\sum p = S$, siendo S el número de clases de un orden taxonómico. Siendo L la longitud de costa total, $\sum p/L$, es una medida de densidad media global geomorfológica, o número de

clases que, por término medio, se encuentran en un punto de la costa. A partir del valor de *q* se analiza y compara la "composición geomorfológica" (*geomorphic composition*) de las costas. Esta comparación se realizó a través del contraste estadístico entre patrones secuenciales observados y posibles (Ferrer-Valero et al., 2018), de la aplicación cruzada del índice de similitud beta de Sorensen y Whittaker (ver cuarto artículo, no publicado).

Las estimaciones de diversidad geomorfológica se hicieron a través de índices de diversidad alfa o cálculos no paramétricos (Magurran, 1988). La diversidad beta a lo largo de los gradientes cronológicos se estimó como tasa de variación de los valores alfa, del tipo $(t_1 - t_0)/t_0$, donde t_0 es el valor inicial o de referencia, histórico (Ferrer-Valero et al., 2017) o inferido (Ferrer-Valero, 2018; Ferrer-Valero et al., 2018), y t_1, el "momento" posterior. Con este mismo propósito, también se exploraron los índices beta de Sorensen y Whittaker (cuarto artículo, no publicado). La riqueza geomorfológica (*geomorphic richness*) se estimó mediante riqueza absoluta o normalizada, en relación al total posible de clases o a la unidad espacial (índice de Margalef y Menhinick). La equiabundancia, mediante índices de entropía de Shannon-Wiener y Gini-Simpson, y la disimilitud o distancia taxonómica, a través del índice de Rao y estimaciones locales. Las formulaciones de estos índices se encuentran detalladas en los artículos.

El número de métricas incorporadas fue creciendo con el progreso de la investigación:

>En el primer artículo (Ferrer-Valero et al., 2017), se estimaron variaciones en la composición geomorfológica en términos absolutos y de diversidad alfa.

>En el segundo (Ferrer-Valero, 2018), se compararon diversidades alfa en riqueza, equiabundancia y disimilitud taxonómica.

>En el tercero (Ferrer-Valero et al., 2018), se compararon composiciones, abundancias/densidades y diversidades alfa en riqueza y equiabundancia, en metodología combinatoria y no combinatoria.

>En el cuarto (no publicado), se compararon composiciones (similitud *beta*), abundancias/densidades, diversidades alfa en riqueza y equiabundancia, y se analizó el fenómeno de "anidamiento" (*nestedness*).

Distorsión fractal

La estimación de la abundancia mediante aproximación espacial, plantea el serio problema de la geometría fractal (Mandelbrot, 1982), hecho ignorado completamente en los trabajos de geodiversidad. La geometría fractal penetra y ocupa los espacios discretos del sistema euclidiano introduciendo la incertidumbre sobre la consistencia escalar de las medidas en líneas y superficies. La línea de costa es un ejemplo de forma fractal, como se sabe desde el trabajo

fundamental de Mandelbrot (1967). La longitud varía según la escala, en una relación potencial. En la práctica del método CDS esto quiere decir que ni los valores absolutos de abundancia ni los relativos (*p*) son escalarmente invariantes. En el segundo artículo (Ferrer-Valero, 2018) se trata este problema diseñando un test de "estrés fractal" para conocer el rango escalar de variación de los valores y su repercusión sobre el error de los índices.

Rarefacción

El tamaño de muestra introduce una incertidumbre de comparación que en ecología se ha llamado rarefacción (Magurran, 2004). Este es un problema presente en esta investigación, por cuanto los perímetros costeros que se comparan no tienen la misma longitud (dos islas nunca la tendrán) y el tamaño de la isla podría, teóricamente, afectar a la riqueza de clases, como se ha demostrado en la diversidad de suelos (Ibáñez y Effland, 2011). En el segundo artículo (Ferrer-Valero, 2018) se trata este problema diseñando una ventana móvil para homogeneizar el tamaño de muestra entre islas y comprobar el impacto en la variabilidad de los índices y en la validez de las comparaciones iniciales.

Aleatoriedad secuencial

Partiendo de que el número posible de configuraciones de la variable *p* en una secuencia de islas temporalmente ordenada, es *n*!, siendo *n* el número de islas, la probabilidad de ocurrencia de cada una de las configuraciones secuenciales, si la variable es aleatoria, es $n/n!$, y $\sum n/n!$=1. En este sentido, se plantea el problema de saber si el conjunto de secuencias de *p* obtenidas empíricamente, así como los valores resultantes de los índices, siguen un patrón determinado, alejándose de la probabilidad aleatoria, o si realmente son aleatorios. Este problema se trata en el tercer artículo (Ferrer-Valero et al., 2018).

Muestreo mínimo

El estudio completo de una costa requiere, cuando tiene una longitud de decenas a cientos de kilómetros, un trabajo laborioso que se puede reducir significativamente mediante el uso de puntos de muestreo. Para conocer el tamaño muestral que permite conocer la diversidad y otros parámetros con un error aceptable, mediante un mínimo número de puntos, se diseñaron curvas de rarefacción (*rarefaction curves*) a partir de remuestreos (*bootstrapping*) sobre islas de estructura geomorfológica conocida (ver cuarto artículo, no publicado).

Artículos

En el siguiente cuadro se resumen las características de los cuatro artículos que se presentan a continuación:

	Primer artículo*	Segundo artículo**	Tercer artículo***	Cuarto artículo****
Publicación	Marzo 2017	Junio 2018	Septiembre 2018	Sin publicar
Número de islas	1	2	3	4
Km de costa analizados	256	454	840	577
Archipiélago	Canarias	Canarias	Canarias	Cabo Verde
Escala temporal de análisis	Histórica	Geológica	Geológica	Geológica
Levantamiento geomorfológico	9 clases (un nivel jerárquico)	14 clases y 42 subclases (dos niveles jerárquicos)	3 clases, 8 subclases y 64 sub-subclases (tres niveles jerárquicos)	21 clases y 60 subclases (dos niveles jerárquicos)
Alcance del levantamiento	Completo	Completo	Completo	Muestreo
Métricas	Var. absoluta y diversidad: Shannon y PLi	Diversidad α: riqueza, equiabundancia y disimilitud.	Composición, abundancia/densidad, riqueza y equiabundancia, Comb. y No-comb.	Sim. *beta*, abundancia/densidad, diversidad, anidamiento, Comb. y No-comb.
Test adicionales	Sensibilidad y varianza	Estrés fractal Ventana móvil	Aleatoriedad secuencial (χ^2)	Remuestreo "bootstrap"

*Ferrer-Valero, N., Hernández-Calvento, L., & Hernández-Cordero, A. I. (2017). *Human impacts quantification on the coastal landforms of Gran Canaria Island (Canary Islands)*. Geomorphology, 286, 58-67.

**Ferrer-Valero, N. (2018). *Measuring geomorphological diversity on coastal environments: A new approach to geodiversity*. Geomorphology, 318, 217-229.

*** Ferrer-Valero, N., Hernández-Calvento, L., & Hernández-Cordero, A. I. (2018). *Insights of long-term geomorphological evolution of coastal landscapes in hot-spot oceanic islands.* Earth Surface Processes and Landforms.

**** *Cape Verde coastal geomorphic chronosequences.* -No publicado-.

Human impacts quantification on the coastal landforms of Gran Canaria Island (Canary Islands)

Nicolás Ferrer-Valero, Luis Hernández-Calvento, Antonio I. Hernández-Cordero

Geomorphology, 286, 58-67

https://doi.org/10.1016/j.geomorph.2017.02.028

Abstract

The coastal areas of the Canary Islands are particularly sensitive to changes, both from a natural perspective and for their potential socio-economic implications. In this paper, the state of conservation of an insular coast is approached from a geomorphological point of view, considering recent changes induced by urban and tourism development. The analysis is applied to the coast of Gran Canaria, a small Atlantic island of volcanic origin, subject to a high degree of human pressure on its coastal areas, especially in recent decades. Currently, much of the economic activity of Gran Canaria is linked to mass tourism, associated with climatic and geomorphological features of the coast. This work is addressed through detailed mapping of coastal landforms across the island (256 km perimeter), corresponding to the period before the urban and tourism development (late 19th century for the island's capital, mid-20th century for the rest of the island) and today. The comparison between the coastal geomorphology before and after the urban and tourism development was established through four categories of human impacts, related to their conservation state: unaltered, altered, semi-destroyed and extinct. The results indicate that 43% of coastal landforms have been affected by human impacts, while 57% remain unaltered. The most affected are sedimentary landforms, namely coastal dunes, palaeo-dunes, beaches and wetlands. Geodiversity loss was also evaluated by applying two diversity indices. The coastal geodiversity loss by total or partial destruction of landforms is estimated at −15.2%, according to Shannon index (H'), while it increases to −32.1% according to an index proposed in this paper. We conclude that the transformations of the coast of Gran Canaria induced by urban and tourism development have heavily affected the most singular coastal landforms (dunes, palaeo-dunes and wetlands), reducing significantly its geodiversity.

Keywords: Oceanic island, Urban development, Coastal landforms changes, Geodiversity.

1. Introduction

Coastal areas attract the population of the planet, either for their multiple resources or as places of residence. Throughout history human activity affects the natural conditions of the coastal territories (Nordstrom, 1994). This has been more significant in recent decades (Jackson and Nordstrom, 2011), when the phenomenon of "littoralisation" has occurred (Bajocco et al., 2012). Currently between 50% and 70% of the world population is concentrated on the coasts (Mimura et al., 2007) and nearly 30% of coastal areas are altered by activities related to human development (Martínez et al., 2007). This has led to an accelerated degradation of the natural coastal systems, which are close to extinction in some cases (Santana-Cordero et al., 2016).

In this context, efforts have been made to address the changing trends on the coast, both from an institutional perspective (e.g., U.S. Geological Survey, European Commission) and by the scientific community. With regard to the latter, numerous papers study coastal erosion problems, at different scales, in recognized problematic areas in the US and Europe (Terich and Levenseller, 1986; Dolan et al., 1990; Amin and Davidson-Arnott, 1997; Aubié and Tastet, 2000; White and Wang, 2003; Cui and Li, 2011; Hapke et al., 2013; Lira et al., 2016) and in other parts of the world, mainly focusing on the analysis of the relationship between observed rates of change and human activities, especially changes in coverage and land-use on sedimentary coasts (Smith and Abdel-Kader, 1988; Narayana and Priju, 2006; El Banna and Frihy, 2009).

Sedimentary shores have been more widely studied in the global context (Naylor et al., 2010). Very few studies have analyzed the conflicts between the human occupation and the rocky shore dynamics, although these environments represent 80% of the world coasts (Emery and Kuhn, 1982). Notable examples of this have been developed on the coast of Algarve, south Portugal, where there are serious problems related to the urban and tourism development along the coastal stretches characterized by high sea-cliff recession rates (Alveirinho Dias and Neal, 1992; Teixeira, 2006; Nunes et al., 2009).

Tourism development plays an important role in the changes in coastal morphology of many parts of the world. The impacts of this activity can caused by the occupation of the coast by infrastructures, the development of recreational activities and the implementation of an inadequate management (Nordstrom, 1994, 2000; Tzatzanis et al., 2003; Grunewald, 2006). In this context, the islands, especially small islands under great tourist pressure, are even more vulnerable territories, due to their limited and scarce resources (Hay, 2013) and strong dependency on goods and services provided by marine and coastal systems (Mimura et al., 2007). The concentration of infrastructures and activities in these fragile environments generates overexploitation of resources and jeopardizes the natural values that these activities are based on, producing serious conflicts (García-Romero et al., 2016).

The effects of changes in island coasts have been addressed through some qualitative and mapping approaches. A study about the Canary Islands by Morales Matos and Santana Santana (1993) and Pérez-Chacón et al. (2007) suggest human coastal development, especially tourism, has produced geomorphological and functional changes in certain ecosystems; García-Romero et al. (2016) relate the rates of changes in aeolian sedimentary systems to urban-tourism development. Other authors relate the development of this activity to direct or indirect changes in aeolian sedimentary landforms, such as the alteration of the wind or the vegetation (Hernández-Cordero et al., 2012; Hernández-Calvento et al., 2014). However, there are few studies that analyze the impacts of human activity on coastal geodiversity (Ruban, 2010), and none of them have been applied to island shores.

This paper aims to develop a methodology to measure the influence of the historical urban and tourism development on the geomorphological transformations on the coast, studying the intensity of human impacts on its natural morphology and geodiversity. The whole coast of Gran

Canaria (256 km) is studied as a pilot area. The proposed methodology is applied as a test, to be later implemented in other areas with similar characteristics.

2. Regional setting

Gran Canaria is an Atlantic volcanic island, which has a roughly circular shape with 50 km of average diameter, located 200 km off north-west Africa (Fig. 1). It has an area of 1560.10 km^2 and a coastline of 256 km (ISTAC, 2009).

It is part of the Canary Islands (Spain), whose origin corresponds to a typical intraplate hot spot archipelago (Carracedo et al., 1998). The displacement of the African plate over the hot spot determines that the geological age increases towards the easternmost islands, whose development phase is called post-erosional volcanism. In this scheme, Gran Canaria (14.5 million years) is the third oldest island of the archipelago (Carracedo et al., 1998).

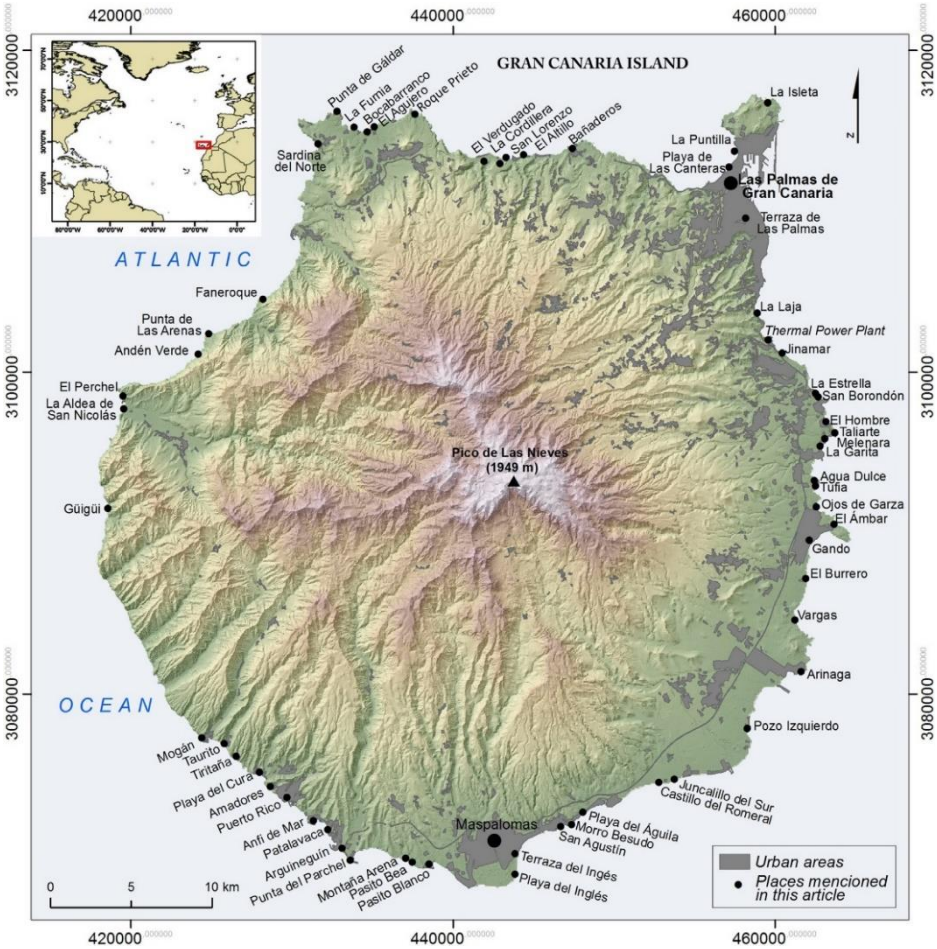

Fig. 1. Study area.

The geological diversity of Gran Canaria, well represented on the coast, is one of the highest in the archipelago (Araña and Carracedo, 1980). The island consists mainly of basic rocks (basalts, basanites), and to a lesser extent, by salic emissions (phonolites, trachytes, rhyolites), extruded in various eruptive processes (flows, pyroclasts, tuffs, ignimbrites). The island formed a single huge stratovolcano, which has intensively been eroded since Mio-Pliocene times. As a result, currently it reaches a maximum altitude of 1949 m above sea level at its center (Pico de las Nieves) and it has

an abrupt relief in which the erosive landforms, such as deeply incised ravines and eroded massifs, predominate in the inland, and rocky shores, such as marine cliffs and shore platforms, predominate along the coast.

Gran Canaria has experienced an intense population and urban growth, particularly throughout the last decades, related to changes in the economic base of the island. Before the 1960s, the economy was organized around the agricultural sector and the population mostly distributed in the interior. Since the 1960s, the economy gave way to a model based on the service sector, mainly tourism, construction and trade. The transformations of the second half of the 20th century triggered an urban growth process mainly in the northern, southern and eastern coasts, leading to the expansion of residential, industrial, commercial, transport fabrics and, above all, tourism infrastructures along the coasts. Previously, during the first half of the 20th century, the urban expansion of the island's capital (Las Palmas de Gran Canaria) was already taking place along the Guanarteme isthmus, in the north-east coast, driven by the implementation and development of the seaport.

Nowadays, the population, urbanization and infrastructures are heavily concentrated on the coast of the island, particularly in the north-east, east and south (Fig. 1). Gran Canaria has currently 829,597 inhabitants and high population density (532 inhabitants/km^2) (ISTAC, 2009). This combined with the large number of tourists visiting the island, 1,681,743 in 2008 (ISTAC, 2009), have recently led to the occupation and degradation of a significant part of the coastal areas (Morales Matos and Santana Santana, 1993).

3. Material and methods

3.1. Sources

The geomorphological mapping is based on the integration of photographic and topographic sources in a Geographic Information System (GIS) and field work. In areas affected by urbanization processes, we proceeded to georeference historical sources in order to reconstruct the situation before the urban and tourism development. For the island's capital, Las Palmas de Gran Canaria (5% of the island perimeter), cartography from late 19th century, before the beginning of its expansion to the north, was used. For the rest of the island (95% of the perimeter) we used aerial photographs from the 1960s of the last century, before the widespread urban and tourism development. For undisturbed areas, the geomorphological interpretation was based on a modern series (2002–2015) of 10 digital orthophotos from the Spatial Data Infrastructure (SDI) of the Canary Islands (IDECanarias, GRAFCAN, S.A., Government of the Canary Islands).

In addition to photographic sources, the geomorphological recognition was also based on the use of Topographic Maps at 1:1000 and 1:5000 scales (GRAFCAN, SA, Canary Islands Government) and LiDAR clouds points from 2009, with a density of 0.5 points/m^2 (National Geographic Institute).

3.2. Coastal geomorphic classification and mapping

The quantification of the urban and tourism impacts on the coasts of Gran Canaria was made comparing the geomorphological map before the urban and tourism development and the currently observed state of the coast.

The classification system used for the geomorphological mapping was based on the individual identification of the main landforms that comprise the shoreline (McGill, 1958; Alexander, 1966; Finkl, 2004; Biolchi et al., 2016), considering only simple first-order landforms, i.e., those that who cannot be grouped into larger landforms, from the Maximum Low Tide Observed (MLTO). Then,

9 first-order landforms, which, in our criterion, represent the entire spectrum of mesoscale coastal geodiversity in Gran Canaria, were selected (summarized in the Table 1). Note that "geodiversity" is a conceptually broader term, but in this paper it is used as a synonym for "geomorphological diversity".

The cartographic method consisted in transposing the identified landforms into the historical reconstructed coastal perimeter by shore-normal projection. Projecting a set of multiple superficial landforms (dunes, beaches, platforms, etc.) on the coastline, allowed us, for analytical purposes, to simplify and integrate a heterogeneous spatial data set in a simple and shared longitudinal dimension. The reconstruction of coastline in disturbed areas was made by the water mark from the historical sources already detailed; in unoccupied areas, the zero level in the Topographic Map 1:5000 (GRAFCAN, S.A., Government of the Canary Islands) was used as a land perimeter.

Table 1. Coastal landforms included in the geomorphological mapping of Gran Canaria's coasts, indicating the conceptual delineation used in the photo interpretation process and topographic analysis.

Landform	*Ad hoc* conceptual delineation
1. Coastal cliffs (Cl)	Modern plunging cliffs and backshore rocky escarps and bluffs, higher than 3m, whose base is in the field of action of waves.
2.Shore platforms (Pt)	Intertidal subhorizontal and slightly seaward sloping rocky surfaces, backed or not by coastal cliffs, subject to marine wetting and drying cycles.
3.Pebble-boulder beaches (Bb)	Modern wave-built accumulations of pebble to boulder dominant grain size, usually forming supratidal ridges.
4.Sandy beaches (Sb)	Modern wave-built foreshore accumulations of sand dominant grain size, usually composed of both emerged and submerged bodies.
5.Coastal dunes (Dn)	Mobile, semi-mobile or stabilized aeolian sands, forming modern backshore dune fields and sand plains.
6.Coastal wetlands (Wl)	Natural depressionary backshore surfaces, where permanent or temporary accumulation of salt water occurs, covering coastal lagoons and salt marshes.
7.Nearshore landforms (Nl)	Isolated and active rocky remnants in the nearshore zone, higher than 5 m above mean sea level (sea stacks) or developed below the mean sea level which can emerge at low tides (rocky reefs).
8.Coastal palaeo-cliffs (Pcl)	Backshore relict slopes originally eroded by the sea, abandoned permanently by marine activity due to external causes: isostatic and eustatic movements and coastal progradation processes.
9.Coastal palaeo-dunes (Pdn)	Backshore extensions of consolidate aeolian sands (eolianites), forming ancient dunes or aeolian mantles, elongated in the direction of the prevailing winds (NNE).

The obtained coastal perimeter of the period before the urban and tourism development was replicated in the GIS for each landform considered (Table 1). Subsequent analysis consisted of identifying the presence or absence of each coastal landform in each section or point of the coastline, without establishing a minimum landform size for mapping. Thus, the resulting nine polylines were divided into *n* segments, which received the code 1 or 0 in the GIS database according to the presence or absence of the landform.

3.3. Data analysis

The current conservation state of the coastal geomorphic features prior to the urban and tourism development of the island is established through four categories of conservation, which are related to the geomorphological transformations observed (Table 2).

The four classes form an impact intensity scale divided in two groups (Table 2). On the one hand, the category "unaltered" corresponds to intact landforms or with minor geomorphological modifications. On the other hand, the category "extinct" corresponds to landforms where the impacts are maximum, causing their total destruction. In intermediate situations we have defined the "altered" and "semi-destroyed" categories. In order to quantify damages to landforms and their impact on coastal geodiversity, the categories "unaltered" and "altered" form the set of "preserved" landforms, while categories "semi-destroyed" and "extinct" have been grouped in "unpreserved" landforms (Table 2).

The changes observed have been analyzed for each of the nine landforms to obtain a comprehensive dataset of the state of coastal conservation from a geomorphological point of view. First, the absolute values were calculated. Diversity indices have then been applied to complete the quantitative data. In order to compare the obtained values in the two periods addressed (before and after urban-tourism development), a common loss-rate formula was applied both to absolute and geodiversity values (Table 3).

Table 2. Categories used in the analysis of human impacts on the coastal landforms of Gran Canaria.

Categories		Definition
Preserved	Unaltered	Unchanged landforms or landforms with no significant modification on their morphological conditions. They are usually found in coastal areas with little or no human occupation, where the low intensity of human activity has allowed the survival of landforms without modifications.
	Altered	Landforms that have experienced remarkable morphological and dynamic disturbances, with visibly modified, often deteriorated, natural conditions. Their original surface has been largely preserved. Usually found in areas with moderate to high levels of human occupation.
Unpreserved	Semi-destroyed	Landforms partially missing due to the elimination of a significant portion of their original area. In some cases they are undergoing severe degradation and are in risk of extinction if human activities responsible for their deterioration persist.
	Extinct	Complete destruction of landforms, which has led to their extinction and generally substitution by artificial elements.

Diversity indices complement the absolute values because they consider the type of classes affected and their impact on the statistical population structure. For comparison purposes, two indices were used. The first is the Shannon index (H'), widely distributed in biodiversity studies (Spellerberg and Fedor, 2003) and recently also applied to geodiversity (Benito-Calvo et al., 2009). It is an alpha index that measures the proportional abundance of all species of a given population sample, expressing the degree of equity or uniformity in the statistical distribution. The formulation of the Shannon index is widely known (Table 3). The second is the Proportional Losses index (PLi), a simple formulation proposed in this paper to calculate the diversity loss, which incorporates the scarcity of the landforms and their proportional losses as a core element. In this approach, the landform classes acquire the initial value=1, that represents a normalized theoretical abundance. Consequently, the total value at the initial time of analysis (PLi_{t-1}) is the total number of landform classes considered (N) (Table 3). The total value at the later time of analysis (PLi_1) is obtained through the sum of the coefficients between the real abundance at the later time (PLi_{t-1}) and the initial time (PLi_t).

Table 3. Calculation methods in the analysis of human impacts on the coastal landforms of Gran Canaria.

Values	Formulation	Loss Rate
Absolutes (T)	$T = \sum_{i=1}^{n}(n_i)$	$\Delta T = (T_t - T_{t-1})/T_{t-1}$
Shannon Index (H')	$H' = -\sum_{i=1}^{n}(p_i \ln p_i)$	$\Delta H' = (H'_t - H'_{t-1})/H'_{t-1}$
Proportional Losses index (PLi)	$PLi_{t-1} = N$ $PLi_t = \sum_{i=1}^{n}(n_{i\,t})/(n_{i\,t-1})$	$\Delta PLi = (PLi_t - PLi_{t-1})/PLi_{t-1}$

Parameters: ΔT, loss rate by absolute values (T); n_i, abundance of each landform class (in km of coastline); ΔH', loss rate by Shannon index values (H'); p_i, probability of occurrence of each landform class (km of coastline/total perimeter); ΔPLi, loss rate by Proportional Losses index values (PLi); N, total number of landform classes; $_{t-1}$, initial time of analysis (before urban and tourism development); $_t$, later time of analysis (after urban and tourism development).

4. Results

Coastal landforms are unequally represented on the island of Gran Canaria (Fig. 2). Before the urban and tourism development, coastal cliffs and shore platforms were dominant (69.4% and 61.8% of coastal perimeter, respectively). Pebble-boulder beaches, palaeo-cliffs and sandy beaches had an intermediate abundance (33.5%, 15.8% and 13.2% of coastal perimeter, respectively); and the less abundant or singular landforms were coastal palaeo-dunes, coastal dune systems, wetlands and nearshore landforms (7%, 5.7%, 4.8% and 3.2% of coastal perimeter, respectively).

This study has been able to estimate the global transformations in the coast of Gran Canaria due to the urban and tourism development (Fig. 3). 570 stretches of the coastline, affected to a greater or lesser extent by human interventions linked to these processes, have been detected. Results show that 14% of coastal landforms are totally or partly devastated (not preserved); 29% are affected in varying degrees of intensity, although they still remain reasonably preserved; and 57% remain unaltered, i.e., conserve their natural morphology.

Overall, it seems clear that the most affected coastal landforms are of sedimentary types (dunes, palaeo-dunes and beaches) and coastal wetlands, also characteristic of low and sedimentary coasts (Fig. 3).

The most notable impacts on the coast of Gran Canaria have occurred on dune systems (Fig. 3). 65% of their extension has currently disappeared, being the best example the growth of the island's capital, Las Palmas de Gran Canaria (Santana-Cordero et al., 2014) (Fig. 4). However, dunes have also disappeared from other coastal areas in the north, east and south of the island (e.g., San Agustín, El Hombre, San Borondón, Jinámar, Bañaderos). Of the remaining dune fields, 32% are partially destroyed and subject to processes of significant deterioration, such as Maspalomas, one of the largest transgressive dune fields of the Canary Islands (Alonso et al., 2011; García-Romero et al., 2016). Only 2.6% of the dune systems of the island can now be considered in optimal conditions. This is the case of small formations in areas of low human pressure (e.g., dune of Güigüi, on the southwest coast).

The palaeo-dune systems had a significant presence on the island. 32% have disappeared due to the occupation by infrastructures and urbanizations (e.g., Gando, Arinaga); 27% are semi-destroyed by extraction of aggregates and the occupation of lands by various infrastructures (e.g., Tufia) (Fig. 4); and 34% are altered, subjected to anthropic deterioration for long periods (e.g., large areas of Arinaga). Only 6% of relict dune systems and aeolian sedimentary palaeo-systems can be considered unchanged or relatively intact (e.g., Punta de las Arenas, on the west coast).

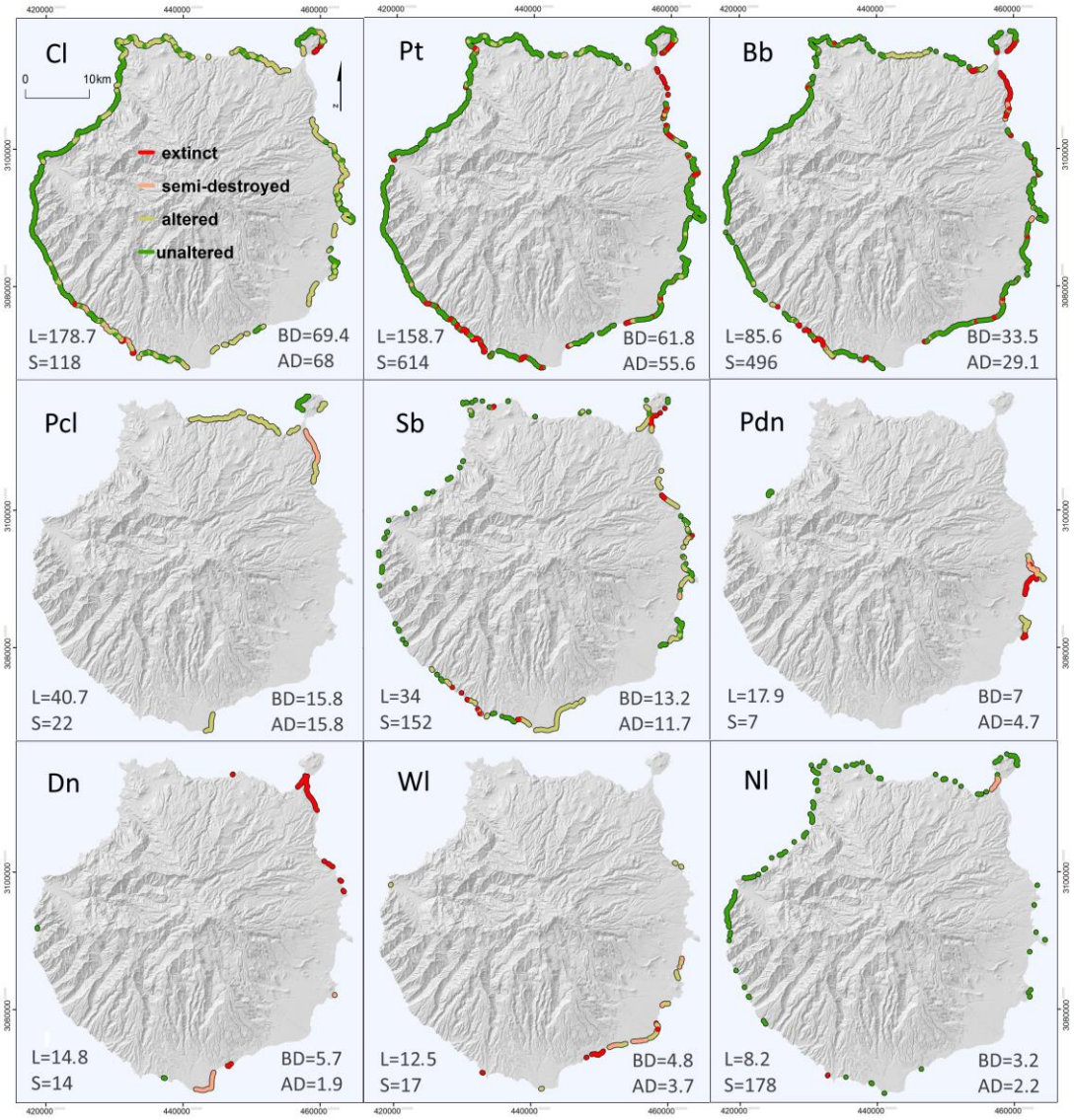

Fig. 2. Distribution of the coastal landforms around the island, indicating their conservation state (colored maps); total length in km (L); number of stretches identified (S); and percentage of coastal perimeter before development (BD) and after development (AD), taking into account just the extinct elements. The sum of percentages exceeds 100% because the landforms overlap along the coast. Cl, coastal cliffs; Pt, shore platforms; BB, pebble-boulder beaches; Pcl, coastal palaeo-cliffs; Sb, sandy beaches; Pdn, coastal palaeo-dune fields; Dn, coastal dune fields; Wl, coastal wetlands; Nl, nearshore landforms.

Some 22% of coastal wetlands have disappeared (Fig. 3), mainly due to the urban occupation and the transformation of the mouth of the ravines (e.g., Playa del Águila and Arguineguín, on the south coast); 27% are partially destroyed or seriously damaged by land use changes, mainly in fan-delta sedimentary plains at the southeast (e.g., Castillo del Romeral, El Burrero). The remaining 52% of coastal wetlands are preserved but altered in varying degrees by channeling, reshaping, degradation, etc. (e.g., Charca de Maspalomas, Juncalillo del Sur, Vargas, La Aldea) (Fig. 4).

The beaches have experienced different impacts according to their grain size characteristics (Fig. 3). The pebble-boulder beaches have been destroyed significantly more than the sandy beaches: 13% and 11%, respectively. In addition, 2% of the pebble-boulder beaches have been partially destroyed, compared to 0.6% of sandy beaches. The pebble-boulder beaches were 38% more abundant than sandy beaches and the difference is even greater in absolute terms. The

most significant contrast, however, lies in the proportion of intact and altered systems. 15% of pebble-boulder beaches are altered and 70% are unchanged, conversely to what happens on the sandy beaches, altered by 68% and 19% unchanged.

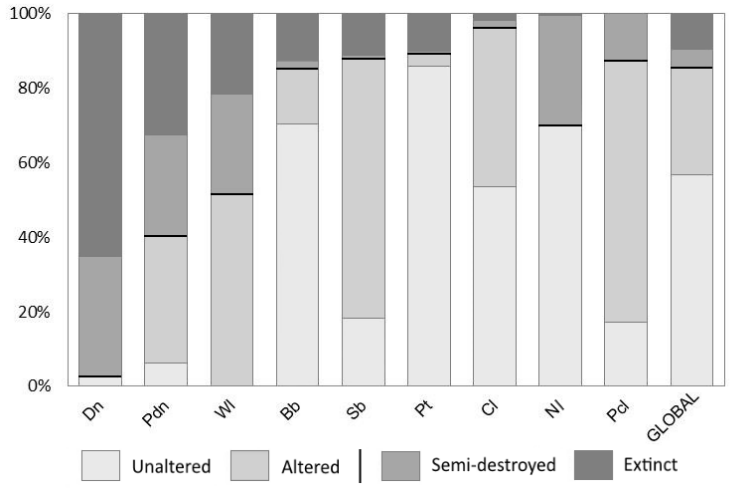

Fig. 3. Human impacts quantification on the coastal geomorphology of Gran Canaria. Dn, coastal dune fields; Pdn, coastal palaeo-dune fields; Wl, coastal wetlands; Bb, pebble-boulder beaches; Sb, sandy beaches; Pt, shore platforms; Cl, coastal cliffs; Nl, nearshore landforms; Pcl, coastal palaeo-cliffs.

The extinction of beaches is mainly concentrated in the northeast and southwest of the island, and it is determined by the development of major infrastructures and urbanizations (e.g., Port of Las Palmas de Gran Canaria, Thermal Power Plant, Taliarte, La Estrella, Pasito Blanco urbanization, Puerto Rico, Amadores, Anfi del Mar, Patalavaca) (Fig. 4). On the other hand, the alteration of beaches, which affects sandy beaches mostly, has resulted in visible coastline retreats (e.g., Maspalomas; Pérez-Chacón et al., 2007), granulometric changes due to alterations in sedimentary balance (e.g., Jinámar), backshore urbanization and reshapings (e.g., Playa de Las Canteras, San Agustín, Bocabarranco, La Garita, Melenara, Ojos de Garza), or the implementation of breakwaters (e.g., Playa del Inglés, Las Burras) and artificial reefs (e.g., La Laja) (Fig. 4), which have modified the sediment transport. The sandy undisturbed beaches are concentrated in coastal areas with low human activity in the west (e.g., Güigüi, Faneroque, El Perchel) (Fig. 4), the south (Pasito Bea, Tiritaña, Montaña Arena) and the east (e.g., San Borondón, Agua Dulce, El Ámbar).

The rocky landforms (coastal cliffs and palaeo-cliffs, shore platforms and nearshore landforms) have been generally less affected (Fig. 3). In particular, shore platforms and coastal cliffs are the most abundant and best preserved landforms of the coast.

Shore platforms have experienced total losses of 10% (Fig. 3), mainly because of coastal infrastructures and urbanizations of the southwest and northeast coasts, as already mentioned. The alteration concerns 3.5% of shore platforms, related to the occupation of the inner edge (e.g., El Altillo, La Puntilla) or to the construction of closing walls in salt-water pools in the north of the island (e.g., San Lorenzo, La Furnia, El Agujero, Punta de Gáldar, Roque Prieto) (Fig. 4).

Just 2% of the coastal cliffs are lost and they correspond with areas where opencast mining has been practiced (Mogán, La Isleta) (Fig. 4) or with large clearances intended to occupy the coastal slopes (e.g., Playa del Cura, Taurito). However, 43% are altered, either by the occupation of the lower-slope (e.g., Arguineguín-Patalavaca section), upper-slope (Morro Besudo, Pozo Izquierdo, Punta del Parchel) and mid-slope areas (e.g., Puerto Rico-Amadores section), or by actions for containment and stabilization of escarpments (e.g., Sardina del Norte, Puerto de La Aldea, Andén Verde, Playa del Inglés).

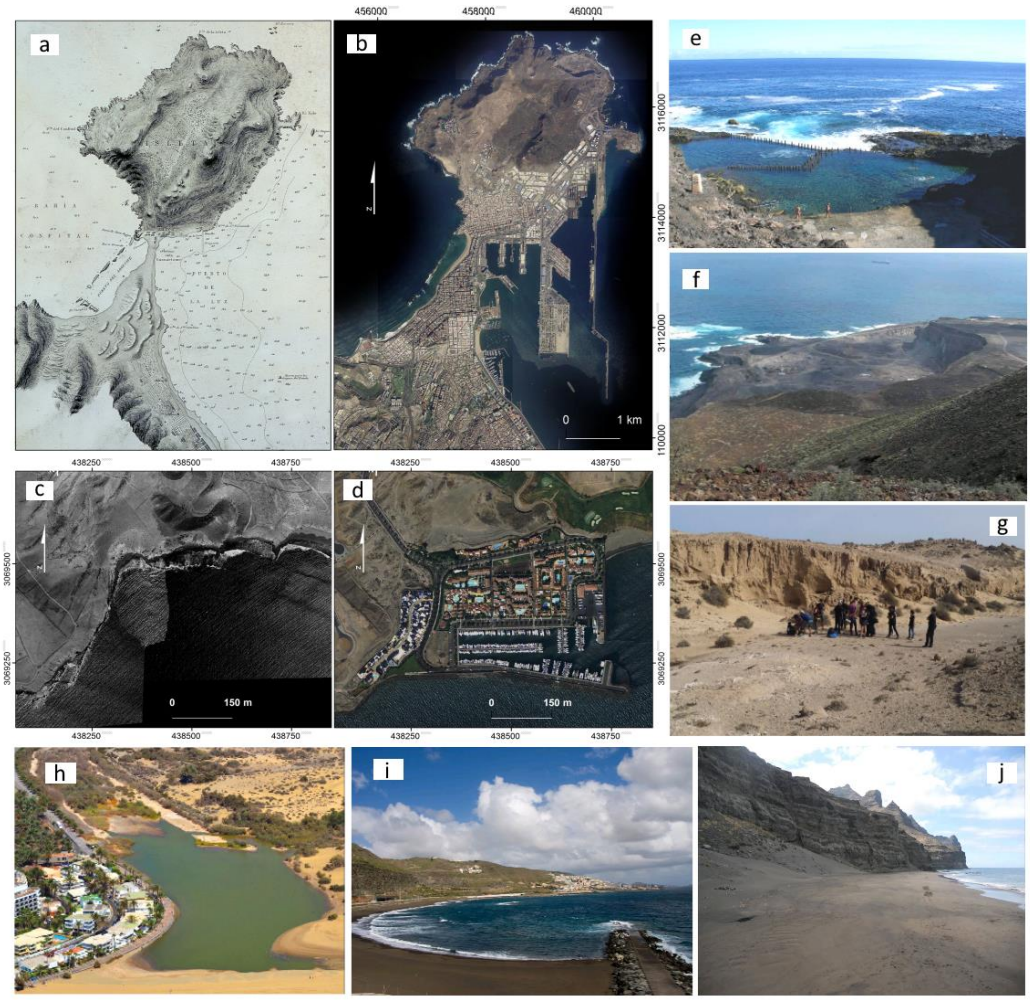

Fig. 4. Some examples of impacts from the urban and tourism development along the coastline of Gran Canaria. a) The *Guanarteme* Isthmus in 1879 according to the *Dirección Hidrográfica*, where a large dune field, rocky reefs, beaches and palaeo-cliffs are identifiable. b) current expansion of *Las Palmas de Gran Canaria* and adjacent seaport in orthophoto (2008), which have let to the total extinction of the dune field and eastern sandy beaches, and the partial destruction of the calcarenitic reef in *Las Canteras* and palaeo-cliffs along the *Terraza de Las Palmas*. c) *Pasito Blanco* bay in orthophoto 1961, where various beaches, cliffs and shore platforms, are observed. d) Urbanization of *Pasito Blanco* in orthophoto (2008), causing the total destruction of beaches and shore platforms, and the drastic alteration of coastal cliff dynamics. e) Shore platform altered by flooding processes due to 0.5 m-high wall on its outer edge that retains the water from tides and overtopping waves (natural pool of *Roque Prieto*) (Photo source: *www.panoramio.com*. Author: *Toni Teror*). f) Extinction of an active-cliff facing along 1km of the coast after half-a-century of mining activities on the basaltic lavas of *La Isleta*, aimed at satisfying constructing demand in nearby city of *Las Palmas de Gran Canaria* (Photo source: *www.conocelaisleta.wordpress.com*). g) Semi-destruction of the palaeo-dune field of *Tufia* due to the persistent extraction of aggregates since the 60s. The group of people are on the lower limit of the exploited aeolian sands that outcrops in the wall behind them (Photo source: *www.teldeactualidad.com*). h) *Charca de Maspalomas*, a costal lagoon severely altered by channeling, reshaping and degradation in the past decades. On its western margin, a 5-star hotel invading part of its natural channel. On the other one, the terminal area of the Maspalomas dune field, affected heavily by sedimentary deficit and rapid plant colonization (Photo source: *www.fotosaereasdecanarias.com*). i) The altered sandy beach of *Playa de la Laja* where a southern breakwater and an artificial reef in the middle have generated additional accumulation of black sands. Note also the road occupying the cliff-beach junction (Photo source: *www.playasdegrancanaria.net*). j) Unaltered coast of *Güigüi*, where a golden sandy beach, cliff-front dune and high coastal cliffs can be observed (Photo source: www.panoramio.com. Author: Almeida Santana).

Some 13% of the palaeo-cliffs have been partially destroyed by excavations (e.g., eastern side of the Terraza de Las Palmas) and altered by 70% due to terraced fields, road infrastructures and urbanization in the upper, mid and lower-slope areas (e.g., Terraza del Inglés, El Verdugado, La Cordillera).

Finally, the nearshore landforms (sea stacks and rocky reefs) have experienced a partial destruction by 29%, which corresponds exclusively with a calcarenitic reef (Pérez-Torrado and Mangas, 1994), located in front of the Playa de Las Canteras, approximately 1.5 km long, where it is estimated that 15,000 m^3 of stone could have been extracted from in recent decades for construction.

To complete the analysis, the absolute results are compared to values resulting from diversity indices, in order to quantify the impacts of the urban and tourism development on the total coastal geodiversity of the island (Table 4). The absolute variation expresses the landform losses in terms of the total amount or length of coastline, regardless of the type considered, while the diversity indices also allow us to analyze the impact of the type of landform affected and its influence on the general structure of the statistical population.

The results show that both the number of coastal landforms and geodiversity have declined significantly (Table 4). The loss rate in absolute terms is −9.5%, taking into account only the extinct landforms and −14.4%, considering the unpreserved group (extinct and semi-destroyed). In the same order, the Shannon index (H′) presents a negative rate of −6.5% to −15.2%, quite similar to absolute values; and the rates of geodiversity loss, according to the PLi, are −17.3% to −32.1%, more than double the previous indices (Table 4).

Table 4. Variation rates by absolute (T) and geodiversity values (H′, PLi), expressed in parts per unit. A sensitivity analysis is included, expressing the isolated impact of each landform change on total values (Σ).

	Absolute values (T)		Geodiversity values			
			Shannon index (H′)		Proportional Losses index (PLi)	
	Extinct	Jnpreserved	Extinct	Unpreserved	Extinct	Unpreserved
Cl	-0.006	-0.012	0.003	0.007	-0.002	-0.004
Pt	-0.029	-0.03	0.013	0.014	-0.011	-0.011
Bb	-0.019	-0.023	-0.003	-0.004	-0.014	-0.016
Sb	-0.006	-0.007	-0.007	-0.008	-0.012	-0.013
Dn	-0.017	-0.026	-0.041	-0.074	-0.072	-0.108
Wl	-0.004	-0.01	-0.01	-0.026	-0.023	-0.053
Pdn	-0.01	-0.019	-0.02	-0.041	-0.036	-0.066
Pcl	0	-0.009	0	-0.008	0	-0.014
Nl	-0.00007	-0.004	-0.0002	-0.012	-0.0005	-0.033
Σ	-0.095	-0.144	-0.065	-0.152	-0.173	-0.321

Cl, coastal cliffs; Pt, shore platforms; Bb, pebble-boulder beaches; Sb, sandy beaches; Dn, coastal dune fields; Wl, coastal wetlands; Pdn, coastal palaeo-dune fields; Pcl, coastal palaeo-cliffs; Nl, nearshore landforms.

The different index outcomes are explained by distinct response to the absolute losses in each class. The absolute losses (T) present low variance between landforms, but diversity values are more sensitive to landforms type in which the loss take place, resulting in a greater variance, which increase substantially by H′ values and even more by PLi, according to the weight of abundance-singularity factor in each index (Fig. 5A–B). On very abundant and relatively little affected classes (shore platforms, cliffs and pebble-boulder beaches), the diversity loss rates are

lower than T, while on scarce and relatively more affected classes (dunes, wetlands and nearshore landforms), the diversity loss rates are higher than T values (Fig. 5A–B). This pattern with regard to T is approximately symmetrical on H′ and clearly asymmetrical on PLi: the last is slightly lower than T in very abundant and relatively little affected classes and strongly higher than T in scarce and relatively more affected classes (Fig. 5B).

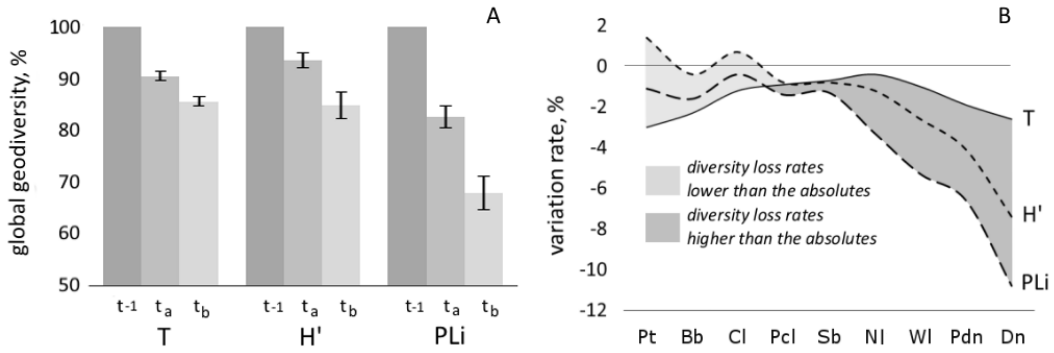

Fig. 5. Loss rates by absolute (T) and geodiversity values (H′, PLi), expressed in percentages. A) Current geodiversity in relation to the state prior to urban and tourism development (t_{-1}), considering extinct features (t_a) and whole unpreserved group ($t_{b)}$. The error bars represent the variance between landforms. B) Behavior of the indices H′ and PLi according to the landform type compared with the rates by absolute values (T). Pt, shore platforms; Bb, beaches; Cl, coastal cliffs; Pcl, coastal palaeo-cliffs; Sb, sandy beaches; Nl, nearshore landforms; Wl, coastal wetlands; Dn, coastal dune fields; Pdn, coastal palaeo-dune fields.

Furthermore, values of H′ are relatively low and similar to T because of two main reasons. Firstly, the losses in abundant classes generate an evident increase in the total geodiversity because H′ is an equity index that evaluates positively the uniformity of population structure. Secondly, the losses in low frequency classes have a limited impact due to their very low initial probabilities. However, in the alternative PLi proposed in this paper, all losses, even those in very abundant classes, produce a negative impact on the total values, and working with proportions instead of probabilities, the impacts on the less abundant (most singular) landforms acquire a significantly higher projection.

The results show that the worst effects on coastal geodiversity come from the impacts on the most singular landforms: modern and relict dunes and coastal wetlands. In this sense, it is particularly relevant the case of modern sand dunes, which represent only 2.6% of the total landforms losses in Gran Canaria but are responsible for about half of the coastal geodiversity loss on the island, according to the Shannon index (H′), and about a third of it according to the PLi index proposed in this paper.

5. Discussion

Coastal territories have a particular interest in the study of the transformation of natural systems in anthropic territories (Delcourt and Delcourt, 1988). Thus Gran Canaria, being a small coastal territory, with a tangible dimension and experiencing an increase in human pressure, represents an ideal scenario for the study of environmental changes induced by human activity.

The impact of human activities on coastal landforms has been studied in various parts of the world. However, most cases focus on quantifying setbacks or morphological changes of the coastline in mainland territories, addressing both local (Terich and Levenseller, 1986; Dolan et al.,

1990; Amin and Davidson-Arnott, 1997; Aubié and Tastet, 2000; Cui and Li, 2011) and regional cases (El Banna and Frihy, 2009; Lira et al., 2016; Hapke et al., 2013). They also focus on the qualitative analysis of transformations in coastal areas by urbanization, industrialization and direct intervention of the coast (Kurt et al., 2010; Farhan and Lim, 2011). As carried out in this work, studies of coastal transformations in island territories are relatively scarce (García-Romero et al., 2016; Hernández-Calvento et al., 2014; Dawson and Smithers, 2010; Fletcher et al., 2003; Norcross et al., 2002; Jones et al., 1993; Lacey and Peck, 1998; Farhan and Lim, 2011).

In many studies, the main objective is to detect and quantify planimetric changes in the coast by widespread erosion or accretion over time, but the coastal erosion in Gran Canaria, with a predominantly igneous and steep coast, is not a general problem. The main problems arise by the intense occupation of the coast in the last century, which has triggered intense degradation processes. Also, most studies on morphological changes in the coasts have focused on the partial analysis of specific landforms: beaches (Norcross et al., 2002; Sallenger et al., 2003), coastal dunes (Ojeda Zújar et al., 2002; Woolard and Colby, 2002; Houser et al., 2008; El Banna and Frihy, 2009; Miccadei et al., 2011; Flor-Blanco et al., 2013; Pye et al., 2014), island barriers (White and Wang, 2003), deltas (Smith and Abdel-Kader, 1988; El Banna and Frihy, 2009), estuaries (Wang et al., 2013) or rocky shores (Pierre, 2006; Dornbusch et al., 2008). Therefore, in this study we propose a comprehensive and quantitative analysis of the changes and conservation state of the complete set of coastal landforms of the island, assuming as a reference the period before the urban and tourism development occurred especially during the second half of the last century. In addition, the results of this work contribute to the knowledge, in relation to other geomorphic systems, of the dunes of the Canary Islands, which have been the subject of extensive studies (Alonso et al., 2002, 2006; Cabrera-Vega et al., 2013; Hernández-Calvento et al., 2014; García-Romero et al., 2016) because of their rarity on oceanic hot-spot islands and their distinguishing characteristics with respect to continental European systems.

The methods used have provided a broad quantitative dataset from the coast of Gran Canaria, which is later used to calculate the temporal evolution of the coastal geomorphological diversity. While geodiversity comprises, in its broadest sense, the abiotic part of the natural environment (Gray, 2008; Thomas 2012), this study considers geodiversity exclusively from the geomorphological point of view. Recent studies on quantification of geodiversity usually focus on continental interior areas in order to compare the geodiversity in two or more spaces (Benito-Calvo et al., 2009; Hjort and Luoto, 2010, 2012; Pereira et al., 2013). On islands, studies have focused on the pedological component (Ibáñez et al., 2005; Ibáñez and Effland, 2011), while geodiversity loss by anthropogenic influence is addressed only in geosites (Ruban, 2010). The quantitative analysis of the evolution of geodiversity in human-impacted coasts of a volcanic island is an issue first explored in this work, where the application of a simple and direct index (PLi) is suggested as an alternative to the Shannon index (H'). The Shannon index arose from the Information Theory to measure the information loss in a system as a result of the entropy increment. Thus, it is a measure of the uncertainty of the internal system configuration, which has been commonly equated with diversity. In this study, the Shannon index doesn't provide a significant additional information respect to the absolute values and, in our view, underestimates the loss of coastal geodiversity in Gran Canaria. Therefore, it was insufficient for the objectives of our study. The alternative index proposed here (PLi) has been specifically developed to estimate the consequences of the losses of elements for geodiversity, given a heterogeneous dataset with numerous classes and differing abundances. The PLi exhibited greater sensitivity to the losses, particularly in the scarcest type of landforms, having results that correspond better to the reality of Gran Canaria.

The results show that human activities, especially the urban and tourism development, have resulted in a significant loss of coastal geodiversity. The island's economy was based on agriculture and most of the population was concentrated in the north of the island due to the existence of abundant water resources. Especially from the 1960s onwards, there was an expansion of infrastructures and urbanizations from the north to the eastern and southern coasts

of the island (Morales Matos and Santana Santana, 1993), due to better climatic and topographic characteristics for urban use and "sun and beach" tourism. Thereafter, the eastern and southern coastal plains and also cliffed shores began to experience an intense process of environmental transformation.

According to our results, sedimentary and low coastal landforms (dunes, beaches and wetlands) have undergone major transformation, becoming the most vulnerable coastal elements. In particular, the study shows, through the rates of variation of diversity indices, the high impact on coastal geodiversity that the processes of degradation and loss of coastal dune fields have had. These have been affected not just by the construction of infrastructures and urbanizations on them but also by altering the marine and aeolian sedimentary dynamics (Cabrera-Vega et al., 2013; Hernández-Calvento et al., 2014; García-Romero et al., 2016). On the other hand, the impacts on the beaches are a true reflection of socioeconomic processes occurring on the island. Coastal tourism exploitation has favored the preservation of sandy beaches with respect to pebble-boulder ones, which have been significantly destroyed and sometimes replaced by artificial infra- structures. As a consequence of that process, however, the sandy beaches are mostly altered.

6. Conclusions

In island territories, which are geographically isolated and where resources are limited (Hay, 2013), it is particularly important to inventory and quantify the damages and losses produced on natural resources and the environment, in order to guide the regional conservation policies. This research is the first one to analyze the evolution of both sedimentary and rocky coastal landforms in an entire island, providing objective, quantitative and comprehensive data about the impacts and losses induced by human activity.

The methodology developed for the analysis of the coastal geodiversity evolution in relation to the human activities has been applied to the case of the Gran Canaria Island, where a new diversity loss index is proposed (Proportional Losses index, PLi). The results demonstrate that the historical urban and tourism development in Gran Canaria has had a significant impact on coastal landforms and geodiversity, and highlights the importance of conducting comprehensive inventories and quantitative analyses of their conservation that incorporate key aspects of impact assessment, such as the uniqueness and vulnerability of natural elements. The most affected landforms, coastal dunes, palaeo-dunes and wetlands, are the most singular landforms, which has a notable negative impact on the coastal geodiversity of the island.

We are convinced that this methodology has the potential to be a future tool in the evaluation of anthropogenic impacts in other coastal areas of the world. Particularly, its application on other islands in the world will be interesting given the role of the islands as closed-system laboratories for understanding the broader impacts of human activities.

Acknowledgments

This work is a contribution to the CSO2013-43256-R project of the Spanish National Plan for R+D+i (innovation), co-financed with ERDF funds, and was supported by a FPI-PhD grant from the Universidad de Las Palmas de Gran Canaria (E-35-2014-0231941) (ULPGC). It was completed while N. Ferrer was a Ph.D. student in the IOCAG Doctoral Programme in Oceanography and Global Change. We would like to acknowledge Leye Beunza Valero, for her assistance in translating the paper, and the recommendations from reviewers that have helped to improve the manuscript.

Measuring geomorphological diversity on coastal environments: A new approach to geodiversity

Nicolás Ferrer-Valero

Geomorphology, 318, 217-229

https://doi.org/10.1016/j.geomorph.2018.06.013

Abstract

Geodiversity can be defined as the spatial variability of geo-elements. Its emergence as a research field is relatively recent, with a wide range of approaches and methods of evaluation and quantification already in use. The work described in this paper was carried out from a novel perspective. Firstly, the emphasis is specifically centred on geomorphological diversity. Secondly, mathematical ecology calculations are applied which tackle the problem on the basis of a larger number of diversity parameters. In addition, whereas most authors have focussed on mountainous and/or continental areas, for the first time a study of this type is applied to coastal landscapes. The analysis covers the full 459 km of volcanic coastline of the islands of Gran Canaria and La Palma (Canary Islands). These two oceanic islands were chosen for purposes of diversity comparison given their differing stages of geomorphic development. In accordance with an *ad hoc* geomorphological taxonomy, as developed in this study, 14 geomorphic groups and 42 subgroups were identified and quantified according to their presence [1] or absence [0] along the coastline. A cartographic-analytical method (coastline data-storing or CDS), based on the computation of binary information in the cartographic vector of the coastline, enabled calculation of the occurrence probability of these groups and subgroups. Both at local level (analyses of *coastal morphoassemblages*) and general level, three components of geomorphological diversity (richness, evenness and dissimilarity) were estimated, through indices of richness (R), Shannon's entropy (H') and Rao's quadratic entropy (Q). The data reveal that geomorphological coastal diversity is between 11.1% and 48.2% higher in Gran Canaria than in La Palma. The method was subjected to a fractal stress test through iterative mapping procedures to assess the effect of scale on the behaviour of the relative frequencies and indices. The variability that was obtained allowed the extraction of corrected values in the indices for La Palma (H'_c=1.88±0.008 and Q_c=0.183±0.004) and Gran Canaria (H'_c=2.11±0.019 and Q_c=0.232±0.003). A moving-window test was also applied as a rarefaction method to confirm the contrast in diversity in coasts of different size. The results enabled to advance hypotheses about the relation between coastal geomorphic diversity and geological age of islands.

Keywords: Geodiversity, coastal geomorphology, oceanic islands, Canary Islands.

1. Introduction

Numerous authors have highlighted the role of natural abiotic elements as economic and cultural resources, as well as their importance in the sustainability of ecosystems, habitats and landscapes (e.g. Gray, 2005; Serrano and Ruiz-Flaño, 2007; Gordon et al., 2012; Thomas, 2012; Hjort et al., 2015). Geodiversity emerged in the 1990s as an analogous concept to that of biodiversity. Since then, it has been conceived as the study of the abiotic part (geology, geomorphology, topography, soils, hydrology, etc.) of natural diversity (Serrano and Ruiz-Flaño, 2007; Gray, 2008). Since the introduction of the concept and its associated problems, a unifying conception has prevailed oriented towards the conservation of natural heritage. For purposes of clarity, a new terminology has been created (*geoconservation, geoheritage, geosites*) and numerous studies have been published identifying, classifying and evaluating sites of potential geo-patrimonial interest (e.g. Bruschi and Cendrero, 2005; Panizza and Piacente, 2009; Feuillet and Sourp, 2011; Brilha, 2015; Çetiner et al., 2018).

Diversity is a universal concept related to heterogeneity and complexity. It can be measured through specific parameters and applied to any reality that can be classified and quantified. Shannon's entropy index, developed in the framework of the mathematical theory of information, has for decades been one of the most common ways to measure diversity. From this perspective, geodiversity comprises the application of a general property of the reality to the components of the geosphere. Gray (2008) defines it as '*the natural range (diversity) of geological (rocks, minerals, fossils), geomorphological (landform, processes) and soil features*'.

Ibáñez et al. (1995) laid the foundation for the study of soil diversity based on the adoption of models and indices developed in mathematical ecology, where biodiversity has been a central topic of importance for decades. Since then, there has been a growing interest in using these techniques to measure soil diversity at different scales and in relation to different variables (e.g. Guo et al., 2003; Ibáñez et al., 2005; Minasny and McBratney, 2007; Minasny et al., 2010). Studies have recently been developed with a view to tackling geodiversity in its strictest sense, namely the spatial variability of geo-elements. Most common has been the adoption of holistic approaches, in keeping with 'foundational' conceptions (Gray, 2008), in which the aim is to calculate total geodiversity, combining variables as lithology, geomorphology, topography, pedology, hydrology and/or morphoclimate. Of these, very few have adopted classical forms of calculation (Benito-Calvo et al., 2009; Argyriou et al., 2016). Most in fact have applied or developed special calculations or *geodiversity indices* (e.g. Serrano et al, 2009; Hjort and Luoto, 2010; Ruban, 2010; Pellitero et al., 2011; Pereira et al., 2013; Ilić et al., 2016; Melelli et al., 2017; Özşahin, 2017; Stepišnik and Trenchovska, 2018), with the most commonly used being that proposed by Serrano and Ruiz-Flaño (2007). The geodiversity indices are generally implemented trough GIS-based algebraic operations, overlaying heterogeneous cartographic information to obtain local estimations of diversity, based fundamentally on richness.

Given the prevalence of the general approaches, it can be argued that geomorphological diversity, in an exclusive sense, has been usually neglected in the field of quantitative geodiversity. Likewise, coastal environments, spaces of high degrees of dynamism and geodiversity at global level (Gray, 2008), have not been an object of study from this perspective. Considering this background, the aim of the present work is to propose analytical procedures for the evaluation and measurement of geomorphological diversity in coastal environments. In alternative to special indices, this work proposes forms of diversity calculation based on parameters of richness, evenness and dissimilarity. As a comparative laboratory, the methods have been implemented of the coasts of two oceanic islands with geomorphological characteristics which are, *a priori*, appreciably different.

2. Study coasts

A study was undertaken of the full extent of the coastal geomorphology of two islands: La Palma and Gran Canaria (Canary Archipelago, Spain) (Fig. 1). The total perimeter analysed was 459 km. The relatively small size of oceanic islands offers practical advantages when performing complete coastline studies. Furthermore, the succession of ages typical of hotspot archipelagos makes these islands particularly interesting for the study of coastal evolution, as geological time induces in them profound geomorphological transformations (Woodroffe, 2014). The Canary Islands are comprised of a chain of volcanic islands arranged in an east-west direction, located opposite the northwest coast of Africa, between 27º-29º north and 13º-18º west. Although the archipelago's geological origin has been the subject of some controversy (Anguita and Hernán, 2000), there is general consensus in associating it to a hotspot model with structural and geodynamical particularities with respect to the Hawaiian prototype (Carracedo et al., 1998; Schmincke and Sumita, 1998; Carracedo, 1999; Carracedo et al., 1999; Carracedo et al., 2001). The hotspot model explains the origin of certain chains of islands based on the movement of a lithospheric plate above a stationary intraplate mantle plume which generates new islands in a direction opposite to that of its movement (Wilson, 1963; McDougall, 1971; Langenheim and Clague, 1987; Moore, 1987).

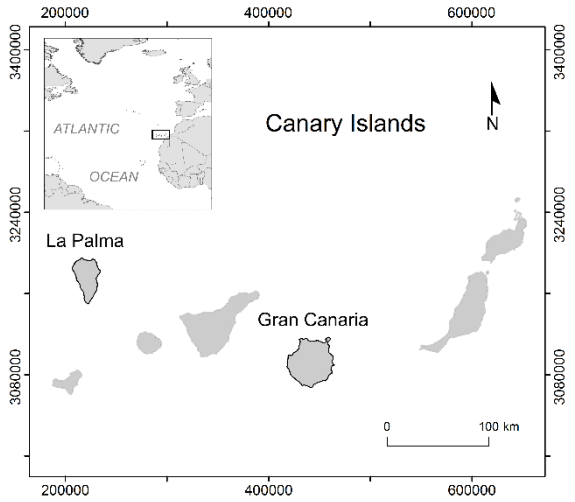

Fig. 1. Study area. Coasts of La Palma (198 km) and Gran Canaria (261 km).

Two islands in different geological stages of development and with distinct general morphological features were chosen to enhance the possibilities of comparison and to generate contrasts in terms of diversity values. La Palma (198 km of coastline) is at the western end of the archipelago. Situated above the theoretical hotspot, it is a young island, date from 1.8 Ma, in a state of intense volcanic activity. It is a growing shield volcano, with a peak height of 2,426 m, comprised in almost its entirety of layers of basalt lava flows cut off at large coastal cliffs. Gran Canaria (261 km of coastline) is older, 14.5 Ma, and is found in a central position in the chain of islands. It is comprised of a single Miocene volcanic shield which evolved into the formation of a stratovolcano during the Pliocene (Roque Nublo), now extinct. After long periods of erosion and volcanic reactivation, its highest point today is in the centre of the island at 1,956 m and the coasts display widely varying topography.

3. Methods

3.1. Test taxonomy

As has been made clear in some review studies (Fairbridge, 2004; Finkl, 2004), coasts have been classified in multiple ways and according to very different criteria. There is no standard international taxonomy with systematization of geomorphological types and their hierarchical and genetic relationships. In view of this deficiency, this research study has developed a proposal a landform-based classification of coastal environments for diversity analyses (Table 1). The table has been constructed as the result of a synthesis of direct observations made of the coasts of La Palma and Gran Canaria, integration of multiple sources in GIS (cartographic, photographic and LiDAR) and field work performed during 2015/16. Different classes are also based on the main scientific literature (Table 1).

Table 1. Taxonomy of geomorphic *groups* and *subgroups* for mesoscale diversity analysis. As can be seen, the *groups* are generic sets which include more specific and defined categories published in the literature. n= number of samples taken along the coasts of Gran Canaria and La Palma. *Local names.

Environments	Groups of landforms	Dimensional Subgroups
Rocky-erosive	**Cliffs group (Cl)**	**Height (m), n= 9,544**
	Sea cliffs (Bird, 2008); *plunging cliffs* (Sunamura, 1992); *bluffs* (Davidson-Arnott, 2010); *hard-soft cliffs* (Davidson-Arnott, 2010); *simple-composite cliffs* (Emery and Kuhn, 1982); *coastal slopes* (Bird, 2008).	Cl_1 Pcl_1 330.1 – 1010 Cl_2 Pcl_2 115.1 – 330.0 Cl_3 Pcl_3 5.000 – 115.0
	Paleo-cliffs group (Pcl)	
	Paleo-cliffs (Zazo, 1999).	
	Platforms group (Pt)	**Width (m), n= 6,415**
	Type A-type B shore platforms (Sunamura, 1992); *low tide-high tide shore platforms* (Bird, 2008); *ledges* (Bird, 2008); *benches* (Kennedy, 2014); *incipient-dissected shore platforms* (Bird, 2008); *cemented pavements* (Brocx and Semeniuk, 2010).	Pt_1 70.01 – 210.0 Pt_2 32.01 – 70.00 Pt_3 2.000 – 32.00
	Terraces group (Mt)	**Surface (ha), n= 4**
	Marine terraces (Zazo, 1999)*; raised platforms* (Stephenson, 2000).	Mt_1 222.4 – 483.1 Mt_2 42.51 – 222.3 Mt_3 42.50
	Remnants group (St)	**Height (m), n= 341**
	Sea stacks, fringing platforms (Pethick, 1984)*; pinnacles* (Bird, 2008); *islets* (Bird, 2008); *roques*, peñas*.*	St_1 27.71 – 80.70 St_2 10.01 – 27.70 St_3 0.400 – 10.00
	Reefs group (Rf)	**Length (m), n= 234**
	Rocky reefs (Bird, 2008); *stumps*; *biogenic reefs* (Brocx and Semeniuk 2010); *barras**, *lajas**, *bajas**, *bajíos**.	Rf_1 349.2– 850.0 Rf_2 57.21– 349.1 Rf_3 3.898 – 57.21
	Lavic group (Ld)	**Surface (ha), n= 23**
	Lava-deltas (Mattox and Mangan, 1997); *islas bajas**.	Ld_1 92.81 – 220.9 Ld_2 31.31 – 92.80 Ld_3 2.600 – 31.30
Clastic-depositional	**Debris group (Db)**	**Volume (m^3), n= 480**
	Rock-falls, topples, slides (Wilkerson, 1997); *collapses* (Carracedo et al., 1999); *scree slopes* (Young and Clayton, 1972)*; talus slopes* (Emery and Kuhn, 1982); *fajanas**.	Db_1 9,895,000-166,200,000 Db_2 3,749,000 – 9,894,000 Db_3 25.85 – 3,748,000
	Gravel beaches group (Gb)	**Length (km), n= 1,254**
	Shingle, pebble and boulder beaches (Bird, 2008); *bouldery shores* (Bird, 2008); *mixed and composite beaches* (Jennings and Shulmeister, 2002); *storm ridges* (Hall et al., 2006).	Gb_1 2.757 – 9.223 Gb_2 0.4972 – 2.756 Gb_3 0.0042 - 0.4971
	Sand beaches group (Sb)	**Length (km), n= 320**
	Sandy beaches (Bird, 2008)*; mixed and composite beaches* (Jennings and Shulmeister, 2002); *sand barriers* (Alexander, 1966).	Sb_1 1.505 – 5.380 Sb_2 0.3933 – 1.504 Sb_3 0.0059 – 0.3932
	Dunes group (Dn)	**Surface (ha), n= 23**

Foredunes, nebkhas, barchans, parabolic dunes, transverse dunes, sand sheets, climbing dunes, falling dunes, cliff-top dunes, stabilized dunes (Hesp and Walker, 2013).	Dn_1 Pdn_1 256.6 – 500.0 Dn_2 Pdn_2 65.51 – 256.5 Dn_3 Pdn_3 0.100 – 65.50
Paleo-dunes group (Pdn) *Aeolianites* (Brooke, 2001)*; palaeodunes* (Criado et al., 2012).	
Wetlands group (Fm) *Salt marshes* (Bird, 2008); *alluvial plains* (McGill, 1958)*; fan-deltas* (Shipman, 2008); *saladares**.	**Surface (ha), n= 99** Fm_1 71.61 – 258.2 Fm_2 21.11 – 71.60 Fm_3 0.010 – 21.10
Lagoons group (Lg) *Coastal lagoons* (Kjerfve, 1994); *ponds* (Davidson-Arnott, 2010); *charcas**.	**Surface (ha), n= 8** Lg_1 0.750 – 3.500 Lg_2 0.200 – 0.750 Lg_3 0.070 – 0.200

The presented classification constitutes an expansion of a previous proposal (Ferrer-Valero et al., 2017). The thematic "resolution" of the classification system is at mesoscale. It is designed, on the one hand, to enable the analysis and comparison of extensive coastal sections and, on the other, to be adaptable to the information that could be obtained about almost any coast in the world using basic primary sources. It is comprised of 14 *geomorphic groups*. They constitute sets of elements which share general morphological features and common links with morphogenetic mechanisms and agents. Seven of these categories constitute morphologies of rocky-erosive origin and the other seven of clastic-depositional origin (Table 1). Four are *groups* of relict landforms and ten of active landforms. In this way, the classification ensures a balance among large coastal environments and avoids the weighting of some coastal processes and mechanisms against others in the analyses of diversity.

The *groups* were further disaggregated into *subgroups* according to the degree of development or state of growth of their elements (size). For this, the significant parameter of each *group* (i.e. the most representative of its dimension) was extracted (Table 1). Systematic measurements of each dimensional parameters were taken until values were obtained of the all the statistical population. For the cliffs and platforms groups, a maximum value was obtained at intervals of 50 m. In the remaining groups, in which the elements can be distinguished from each other (e.g. one beach from another), measurements were taken of each individual element. In total, 21,267 measurements were taken. Each obtained frequencies distribution were clustered by natural breaks (Jenks, 1967) into three groups: g_3-small, g_2-medium and g_1-large (Fig. 2b). In this way, the *subgroups* were established in accordance with the actual data and not arbitrary thresholds, thereby allowing a reliable comparative analysis.

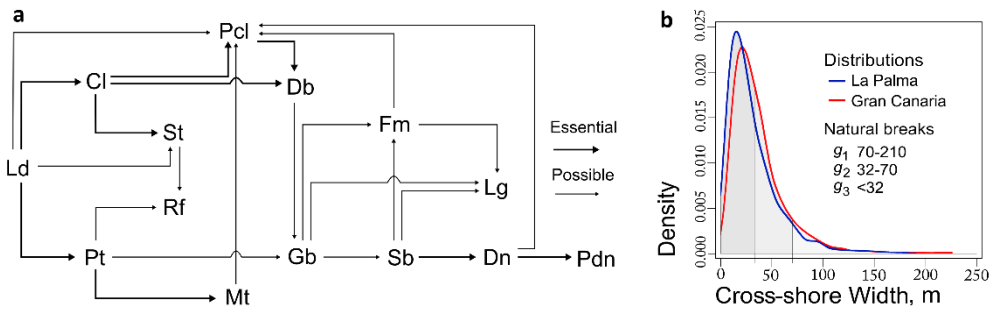

Fig. 2. Additionally factors in taxonomic distance calculation; a) genetic dependencies between landforms (see Table 1 for acronym definitions). The dependence is considered 'essential' when there is a theoretic direct cause-effect relation between *groups*, and 'possible' when a *group* is spatially correlated with other, becoming potential factor of their development; b) example of classification of Platforms group in 3 dimensional *subgroups* according to natural breaks of 6,415 measurements of width.

3.2. Test diversity components

Three components of diversity were analysed using non-parametric models, also known as diversity indices (Marrugan, 1988). The first, *richness*, is the simplest component and, in itself, one of the most informative with respect to diversity. It represents in absolute values the number of classes present in the space under analysis without considering their frequencies. A normalisation (R) is used in its calculation.

$$R = S \,/\, S_{max}$$

Where *S*, the number of classes present; S_{max}, total number of classes considered.

The second component is *evenness*. It represents the degree of balance in the frequencies distribution of the classes which make up the sample appear. It is positively related with diversity, increasing in those populations in which the classes are more evenly represented. Shannon's entropy index (H') was used to measure this component.

$$H' = -\sum_{i=1}^{S} p_i \log p_i$$

Where p_i, indicates the probability of occurrence of class *i*. This index has the quality of also incorporating richness in the diversity estimations.

The third component considered is *dissimilarity*. This represents the general degree of relationship (or taxonomic distance) that exists between the classes of a sample. Diversity is positively related with taxonomic dissimilarity, decreasing when the classes present belong to just one part of the spectrum of a distances matrix or taxonomic tree. Rao's quadratic entropy index (Q), which also incorporates richness, was used for its calculation (Rao, 1982). It is defined as the expected distance between two randomly selected individuals:

$$Q = \sum_{i=1}^{S} \sum_{j=1}^{S} p_i \; d_{ij} \, p_j$$

Where d_{ij} is the taxonomic distance between classes *i* and *j*.

The probabilities of coastline occurrence of the classes are normalized by the sum total of probabilities, so that the condition $\sum p_i = 1$ is met, maintaining the ratio of proportionality. At local level, dissimilarity was calculated as mean distance (δ_m).

$$\delta_m = \frac{1}{n^2} \sum_{i=1}^{n} \sum_{j=1}^{n} d_{ij}$$

Estimation of the degree of kinship between classes was not developed in geomorphology. In other fields it has been addressed by constructing distance matrices from phylogenetic trees (Owens and Bennet, 2000; Clarke and Warwick, 2001; Faith, 2002) or tables of key properties (Minasny et al., 2010; Van Huyssteen et al., 2014; Smirnova and Gerasimova, 2017). In this case, a table of identification properties was designed (Table 2). In this table, the different geomorphic *groups* are evaluated according to 15 variables, with values of [0.0], [0.5] and [1.0] according to their properties. Both morphodynamic and morphometric variables are taken into consideration.

Complementary, the existence of direct genetic dependencies between landforms and the state of growth of landforms, have been considered as a kinship factors (Fig. 2). Taxonomic distance has been finally calculated as a Euclidean distance in matrix, with two additional terms:

$$d_{ij} = dep\left[\left(x_i - x_j\right)^T\left(x_i - x_j\right)\right] + g_n$$

Where x_i and x_j, the vectors-rows of properties in the matrix; *dep*, the existence of necessary (*dep*=0.50) or possible (*dep*=0.75) genetic dependence between two landforms; and g_n, the membership of a *subgroup* of size *n*, where g_3=0.00, g_2=0.05 and g_1=0.10 (Fig. 2b).

Table 2. Table of key attributes for the calculation of taxonomic distances (see acronyms in Table 1).

Variables	Properties		Cl	Pcl	Pt	Mt	St	Rf	Ld	Db	Gb	Sb	Dn	Pdn	Fm	Lg
Causative	Erosive	1.0	x	x	x	x	x									
dynamic	Mixed	0.5						x							x	x
	Accretive	0.0							x	x	x	x	x	x		
Triggering	Marine	1.0			x	x	x	x			x	x				
agent	Mixed	0.5	x	x					x	x					x	x
	Derived	0.0											x	x		
Activity	Active	1.0	x		x		x		x	x	x	x	x		x	x
	Relict	0.0		x		x		x						x		
Evolutionary	High	1.0										x	x	x	x	x
degree	Medium	0.5		x		x	x	x			x					
	Low	0.0	x		x				x	x						
Standard	High	1.0									x	x	x	x	x	x
dynamism	Medium	0.5								x						
	Low	0.0	x	x	x	x	x	x	x							
Shore-relative	Backshore	1.0		x		x			x				x	x	x	x
position	Foreshore	0.5	x		x					x	x	x				
	Nearshore	0.0					x	x								
Dominant	Rock	1.0			x		x	x	x					x		
composition	Indifferent	0.5	x	x		x										
	Sediment	0.0								x	x	x	x		x	x
Granulometry	Coarse	1.0			x	x	x	x	x	x	x					
	Indifferent	0.5	x	x												
	Fine	0.0										x	x	x	x	x
Surface-water	Permanent	1.0														x
retention	Episodic	0.5			x										x	
	None	0.0	x	x		x	x	x	x	x	x	x	x	x		
Signature	High	1.0	x	x			x									
slope	Medium	0.5								x	x					
	Low	0.0			x	x		x	x			x	x	x	x	x
Cross-shore	Represent	1.0	x	x												
height	Significat	0.5				x			x			x				
	Non-sign	0.0			x		x	x		x	x		x	x	x	x
Cross-shore	Representat.	1.0			x	x										
width	Descriptive	0.5						x	x		x	x	x	x		x
	Non-descrip.	0.0	x	x			x			x					x	
Longshore	Representat.	1.0						x			x	x				
length	Descriptive	0.5	x	x	x	x	x		x	x			x	x	x	x
	Non-descrip.	0.0														
Volume	Representat.	1.0								x						
	Descriptive	0.5						x	x				x	x		
	Non-descrip.	0.0	x	x	x	x	x				x	x			x	x
Planimetric	Representat.	1.0							x				x	x	x	x
Surface	Descriptive	0.5				x	x	x		x	x	x				
	Non-descrip.	0.0	x	x	x											

3.3. Computation of abundances

Measuring geomorphological evenness and dissimilarity requires a knowledge of frequencies and their expression as a probabilities (see Eq. 2 and 3). In geodiversity it is not always possible or desirable to differentiate between and count "individuals". In its stead, a spatial proxy may be required which represents the abundance of the elements. In pedodiversity, the planimetric area of the different groups of soils in the space has been used (Guo et al., 2003; Ibáñez et al., 2005;

Minasny and McBratney, 2007), but in coastal geomorphology this parameter is not representative in all the classes (e.g. 'cliffs'). Furthermore, the planimetric surface development of some landforms and others is intrinsically different, and so the ratio of frequencies when operating with this would be always skewed. In this work, length of coast has been used as reference element for the normalization of abundances. The coastline employed is elevation 0 of the 1:5,000 topographic map of the Canary Islands (Grafcan S.A., Gobierno de Canarias).

The procedure, implemented in GIS, has been named Coastline Data-Storing (CDS). It consists of the computation of binary information (presence [1] or absence [0] of the classes) in a spatial database supported in a cartographic vector (coastline), so that the abundance of each element is defined, in absolute terms, by the length of coast which it occupies and, in relative terms, by its relationship with the total coastal perimeter under consideration (Fig. 3). The procedure entails the difficulty of determining the coastal segment occupied by each landward (e.g. *dunes*) or seaward element (e.g. *stacks*). In such cases, it is necessary to project the cartographic features. Tangent planes defined by parallel straight lines were used for this purpose. The projection plane encompasses the cartographic feature which is projected on the coastline so that the end points of the intersection are connected by a perpendicular line to that plane (Fig. 3).

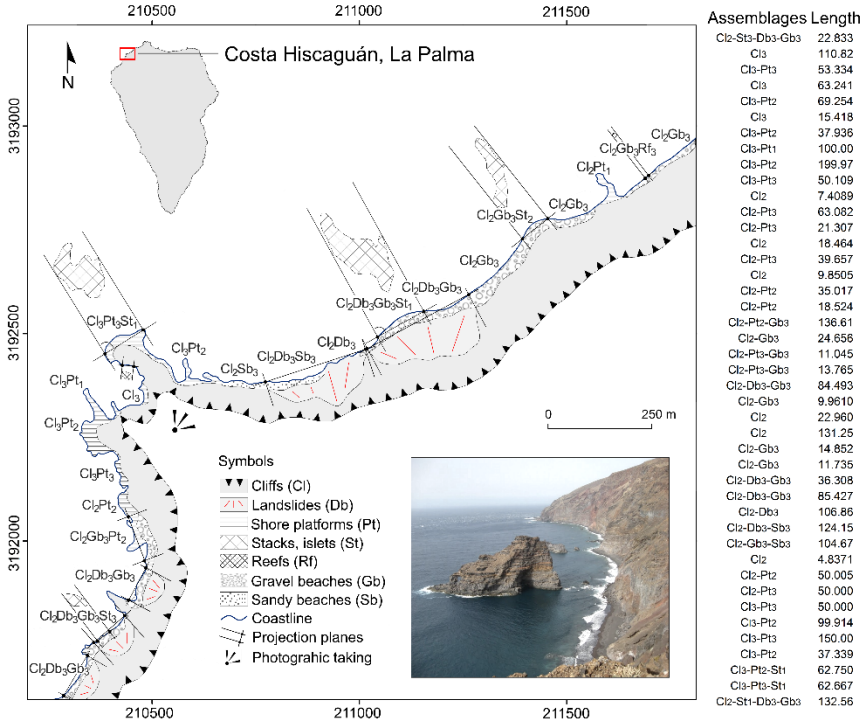

Fig. 3. Graphic representation of the CDS procedure and corresponding spatial database along a 3-km coastline sector of La Palma (Hiscaguán).

As well as generating diversity values for sets (in this case an entire coastline), the CDS procedure enables combinatorial analyses and local calculations to detect high-diversity points. The transposition of the landforms to the coastline allows a reading of the various combinations that take place along it and their characterisation according to the type and size of cross-shore landform associations or *coastal morphoassemblages* (e.g. cliff-platform, beach-dune, cliff-beach-platform). Maps of local richness (R) and mean taxonomic distance (δ_m) have been elaborated based on it. In CDS, the coastline is finally divided into a number of sections of variable length. Each alongshore section differs from the contiguous ones by the particular combination

of a class or classes. The number of sections (*s*) of a category is independent of its relative frequency (*p*). In CDS, if $p=0.0 \leftrightarrow s=0$ and if $p=1.0 \rightarrow s=1$. Otherwise, any relationship between *p* [0,1] and *s* [0,∞] is possible, allowing other landscape structure measurements like fragmentation (not covered in this paper).

3.4. Evaluation of uncertainties

Due to the fractal nature of coastlines, their morphology and length depend on the measurement scale (Mandelbrot, 1967). The relative frequencies of the CDS will, for this reason, experience scalar modifications which generate alterations in the indices (except in richness). It should therefore be considered that the results of two samples, though comparable on a constant scale, are not scale-invariant. With this in mind, the influence of a change in scale on the values of the indices obtained by the CDS procedure was evaluated. A total of 28 scale decreases were simulated using the polynomial approximation with exponential kernel (PAEK) algorithm (Bodansky et al., 2002) for each of the islands (Fig. 4a). This algorithm permits a vector generalization, cartographically highly optimal, modifying a parameter of tolerance. In this way, the scale was progressively decreased from the baseline of 1:5,000 to approximately 1:500,000. An iterative procedure of the automatic projection of tangent planes was applied to transpose the original information contained in the 1:5,000 scale to each new scale. For a greater understanding of scale behaviour, the probabilities of the occurrence of a particular class and the H' and Q indices were recalculated 56 times. The scalar variations were represented in terms of their fractal dimension (*D*), estimated using the box-counting method (Xu et al., 1993; Xiaohua et al., 2004; Piña-García et al., 2016).

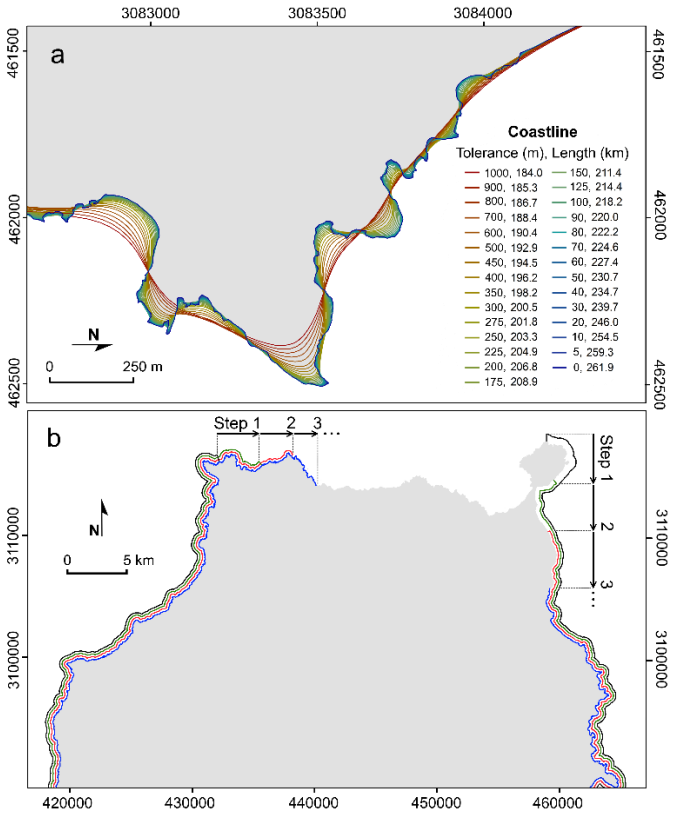

Fig. 4. Evaluation of uncertainties; a) fractal stress analysis, showing the effect of generalization on the shape and length of the coastline. It can be seen how the scalar distortions are more pronounced in rocky sections, which are more irregular, and the lines tend to converge towards the upper right-hand quadrant of the sheet where the coast becomes sedimentary; b) graphic representation of the moving-window method: the window shifts unidirectionally from the northernmost tip of the island at constant 500 m

intervals (exaggerated in the figure to enable its visualisation). The method generates an almost continuous scanning (>99% of overlapping) of equivalent sections along the whole perimeter.

The comparison of coastal geomorphic diversity poses another element of uncertainty related to so-called rarefaction, when the size of the samples (coastlines compared) are not equivalent. Because the size of the coast can theoretically influence its diversity, the differences observed could be due to this fact and interfere in other interpretations. Between La Palma and Gran Canaria there is a difference in coastal length of around 25% at larger scales and around 30% at smaller scales. To evaluate the effect of the size of the coast on the CDS-derived diversity values, a moving-window technique was applied, implemented through R-Studio® coding. This technique entails the adoption of a linear sampling 'window' of length *n* which is shifted at constant longitudinal intervals, partially overlapping with previous windows (Fig. 4b). The set of values obtained offers a perspective of the diversity of largest sample in reference to the size of the smaller sample. The experiment was replicated for the island of Gran Canaria with a sample size equivalent to the perimeter of La Palma (198,620 m at a 1:5,000 scale) at constant displacements of 500 m (99.75% overlapping), beginning at the northern end of the island and covering the whole perimeter, with a resulting 523 comparable replicates of R, H' and Q.

4. Results

According to the proposed geomorphological taxonomy (Table 1) and cartographic-analytical procedure (Fig. 2b, Fig. 3), it was possible to distinguish a total of 4,092 sections in La Palma and 3,834 in Gran Canaria at *group* level, and 8,430 sections in La Palma and 9,141 in Gran Canaria at *subgroup* level (Fig. 5a). These values (*s*) are a proportional reflection of the resolution and mapping effort employed.

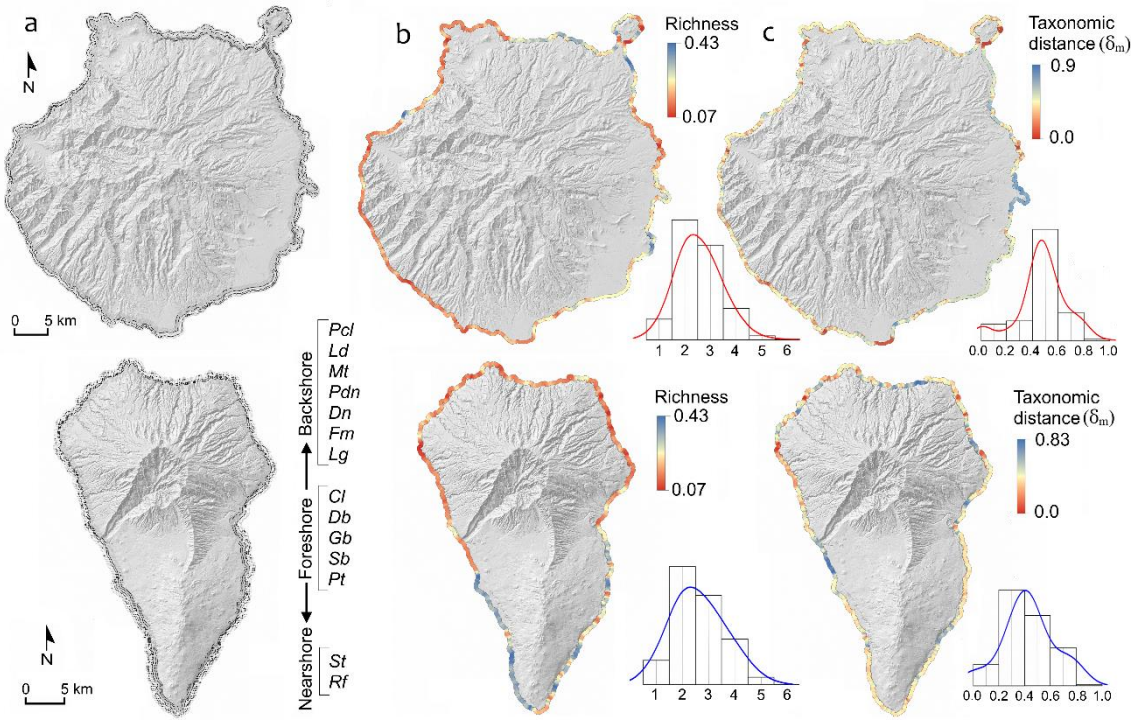

Fig. 5. Results of the local analysis based on combinatorial operations in GIS; a) mapping of the 4,092 differentiated sections in La Palma and the 3,834 in Gran Canaria at *group* level. In the original analytical mapping all the information is contained in the same line (see Table 1 for acronym definitions); b) local

analysis mapping and histograms of richness (R) in La Palma and Gran Canaria; c) local analysis mapping and histograms of mean taxonomic distance (δ_m) in La Palma and Gran Canaria.

The results for the diversity components considered (richness, evenness and dissimilarity) indicate a significant contrast in the geomorphological diversity of the samples studied (coasts of La Palma and Gran Canaria).

As can be deduced from the length of the series on the x-axis in the rank-abundance plots (Fig. 6a-6b), there is an evident contrast of richness (R) between the two islands. In La Palma 12 of the 14 *groups* (R=0.86) were found, and in Gran Canaria all 14 (R=1.0). This is equivalent to a 16.7% increase in richness (R) of the second island over the first. The increase is significantly higher (48.3%) at *subgroup* level, with La Palma having 27 of the 42 taxonomic features (R=0.66) and Gran Canaria 41 (R=0.98) (Fig. 6c).

Calculating R at each point of the coasts gives the local geomorphological richness (Fig. 5b). In no section of La Palma or Gran Canaria is the joint presence of 6 *groups* exceeded (of the total of 14), while the number of *groups* is always greater than 0. The results allow the observation of significant contrasts by zones. In La Palma, the minimum R values (1.0) are concentrated in the north, where low values of richness are common, while high values (4.0, 5.0) are found in the south. The maximum values (6.0) are found at very localised points in the southwest of the island. In Gran Canaria, the minimum R values (1.0) are concentrated on the west coast and the high values (4.0, 5.0) on the east coast. Maximum values (6.0) are only found in the oriental region. However, occupying 73% of the La Palma coast and 78.9% of the Gran Canaria coast, the combinations of 2 and 3 *groups* are widely distributed without any geographic pattern along the coasts of both islands.

The richness and spatial distribution of the landforms along the coast of La Palma, lead to 156 types of specific morphoassemblages were found at *group* level. The predominant association was that of cliffs and gravel beaches (Cl-Gb). By contrast, in Gran Canaria a total of 234 morphoassemblages were found (Δ50.0%), with the predominant association being that of cliffs and platforms (Cl-Pt). At *subgroup* level, the number of morphoassemblages rises to 510 in La Palma and 666 in Gran Canaria (Δ30.6%).

The slope of the series in the rank-abundance plots (Fig. 6a-6b) reveals a greater evenness of classes for the coasts of Gran Canaria than for those of La Palma. Shannon entropy (H'), which incorporates this component in the value of diversity, shows that diversity at *group* level is 12.1% lower in La Palma (H'=1.87) than in Gran Canaria (H'=2.09). Diversity increases markedly at *subgroup* level both in La Palma (H'=2.66) and Gran Canaria (H'=2.96), by virtue of a logical increase in richness and general decrease in dominance. Nonetheless, the proportional difference remains practically constant at this taxonomic order (Δ11.1%) (Fig. 6c). Shannon index was not applied to the local analysis as the relative frequency of the classes is constant (p=1.0) when the coastal sections are defined beforehand by morphoassemblages.

The taxonomic distances resulting from specified methods (Fig. 2, Table 2), on which Rao's index (Q) is calculated, are gathered in the matrix of Table 3. The matrix meets the properties of symmetry: $d_{ij}=d_{ji}$, non-negativity: $d_{ij}\geq 0$, zero self-difference: $d_{ii}=0$, and triangle inequality: $d_{ij}\leq(d_{ik}+d_{kj})$ from key attributes (Ricotta and Avena, 2005). To evaluate the coherence of the d values, the statistics of the matrix were calculated by regions: (1) Rocky-erosive, (2) Mixed and (3) Clastic-depositional (Table 3, see statistical values). These values confirm that the distances are lower in regions 1 and 3, the extremes of the matrix, than in region 2, formed by their intersection. At the same time, the d statistics are very similar between regions 1 and 2, which ensures an equal weight of the macro-environments in the diversity calculations.

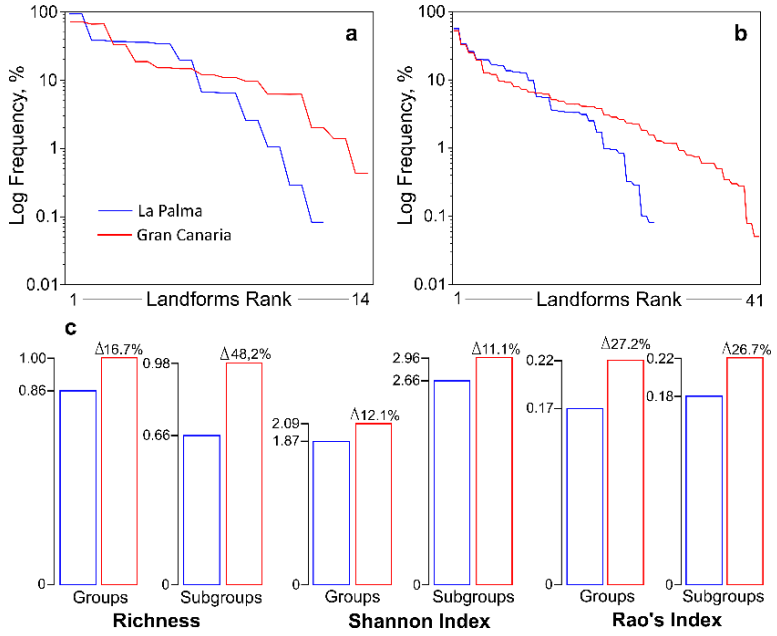

Fig. 6. Global results for the islands of La Palma and Gran Canaria; a) rank-abundance plot at *group* level; b) rank-abundance plot at *subgroup* level; c) comparison between islands of the values of richness (R), Shannon's index (H') and Rao's quadratic entropy index (Q), in *groups* and *subgroups* and showing their proportional variations.

At *group* level, Rao index has an overall value of Q=0.17 for the coasts of La Palma and Q=0.22 (Δ27.2%) for those of Gran Canaria (Fig. 6c). At subgroup level, the indices do not vary significantly, neither in absolute nor comparative terms, as the weight of differentiation by size is relatively low within the matrix of distances. At local level, the Q index was transformed into mean distance (δ_m) by discarding richness and abundances. The mapping (Fig. 5c) shows high spatial variability of δ_m without any clearly defined geographic pattern or significant spatial correlation with richness (r^2=0.03 in La Palma and r^2=0.17 in Gran Canaria). The frequency distribution of δ_m in Gran Canaria gives a leptokurtic-shaped curve, strongly concentrated in the modal interval [0.4, 0.6]. In La Palma, the distribution gives a positively-skewed asymmetric bell-shaped curve, less concentrated in the modal interval [0.2, 0.4] (Fig. 5c, see histograms). These distributions mean a general lower similarity (higher taxonomic distance) between the landforms which make up the coast of Gran Canaria than between those of La Palma, what is consistent with Q values.

Table 3. Taxonomic distances *d* derived from the key attributes and genetic dependencies (see Table 1 for acronym definitions).

Rocky/erosive (1)							Mixed (2)								
Cl	Pcl	Pt	Mt	St	Rf	Ld	Db	Gb	Sb	Dn	Pdn	Fm	Lg		
0.00	0.10	0.45	0.65	0.18	0.70	0.38	0.23	0.65	0.80	0.80	0.90	0.75	0.85	Cl	
0.10	0.00	0.65	0.38	0.45	0.75	0.45	0.33	0.75	0.90	0.64	0.70	0.56	0.85	Pcl	
0.45	0.65	0.00	0.20	0.40	0.30	0.30	0.60	0.45	0.75	0.90	0.85	0.75	0.80	Pt	Mixed (2)
0.65	0.38	0.20	0.00	0.50	0.45	0.40	0.70	0.50	0.65	0.80	0.55	0.70	0.70	Mt	
0.18	0.45	0.40	0.50	0.00	0.26	0.53	0.50	0.50	0.75	0.90	0.85	0.80	0.90	St	
0.70	0.75	0.30	0.45	0.26	0.00	0.34	0.55	0.35	0.38	0.75	0.60	0.75	0.75	Rf	
0.38	0.45	0.30	0.40	0.53	0.34	0.00	0.38	0.60	0.75	0.60	0.25	0.70	0.70	Ld	
							0.00	0.30	0.65	0.60	0.75	0.70	0.80	Db	
Mean (1)=0.42				Min (1)=0.10			0.30	0.00	0.25	0.60	0.75	0.45	0.45	Gb	Clastic/depos.
Mean (2)=0.67				Min (2)=0.23			0.65	0.25	0.00	0.18	0.60	0.26	0.26	Sb	
Mean (3)=0.45				Min (3)=0.08			0.60	0.60	0.18	0.00	0.18	0.30	0.30	Dn	
σ (1)=0.17				Max (1)=0.75			0.75	0.75	0.60	0.18	0.00	0.55	0.55	Pdn	
σ (2)=0.18				Max (2)=0.90			0.70	0.45	0.26	0.30	0.55	0.00	0.08	Fm	

σ (3)=0.21	Max (3)=0.80	0.80	0.45	0.26	0.30	0.55	0.08	0.00	Lg						

In the first of the tests to determine the consistency of the CDS model (Fig. 4a), the *p* values were subjected to successive changes of scale to observe their behaviour and the impact of the changes on the indices. Table 4 shows the variation in *p* for all the *groups* in each generalization step, from the initial scale of 1:5,000 to a scale of approximately 1:500,000 (T=1,000 m). In the test, the coastal length of La Palma contracted by 38.9% and of Gran Canaria by 29.7%. This means that La Palma has greater irregularity at finer scales. This is shown by the fractal dimension (D) at the 1:5,000 scale, which acquires a value of D=1.104 in La Palma and D=1.065 in Gran Canaria.

Table 4. Results of the fractal stress test. Generalization increases with the PAEK tolerance (T), decreasing coastal length (km) and fractal dimension (D), and inducing different behaviours in the *p* values of the geomorphic *groups* (see Table 1 for acronyms).

T	km	D	*p*-Cl	*p*-Pcl	*p*-Pt	*p*-Mt	*p*-St	*p*-Rf	*p*-Ld	*p*-Db	*p*-Gb	*p*-Sb	*p*-Dn	*p*-Pdn	*p*-Fm	*p*-Lg
La Palma																
-	198.6	1.104	.9015	.3267	.3518	.0000	.0620	.0101	.369	.1862	.3440	.0626	.0028	.0000	.0246	.0008
5	196.6	1.103	.9027	.3252	.3532	.0000	.0630	.0108	.3650	.1880	.3482	.0635	.0028	.0000	.0250	.0008
10	192.5	1.100	.9037	.3220	.3486	.0000	.0626	.0107	.3609	.1895	.3526	.0641	.0027	.0000	.0254	.0008
20	184.4	1.093	.9054	.3156	.3398	.0000	.0614	.0107	.3525	.1930	.3614	.0655	.0027	.0000	.0264	.0008
30	177.8	1.086	.9065	.3101	.3326	.0000	.0600	.0108	.3451	.1966	.3695	.0667	.0027	.0000	.0273	.0008
40	172.4	1.079	.9071	.3056	.3267	.0000	.0586	.0109	.3390	.2000	.3764	.0678	.0028	.0000	.0280	.0008
50	167.9	1.073	.9074	.3019	.3217	.0000	.0575	.0109	.3339	.2030	.3824	.0687	.0028	.0000	.0286	.0008
60	164.1	1.069	.9077	.2989	.3176	.0000	.0565	.0111	.3296	.2058	.3879	.0696	.0029	.0000	.0292	.0008
70	160.8	1.065	.9077	.2963	.3138	.0000	.0554	.0110	.3260	.2083	.3929	.0704	.0029	.0000	.0297	.0008
80	157.9	1.060	.9078	.2941	.3106	.0000	.0544	.0111	.3228	.2106	.3975	.0712	.0030	.0000	.0301	.0008
90	155.4	1.055	.9077	.2922	.3077	.0000	.0535	.0112	.3201	.2126	.4016	.0718	.0030	.0000	.0305	.0008
100	153.1	1.052	.9077	.2904	.3051	.0000	.0527	.0112	.3176	.2145	.4054	.0724	.0031	.0000	.0309	.0008
125	148.5	1.045	.9076	.2869	.2996	.0000	.0513	.0113	.3126	.2187	.4139	.0737	.0032	.0000	.0317	.0008
150	144.8	1.038	.9073	.2842	.2953	.0000	.0502	.0114	.3088	.2220	.4212	.0747	.0033	.0000	.0324	.0009
175	141.8	1.034	.9070	.2820	.2919	.0000	.0494	.0117	.3056	.2248	.4275	.0757	.0033	.0000	.0330	.0009
200	139.4	1.031	.9067	.2803	.2892	.0000	.0488	.0118	.3033	.2269	.4329	.0766	.0034	.0000	.0334	.0009
225	137.5	1.028	.9064	.2792	.2874	.0000	.0483	.0118	.3015	.2287	.4378	.0774	.0034	.0000	.0338	.0009
250	135.8	1.025	.9060	.2783	.2858	.0000	.0482	.0120	.3003	.2301	.4417	.0780	.0034	.0000	.0341	.0009
275	134.4	1.023	.9057	.2778	.2843	.0000	.0478	.0122	.2994	.2313	.4452	.0784	.0035	.0000	.0344	.0009
300	133.1	1.022	.9054	.2774	.2828	.0000	.0476	.0121	.2986	.2325	.4485	.0790	.0035	.0000	.0346	.0009
350	131.1	1.018	.9048	.2769	.2813	.0000	.0473	.0122	.2977	.2340	.4541	.0797	.0035	.0000	.0350	.0009
400	129.6	1.019	.9044	.2767	.2798	.0000	.0471	.0124	.2979	.2352	.4580	.0803	.0035	.0000	.0353	.0009
450	128.3	1.014	.9038	.2769	.2787	.0000	.0473	.0126	.2972	.2364	.4618	.0810	.0036	.0000	.0355	.0009
500	127.2	1.014	.9035	.2771	.2779	.0000	.0474	.0127	.2978	.2372	.4651	.0815	.0036	.0000	.0358	.0009
600	125.5	1.012	.9035	.2771	.2779	.0000	.0474	.0127	.2978	.2372	.4651	.0815	.0036	.0000	.0358	.0009
700	124.1	1.010	.9028	.2780	.2763	.0000	.0478	.0129	.2977	.2389	.4745	.0832	.0036	.0000	.0364	.0009
800	123.0	1.008	.9023	.2786	.2756	.0000	.0480	.0131	.2981	.2399	.4783	.0839	.0037	.0000	.0367	.0009
900	122.1	1.007	.9020	.2791	.2751	.0000	.0481	.0132	.2983	.2406	.4812	.0844	.0036	.0000	.0368	.0009
1000	121.3	1.005	.9017	.2794	.2750	.0000	.0482	.0131	.2986	.2412	.4835	.0851	.0037	.0000	.0369	.0009
Var%	-38.9	-9.0	0.03	-14.5	-21.8	0.0	-22.2	30.0	-18.6	29.5	40.5	35.9	31.6	0.00	49.9	17.8
Gran Canaria																
-	261.9	1.065	.6841	.1447	.6298	.1400	.0133	.0192	.0592	.1135	.3157	.1769	.0588	.0926	.1036	.0041
5	259.4	1.064	.6836	.1447	.6308	.1414	.0135	.0196	.0591	.1138	.3196	.1790	.0595	.0927	.1049	.0042
10	254.5	1.061	.6807	.1441	.6274	.1409	.0134	.0197	.0588	.1129	.3227	.1815	.0605	.0926	.1067	.0043
20	246.1	1.055	.6762	.1428	.6214	.1399	.0131	.0199	.0582	.1120	.3313	.1868	.0623	.0927	.1099	.0044
30	239.7	1.050	.6726	.1416	.6159	.1390	.0127	.0197	.0575	.1114	.3335	.1895	.0637	.0929	.1123	.0045
40	234.7	1.047	.6703	.1405	.6115	.1382	.0123	.0200	.0569	.1114	.3396	.1929	.0649	.0932	.1143	.0046
50	230.7	1.043	.6683	.1395	.6081	.1375	.0120	.0200	.0564	.1113	.3425	.1951	.0659	.0935	.1159	.0047
60	227.4	1.040	.6667	.1387	.6055	.1369	.0117	.0200	.0559	.1113	.3449	.1969	.0666	.0937	.1173	.0047
70	224.6	1.037	.6654	.1379	.6033	.1363	.0112	.0200	.0554	.1113	.3468	.1984	.0673	.0939	.1184	.0048
80	222.2	1.036	.6643	.1373	.6016	.1358	.0112	.0200	.0550	.1113	.3484	.1996	.0679	.0941	.1194	.0048
90	220.1	1.033	.6633	.1367	.6002	.1354	.0110	.0200	.0547	.1114	.3497	.2007	.0683	.0942	.1202	.0049
100	218.2	1.031	.6625	.1363	.5990	.1350	.0108	.0200	.0544	.1114	.3509	.2015	.0688	.0943	.1210	.0049
125	214.4	1.027	.6609	.1354	.5964	.1342	.0105	.0201	.0537	.1116	.3543	.2036	.0697	.0943	.1225	.0050
150	211.4	1.024	.6597	.1348	.5945	.1337	.0104	.0203	.0532	.1118	.3570	.2053	.0703	.0942	.1237	.0050
175	208.9	1.023	.6587	.1345	.5932	.1333	.0103	.0204	.0528	.1119	.3595	.2067	.0709	.0939	.1248	.0051
200	206.8	1.020	.6578	.1343	.5920	.1330	.0102	.0205	.0524	.1120	.3616	.2079	.0714	.0937	.1256	.0051
225	204.9	1.018	.6571	.1342	.5908	.1328	.0101	.0206	.0520	.1121	.3635	.2089	.0718	.0935	.1263	.0052
250	203.3	1.017	.6565	.1341	.5897	.1327	.0100	.0207	.0517	.1121	.3653	.2099	.0722	.0932	.1270	.0052
275	201.8	1.017	.6559	.1341	.5888	.1325	.0100	.0208	.0514	.1123	.3668	.2106	.0725	.0930	.1275	.0052
300	200.5	1.016	.6554	.1341	.5879	.1325	.0100	.0209	.0511	.1123	.3684	.2113	.0728	.0927	.1280	.0053
350	198.2	1.014	.6545	.1342	.5865	.1324	.0099	.0210	.0506	.1125	.3708	.2127	.0733	.0922	.1289	.0053
400	196.2	1.011	.6531	.1345	.5835	.1324	.0099	.0214	.0502	.1129	.3748	.2149	.0738	.0917	.1303	.0054
450	194.5	1.010	.6529	.1347	.5839	.1324	.0099	.0212	.0499	.1128	.3751	.2148	.0741	.0912	.1305	.0054

500	193.0	1.009	.6522	.1350	.5829	.1325	.0099	.0213	.0497	.1129	.3768	.2157	.0744	.0908	.1313	.0054
600	190.4	1.007	.6511	.1356	.5812	.1327	.0098	.0215	.0493	.1131	.3798	.2171	.0750	.0900	.1323	.0055
700	188.4	1.006	.6502	.1361	.5797	.1329	.0099	.0215	.0491	.1134	.3824	.2183	.0754	.0894	.1332	.0055
800	186.7	1.005	.6493	.1366	.5786	.1331	.0100	.0215	.0489	.1137	.3843	.2185	.0758	.0887	.1342	.0055
900	185.3	1.004	.6486	.1369	.5775	.1333	.0100	.0217	.0488	.1142	.3859	.2202	.0761	.0881	.1348	.0055
1000	184.0	1.004	.6480	.1374	.5764	.1334	.0100	.0218	.0487	.1144	.3874	.2211	.0764	.0875	.1355	.0055
Var%	-29.7	-5.7	-5.3	-5.1	-8.5	-4.7	-24.9	13.4	-17.7	0.8	22.7	25.0	29.9	-5.6	30.7	33.8

Each *group* experiences a different evolution according to its frequency and fractality. First, the higher the frequency of *groups*, the higher the variation in absolute terms of linear units (r_s=0.942, p<0.01). Second, the lower the frequency of groups, the higher variation in relative terms of proportionality (r_s=-0.453, p<0.05). In addition, the relative loss of length has a greater effect on the *rocky-erosive groups* (T-Test=-10.57, p<0.01), in which irregularity is commonly higher. In these *groups*, where there was originally 1 m of coast this value had contracted by the end of the test to, on average, 0.60 m. The corresponding final value for the *clastic-depositional groups* was 0.83 m. Likewise, negative balances of *p* at the end of the test affected the *groups* with greater frequency (*Pcl*, *Pt*, *Ld* and *St*, in La Palma; *Cl*, *Pcl*, *Pt*, *Ld*, *St*, *Mt*, and *Pdn*, in Gran Canaria). In the generalization process, the relative frequency of these, more irregular landforms, tends to decrease, whereas for the other landforms it tends to increase. The *Mt* and *Pcl groups*, in Gran Canaria, and *Pcl*, in La Palma, change from a negative to a positive tendency around D=1.01. In the *Db group* of Gran Canaria, this occurs at D=1.04. Conversely, in the *Pdn group* of Gran Canaria and *Cl* of La Palma, a positive tendency becomes negative. In the first at D=1.03 and the second at D=1.06.

The effect of the behaviours of *p* on the Shannon (H') and Rao (Q) indices is shown in Figure 7. It can be seen how the indices of diversity tend to grow with cartographic generalization. This growth can be explained through the general increase of evenness (decrease and increase of *p*, respectively, in the more and the less abundant landforms) and the general increase of density (from 2.59 km to 2.63 km of landforms per km of coast). The values of H' and Q tend to stabilise as the T values of the algorithm increase. However, this stabilisation is not observed with respect to the fractal dimension (D) decrease, except in the Q values in Gran Canaria. The values of diversity in the bounds of D are unknown. However, the narrow range of variation of the values in the test indicates the consistency of the CDS procedure within reasonable scales in practical mapping. This range of variation can be considered the expected error in the choice of coastline scale and allows estimation of corrected Shannon (H_c') and Rao (Q_c) values. In La Palma, these values are H_c'=1.88±0.008 and Q_c=0.183±0.004; and in Gran Canaria, H_c'=2.11±0.019 and Q_c=0.232±0.003. The corrected values are slightly higher than the original ones, but the differences between islands remain stable (Δ12.8% in H_c' and Δ26.8% in Q_c). Despite the important metric and morphologic variation between the cartographic scales of 1:5,000 and 1:500,000, with significant changes in the values of *p*, the error range in the indices is below 2%.

The second test was performed to enable a comparison of geomorphological diversity values in coasts of different size (Fig. 4b). The results are shown in Figure 8. The values for La Palma are the total values obtained previously. Those for Gran Canaria, however, are the result of applying a moving-window with the size of the coast of La Palma (198 km). Firstly, it can be seen that richness (R) at *group* level does not suffer any variation. This means that in Gran Canaria all the *groups* are included in any 198 km section. Variation was, however, detected at *subgroup* level: no 198 km section includes all the *subgroups*, as the maximum value obtained is equivalent to the total value and the minimum value is significantly above the total value of La Palma. In Shannon's entropy index (H'), both in *groups* and *subgroups*, the maximum value obtained exceeds the total value, which lies between the mean and the 75th percentile, while the minimum value is slightly above the total value of La Palma. Finally, the values of Rao's index (Q), similar between *groups* and *subgroups*, have a fairly symmetric distribution, with the maximum value above the total value, the total value very close to the mean value, though above it, and the minimum value clearly above the total value of La Palma. It is shown, therefore, that, although a

greater sample size can entail an increase in diversity (mean values of the moving-window compared with total values of Gran Canaria), no section of the Gran Canaria coast of same size as the coastal perimeter of La Palma has less diversity than La Palma (minimum values of the moving-window compared with total values of La Palma).

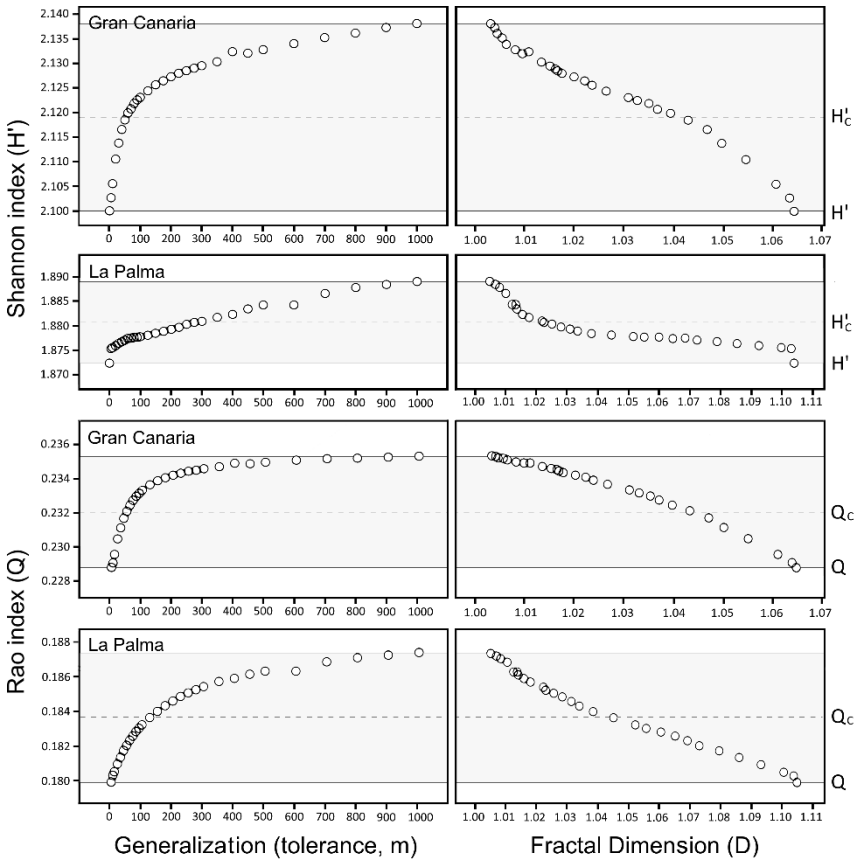

Fig. 7. Effect of scalar fluctuations of *p* on the Shannon entropy (H') and Rao (Q) indices. The grey areas represent the range of variation (scale error approximation), and the dashed line the corrected Shannon (H'_c) and Rao (Q_c) values.

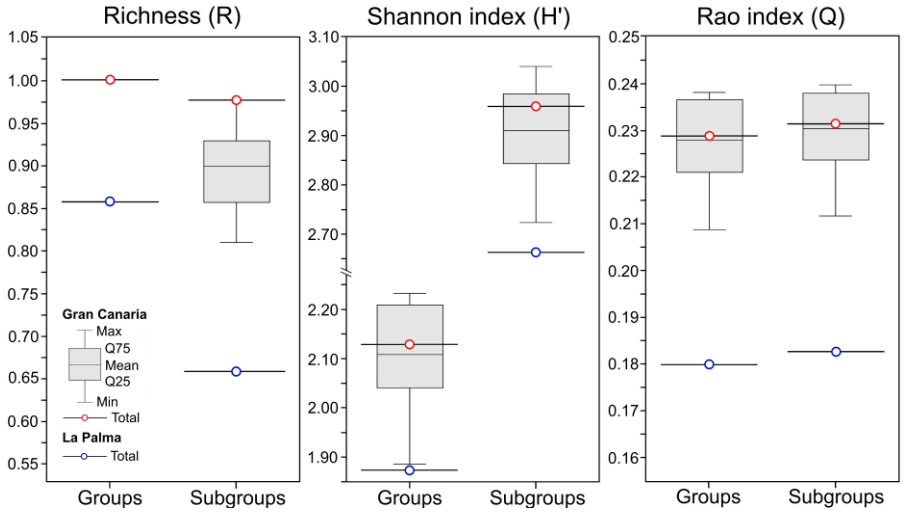

Fig. 8. Box plot showing the results of the moving-window test.

5. Discussion

5.1. Towards a quantitative geomorphological diversity

The geodiversity is used in abundance as a conceptual backdrop to refer the set of nature's abiotic elements, prefigured as being a diverse or heterogeneous totality, but without a particular interest to measure it. In few occasions, as in this study, is there any actual attempt made to tackle the problem of estimating or measuring the spatial heterogeneity or variability of the geo-elements. This study entails a conceptual and methodological contribution to advances in quantitative geodiversity as a growing research field, in which diversity is the problem itself and not only an implicit and preconceived characteristic of the abiotic nature.

A general ambition to measure geodiversity in a 'holistic' manner (Zwoliński et al., 2017) has led to a tendency to lump together all, or at least a large part, of what are considered elements of geodiversity (geology, geomorphology, edaphology, etc.) in the same analytical process (Benito-Calvo et al., 2009; Serrano et al., 2009; Hjort and Luoto, 2010; Ruban, 2010; Pellitero et al., 2011; Pereira et al., 2013; Argyriou et al., 2016; Ilić et al., 2016; Kot, 2017; Melelli et al., 2017; Özşahin, 2017; Stepišnik and Trenchovska, 2018). In some of these cases, the sheer amount of heterogeneity in the primary data can cause major difficulties when it comes to interpreting the results. Specific approaches which focus on a single component of geodiversity are few. The advances in pedodiversity studies (Ibáñez et al., 1995; Guo et al., 2003; Ibáñez et al., 2005; Minasny and McBratney, 2007; Minasny et al., 2010) show that while the 'all-encompassing' perspective is the defining feature of the conceptual framework of geodiversity (Gray, 2005, 2008), it should not exclude the development of sub-topics which allow a more in-depth analysis into specific aspects. In this respect, the present work undertakes a specific development in the field of geomorphological diversity. Although the importance of the geomorphology as a natural component in the configuration of landscapes and ecosystems has been underlined (sufficient justification for its separate and in-depth treatment), it has tended in the end to be combined with other variables in the geodiversity studies (e.g. Kot, 2017; Melelli et al., 2017).

As for the methodological problems, Jie et al. (2001) argue that geodiversity as a practice is not exempt from uncertainty; if biodiversity has a physically well delimited reference in the individual, geodiversity operates over a *continuum* (the Earth surface), where the boundaries of classes are diffuse and scale-dependent. Despite of this, the central role that is played by categories (landforms) in the geomorphology science means that the question of diversity must be structured around them. While geomorphology is conceptually rooted in the use of categories, no relational and standardised system of classes exists, which does not guarantee an appropriate framework for spatio-temporal analyses and comparisons. The presented classification of coastal landforms is a step in this direction. In its hierarchical structure, the *groups* are the central categories (cliffs, beaches, platforms, etc.) and the *subgroups* are parametric intervals of Euclidean measuring series, which add relevant information about the spatial development of the landforms and landscape structure (Table 1).

On the quantification of geodiversity, the main component usually analysed is richness (Serrano et al., 2009; Hjort and Luoto, 2010; Ruban, 2010; Pellitero et al., 2011; Pereira et al., 2013; Ilić et al., 2016; Melelli et al., 2017; Özşahin, 2017; Stepišnik and Trenchovska, 2018), generally using the special index proposed by Serrano and Ruiz-Flaño (2007). In this formulation the number of distinct elements (richness), multiplied by a parameter of terrain roughness, is divided by the log of the surface area, which apparently invokes an adaptation of Margalef's richness index (1958) to the problem of geodiversity. Other components or parameters of diversity are rarely taken into consideration (Benito-Calvo et al., 2009; Malinowska and Szumacher, 2013; Argyriou et al., 2016; Ferrer-Valero et al., 2017). In this work, in addition to richness, evenness and dissimilarity have been incorporated. In particular, dissimilarity has not

been reported in any other geodiversity study. It has been analysed through the identification of key attributes (Table 2), genetic dependencies (Fig. 2a) and sizing differentiation of the landforms (Fig. 2b). This proposal is based on previous developments in the fields of pedodiversity (Minasny et al., 2010; Van Huyssteen et al., 2014; Smirnova and Gerasimova, 2017) and biodiversity (Owens and Bennet, 2000; Clarke and Warwick, 2001; Faith, 2002).

5.2. Solutions and results on coasts

The geomorphological diversity analysis has been carried out in coastal environments, recognized high-geodiversity environments (Gray, 2008) where no other studies have been undertaken from this perspective.

One of the peculiarities of coasts as opposed to other environments is the existence of a constant spatial reference which structures the landscape. This reference is the land-sea limit, or coastline, which allows the expression of the abundance of any entity by its extension along it. Thus, the coastline data-storing procedure (CDS) proposed in this work becomes a proxy of presence and abundance in coastal environments, an alternative to widespread used surface-area estimations. As it is shown, CDS is an efficient way to describe and analyse the structure of coastal landscapes. It enables probabilistic computation, significantly reducing the cartographic work required, and opens up the possibilities of a crosswise interpretation which shows the spatial combination of landforms alongshore (morphoassemblages) (Fig. 3).

The results obtained offer quantitative data of geomorphological diversity and show that the CDS method is robust to compare samples, having evaluated the fractal and rarefaction issues by specific methodologies (Fig. 4). CDS has enabled to observe inside-island contrasts of diversity from the local analyses of cross-shore morphoassemblages (Fig. 5), as well as the comparison the overall diversity between of two entire coasts (Fig. 6). The comparison clearly shows that the island of Gran Canaria has greater coastal diversity than the island of La Palma in its three components: richness, evenness and dissimilarity (Fig. 6). Evaluated, respectively, through the indices of richness (R), Shannon's entropy (H') and Rao's quadratic entropy (Q), a minimum value of proportional variation was obtained of Δ11.1% (H'-*subgroups*), a maximum of Δ48.2% (R - *subgroups*) and an overall mean of Δ23.6%. It can be seen that the contrast of diversity is more pronounced in richness and taxonomic dissimilarity than in evenness. Likewise, it is seen that the disaggregation of the *groups* into dimensional *subgroups* by natural breaks method (Jenks, 1967) generates an increase of differentiation and, as is logical, an increase of diversity in the three indices of both islands. In particular, the disaggregation into *subgroups* has enabled a notably amplified observation of the general geomorphological richness of these coastal landscapes. By contrast, Rao's index, calculated on the basis on a taxonomic distance matrix (Table 3), experiences only a slight increase, and so in future studies it is proposed to work increasing the taxonomic distance on the grounds of size with a view to enabling detection of bigger differences with the process of parametric disaggregation.

Before stating definitively that the coast of Gran Canaria is more diverse than that of La Palma, the influence of two methodological uncertainties derived from CDS was examined. First, the fractal influence. The frequency values and the results of the indices were subjected to a fractal stress test to determine the soundness of the method. As a result of the test, a small scalar variation was obtained which determines an acceptable error in the choice of the cartographic resolution of the coastline (Table 4, Fig. 7). Second, the influence of size of the coast on the final values. As the general behaviour of geomorphological diversity with coastal length was unknown, the use of coefficients was avoided (Margalef, 1958; Serrano and Ruiz-Flaño, 2007) and a re-sampling technique based on the moving-window method was implemented. Linear moving-windows have been widely used in the boundaries detection in ecological communities (Erdős et al., 2014), but in the present study it is used as a rarefaction technique in coastal geodiversity. Through the moving-window analysis it was possible to precisely determine that the diversity of

equivalent portions is, in all the indices and taxonomic levels, always higher in Gran Canaria (Fig. 8).

The explanation for the diversity contrasts found between these two hotspot intraplate islands could lie in the geological age of the two islands. Whereas La Palma is a fully active recent volcanic shield, Gran Canaria is an extinct stratovolcano in an erosional process (Carracedo et al., 1998). More than 12 million years separate the origin of the two islands, and so the development of coastal morphologies is linked to the passage of time at different scales. The contrast in diversity that was observed could reveal a pattern of increase in the complexity of coastal systems in the first few millions of years after the emergence of a submarine volcano and the formation of a new land-sea boundary. In consequence, the interpretation of these results from an evolutionary perspective can open the door to new research hypotheses in the question of coastal evolution, additionally demonstrating the scientific potential of such specific approaches in geodiversity.

6. Conclusions

The methodology developed in the present study integrates new cartographic, taxonomic and numerical procedures for the estimation of coastal geomorphologic diversity. It was applied to two coasts of hotspot volcanic islands in the Canary archipelago (La Palma and Gran Canaria). Given the absence of geomorphological mapping for these areas, the information was obtained by direct methods through the analysis of remote sources, mainly aerial orthophotos and LiDAR-based terrain digital model (TDM), and *in situ* verification. In consequence, an extensive database was obtained differentiating more than 17,500 sections along 459 km of coastline. Such a volume of data ensures the statistical significance of the results, which indicate the existence of a notably higher geomorphological diversity in Gran Canaria compared to La Palma. This difference is seen in different proportions in the three components of diversity that were analysed: richness, evenness and dissimilarity.

The main contributions of this work are as follows: i) a specific approach to geomorphological diversity, including a significant effort in the direct gathering of the primary data; ii) the application of this approach to coastal environments, with the development of a geomorphological taxonomy specifically designed for the analysis of diversity; iii) the incorporation of indices and components which have not previously been contemplated in geodiversity; and iv) the development of an alternative analytical mapping procedure for the execution of the analyses.

The results open up a new line of research based on the hypothesis of a correlation between the diversity-complexity of coastal systems and geological time in intraplate hotspot volcanic islands. This shows how specific approaches in geodiversity can lead to a more in-depth understanding of the subject and contribute to its scientific potential.

Acknowledgments

This work is a contribution to the CSO2013-43256-R and CSO2016-79673-R projects of the Spanish National Plan for R+D+i (innovation), co-financed with ERDF funds, and was supported by a FPI-PhD grant from the Universidad de Las Palmas de Gran Canaria (E-35-2014-0231941). It was completed while N. Ferrer Valero was a Ph.D. student in the IOCAG Ph.D. Program in Oceanography and Global Change. Special thanks are expressed to Luis Hernández-Calvento (Oceanography and Global Change Institute, ULPGC) and Juan Bautista Gallego Fernández (Plant Biology and Ecology Department, US) for their recommendations that have helped to improve the quality of manuscript.

Insights of long-term geomorphological evolution of coastal landscapes in hot-spot oceanic islands

Nicolás Ferrer-Valero, Luis Hernández-Calvento, Antonio I. Hernández-Cordero

Earth Surface Processes and Landforms

DOI: 10.1002/esp.4518

Abstract

The Canary Islands form a volcanic archipelago in which a W-E chain of progressively older and less active islands can be observed. In the Canary Islands, unlike most hot-spot archipelagos, certain geodynamic peculiarities have promoted longer periods of island survival, exceeding 20 My. This factor makes these islands a suitable context for this work, which aims to analyze extensively the coastal geomorphic structure on islands with different development states. For this, three islands in different volcanic phases were selected: La Palma (1.8 My), Gran Canaria (14.5 My) and Fuerteventura (22.6 My). An ad hoc landform-based hierarchical taxonomy was designed to analyse the coastal geomorphic structure of the three islands. Based on a multi-sourced analysis in GIS and field recognition, a comprehensive cartographic database was collected using the CDS method as a feature abundance proxy. Three different aspects of the geomorphological structure were compared and related between the islands: (i) composition, (ii) abundance and (iii) diversity. Through their comparison, we attempt to explore geomorphological aspects of coastal evolution over geological spatiotemporal scales. Composition was explored analyzing the distribution of the feature's longshore frequencies (p). Abundance, by metrics of Local abundance ($N_{\cap}$) and Whole density (N_{U}). Diversity, through four indices: Normalized Richness (S) and Margalef index (M) to estimate richness; Simpson (D) and Shannon (H') indices to estimate evenness. We identified a systematic transformation in the dominant landform composition and a systematic trend in increasing geomorphological abundance and diversity from younger to older islands. The results show a long-term structural pattern defined by the increase in coastal geomorphic complexity (abundance and diversity) over geological time, as the coasts evolve from predominantly rocky-erosive to increasingly clastic-depositional environments. This long-term geomorphological pattern may be a general aspect of hot-spot island archipelagos, which can bring a new perspective to the knowledge of their coastal evolution.

Keywords: Landscape evolution; coastal landforms; geodiversity; Canary Islands.

1. Introduction

Intraplate hot-spot oceanic islands (e.g. Hawaii, Canary Islands, Cape Verde or Reunion, among others) represent a very small proportion of the Earth's land surface (around 0.04% of emerged landmasses), forming highly singular geotectonic contexts. The prototypical model of hot-spot islands involves the movement of a lithospheric plate over a stationary mantle plume, which results in an alignment of progressively more youthful islands in the opposite direction of the plate movement (Wilson, 1963; McDougall, 1971; Langenheim and Clague, 1987; Moore, 1987). The specificity of this geophysical process leads to the particular configuration of these archipelagos. The intraplate oceanic islands can form clustered groups or isolated islands (Nunn, in Finkl, 2004), but the prototypical result of hot-spot processes is a chain with an orderly progression of ages. For this reason, these archipelagos have been of interest for the study of the evolution of terrestrial and submarine reliefs since the nineteenth century (Menard, 1986), making them especially interesting for the study of coastal evolution (Woodroffe, 2014).

Geochronological, seismic and geochemical studies, conducted throughout the Canary Islands, indicate the necessary intervention of a mantle anomaly in its formation. In this way, the origin of the Canary Islands responds to a hot-spot model (Carracedo, 1999; Carracedo et al., 1998, 2001; Hoernle and Carracedo, 2009). However, the existence of an old, thick and rigid lithosphere, with slow displacement, is a regional geophysical peculiarity of the Canary Islands which determines geodynamic differences with respect to the Hawaiian hot-spot model, the most studied of the hot-spot archipelagos. The most important aspect for this study is the long periods of survival of the Canary Islands due to the absence of long-term tectonic subsidence after the hot-spot separation, as it is observed in the Hawaiian archipelago. In general, the islands of the Pacific hot-spot archipelagos do not survive beyond 5 My before being submerged, whereas in the Canary Islands, 20 My are exceeded (Carracedo et al., 1998; Schmincke and Sumita, 1998; Acosta et al., 2003, 2005). These long periods of survival of the islands are an opportunity to observe costal geomorphic processes and transformations that take place over longer periods of time.

Theories of long-term coastal evolution have traditionally supported the concepts of youth and maturity. These classical schemes try to establish how coasts change their morphology over time and suggest progression from characteristic coastal structures and typologies. Johnson (1919), inspired by the 19th-century ideas of Danna and Davis, recognized the existence of emergence, submergence and neutral coasts, and tried to systematize their evolution into a scheme of sequential stages: initial, young, mature and old. Shepard (1937, 1976), as an alternative to Johnson's scheme, introduced a simple classification system based on the genetic-evolutionary concepts of (i) primary or youthful coasts, where dominant morphology is related to non-marine processes (volcanic, fluvial, glacial, etc.), and (ii) secondary or mature coasts, where marine modelled landforms have already been developed. Inman and Nordstrom (1971), on the basis of previous authors (Cotton, 1954; Mitchell and Reading, 1969) and using also the 'youthful' and 'mature' conceptualizations, divided the coasts of passive margins into (i) neo-trailing-edge coasts, (ii) afro-coasts and (iii) amero-coasts.

This paper addresses the study of quantifiable key aspects of the geomorphological evolution of coastal landscapes at geological time-scales. For this, a space-for-time substitution (Pickett, 1989) is applied to three oceanic hot-spot islands of the Canary archipelago, with progressively older ages and highly differentiated evolutionary states. The islands are similar in terms of lithological composition, allowing control of dynamic factors, and in consequence, allowing time as a dimension to be isolated. The space-for-time reasoning assumes that spatial and temporal variation are equivalent to inferring long-term trends from a study of different-aged sites (Pickett, 1989). In this way, observing three common-origin islands with different ages, we could infer evolutionary features of one theoretical island. This reasoning for island chains was adopted by Darwin (1842) in relation to the evolution of coral reefs, or by Dana (1890) to deduce

the existence of temporal sequences in the subaerial erosion of oceanic volcanoes (Menard, 1986).

From an exhaustive geomorphological mapping and metrics comparison between the coasts of geologically similar but different-aged islands, we aim to analyze the spatiotemporal relations between (i) the typological long-term changes in the dominant coastal landform composition, (ii) the general long-term proliferation, or abundance, of landforms on the coasts, and (iii) the long-term evolution of coastal geomorphic diversity. Hereinafter, abundance and diversity are jointly referred to as geomorphic complexity. It is not therefore used in the same sense as 'coastal complexity', which commonly refers to the planform of coastlines (e.g. Bartley et al., 2001; Porter-Smith and McKinlay, 2012).

This approach can contribute to the knowledge of coastal evolution from a novel perspective, and represents a new application in the growing field of geodiversity (Gray, 2005; Serrano and Ruiz-Flaño, 2007; Gray, 2008; Benito-Calvo et al., 2009; Hjort and Luoto, 2010; Pellitero et al., 2011; Pereira et al., 2013; Melelli et al., 2017) and its relationship with the provisioning of habitats for biodiversity (Hjort et al., 2012; Tukiainen et al., 2017).

2. Study coasts

The Canary archipelago is an E-W oriented island chain, formed by 7 main islands and some islets, located on the African plate, between 27º-29º latitude North and 13º-18º longitude West (Figure 1). The entire coasts of La Palma, Gran Canaria and Fuerteventura, 844 km in total, were analyzed for the purposes of this study. Each of these islands is highly representative of the different evolutionary stages of the oceanic hot-spot islands.

La Palma, located at the western end of the archipelago, 400 km offshore of Africa, is the youngest island selected, less than 1.8 My old. Located on top of the theoretically inferred hot-spot, it is in a state of intense volcanic activity. It is a growing volcanic shield, composed of alkaline mafic lavas, with a Pleistocene subcircular volcano in the north, Taburiente, and a rift system, Cumbre Vieja, formed in the south during the Upper Pleistocene and Holocene (Carracedo et al., 2001; Acosta et al., 2003, 2005; Hoernle and Carracedo, 2009). This structure gives the island an inverted triangle shape, with a perimeter of almost 200 km, an area of 708 km^2 and an altitude of 2,426 m at its highest point.

Gran Canaria has an intermediate age, 14.5 My, and occupies a central position in the archipelago. It is composed of a single Miocene volcanic shield made of mafic lavas, which later produced explosive eruptions (ignimbrites) and extrusions of large volumes of differentiated lavas. The Plio-Quaternary post-erosive volcanism began about 3.7 My, after an erosive hiatus of approximately 4 My (Schmincke and Sumita, 1998; Hoernle and Carracedo, 2009; Karátson et al., 2016). The most recent reconstructions indicate that Gran Canaria reached an altitude of more than 3,000 m in its highest growth phase (Karátson et al., 2016). After long periods of erosion, it currently reaches a maximum altitude of 1,956 m, with a total area of 1,560 km^2 and a subcircular perimeter of 261 km.

Fuerteventura is the closest island to the African continental margin (100 km). The first subaerial emissions began more than 20 My ago, forming as such one of the longest-lived hot-spot islands on the Earth. The subaerial volcanism of Fuerteventura is composed mainly of three independent Miocene shields, north, south and central, arranged in a NE-SW direction (Ancochea et al, 1996), followed by Plio-Pleistocene eruptions after approximately 5 million years of volcanic inactivity (Hoernle and Carracedo, 2009). This structure gives it an elongated form, with an extension of 1,659 km^2 and a perimeter of 385 km. The prolonged erosive period has generated low altitudes, reaching a maximum of 817 m in the Jandía peninsula. However, it is estimated that the Miocene shields could have reached 3,000 m altitude during their phases of maximum growth (Stillman, 1999).

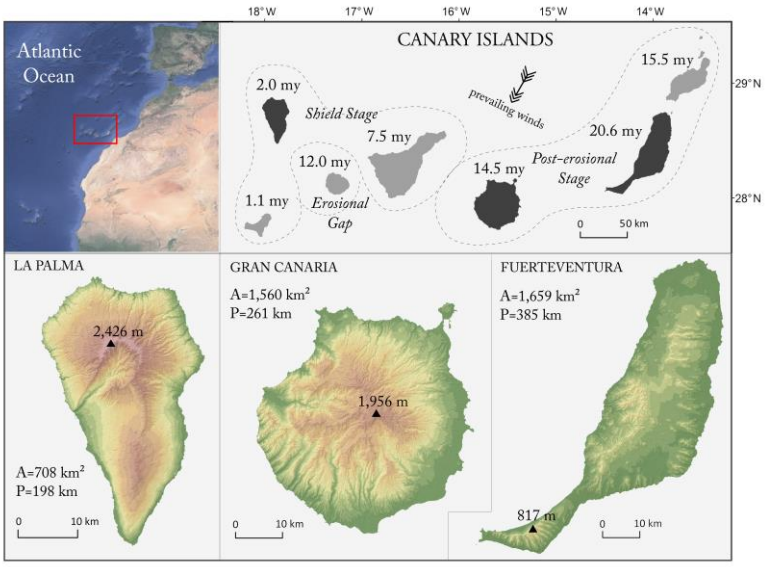

Fig 1. Study area. Ages of the islands (my, millions of years) and phases of the volcanic evolution of the Canary Islands according to Carracedo et al. (1998). Below, hypsometric maps of the islands studied; A, area; P, perimeter at 1:5000 scale.

The prevailing climate in the Canary Islands is subtropical. The NNE trade winds regime determines average annual temperatures close to 20°C at the coasts, although the temperature varies significantly with altitude and exposure to prevailing winds. Aridity is widespread at sea level. It becomes more accentuated on the leeward southern-slopes of the islands, where annual precipitation is lower than 100 mm in many areas, and from the western towards the eastern islands (Marzol Jaén, 1987).

The Canary Current generates mean water temperatures close to 20°C, relatively cold for the latitudinal position of the archipelago. These conditions inhibit the formation of coral reefs around the islands, and largely determine the modern marine dynamics of the archipelago and its coastal evolution (Menard, 1986; Ramalho et al., 2013, Woodroffe, 2014). A medium-energy wave regime is produced by the combined effect of swell and wind waves, presenting important contrasts between the exposed north and the sheltered south, as well as between the coasts of the more energetic western islands and the less energetic eastern ones. The tidal regime is semi-diurnal and meso-tidal, with a maximum range of 3 m.

3. Materials and methods

3.1. Primary sources

The coastal landforms of La Palma, Gran Canaria and Fuerteventura were systematically classified and mapped in detail by integrating photographic and cartographic sources into geographic information systems (GIS) and fieldwork for recognition. The sources integrated in GIS cover all the islands and are mainly 10 series of digital orthophotos (2002, 2005, 2007, 2008, 2009, 2011, 2012, 2013, 2014, 2015), with spatial resolutions between 10 and 50 cm/pixel (Spatial Data Infrastructure of the Canary Islands, https://www.idecanarias.es); LiDAR altimetry with a resolution of 0.5 points/m^2 (Instituto Geográfico Nacional, IGN); geological maps 1:25,000 (Instituto Geológico y Minero de España, IGME); and vegetation maps 1:25,000 (del Arco et al.,

2006). In addition, the field work, conducted over 2015/16, included numerous photo campaigns by land and three campaigns by sea aboard light boats.

Due to the profound anthropogenic transformation of some coastal areas of the Canaries during the second half of the 20th century (Pérez-Chacón et al., 2007; Hernández-Calvento et al., 2014; García-Romero et al., 2016; Santana-Cordero et al., 2016; Hernández-Cordero et al., 2017), particularly severe on Gran Canaria (Ferrer-Valero et al., 2017), it has been necessary to reconstruct the original landforms and perimeter characteristics of some sections of the coast using historical sources. To this end, a series of aerial photographs and digital orthophotos from the 1960s was used, as well as historical field photographs from the archives of the FEDAC Foundation (Cabildo de Gran Canaria) and maps prior to the 20th century for the cities of Las Palmas de Gran Canaria and Santa Cruz de La Palma.

3.2. Coastal geomorphic taxonomy

The absence of taxonomic standards in coastal geomorphology (see Fairbridge, 2004; Finkl, 2004), which establish internationally accepted frameworks for spatiotemporal comparisons, constrains this analysis. For that reason, an appropriate *ad hoc* geomorphological taxonomy was developed based on exhaustive observations of the coasts of the Canary Islands (Figure 2, Annex 1). This classification constitutes an expansion of previous proposals (Ferrer-Valero et al., 2017; Ferrer-Valero, 2018). It (i) incorporates the complete spectrum of mesoscale landforms of the study area; (ii) is spatially consistent, i.e. it can be applied continuously alongshore; (iii) avoids double-counting or redundancies, i.e., repeated criteria between categories; and (iv) is hierarchical. The hierarchical structure contributes to maintain a balance between classes, avoiding the weighting of particular processes, and allows future studies to adapt the detail level of analysis according to source availability.

The first taxonomic order defines coastal Environments. It is based on the common distinction between rocky-erosive and clastic-depositional coasts (e.g. Davies, 1980; Finkl, 2004), according to the presence alongshore of endomorphic erosive landforms, allomorphic sedimentary-derived landforms or combinations of both types (mixed coasts) (Figure 2). The second order establishes Groups of landforms (8 taxonomic units) according to common morphological features, genetic processes and physical agents (gravitational, marine, aeolian, etc.). They form 7 marine-genetic Groups (with direct or indirect intervention of marine agents), plus a morphostructural Group composed of the main volcanic morphologies affected by coastal dynamics in the Canary Islands. The third order segregates 4 Subgroups of landforms from each second-order Group, resulting in 32 taxonomic units. Order 3a is composed of Typological Subgroups and order 3b is composed of Dimensional Subgroups (Figure 2).

The Subgroups of order 3b are derived from the systematic measurements of the most characteristic dimensional metric of each Group of landforms (Figure 2). This provides additional landscape information about the size (stage of growth) of the features of each Group (e.g. cliffs→heights, platforms→widths). A total of 29,869 measurements of various parameters were collected, later clustered using the algorithms appropriate to each distribution. The Groups Cl and Pt (see acronyms in Figure 2) constitute sets of non-systematically differentiable features alongshore (e.g. one cliff from another), so that the measurements of height and width were made through systematic spatial sampling each 50 m, obtaining 25,350 records classified by quantiles in Cl Group, and by natural breaks (Jenks, 1967) in Pt Group (Figure 2). The other Groups are composed of differentiable features (e.g. one beach from another), so that the samples were collected for 'individuals'. As a result, 4,519 records were obtained, classified by geometric intervals.

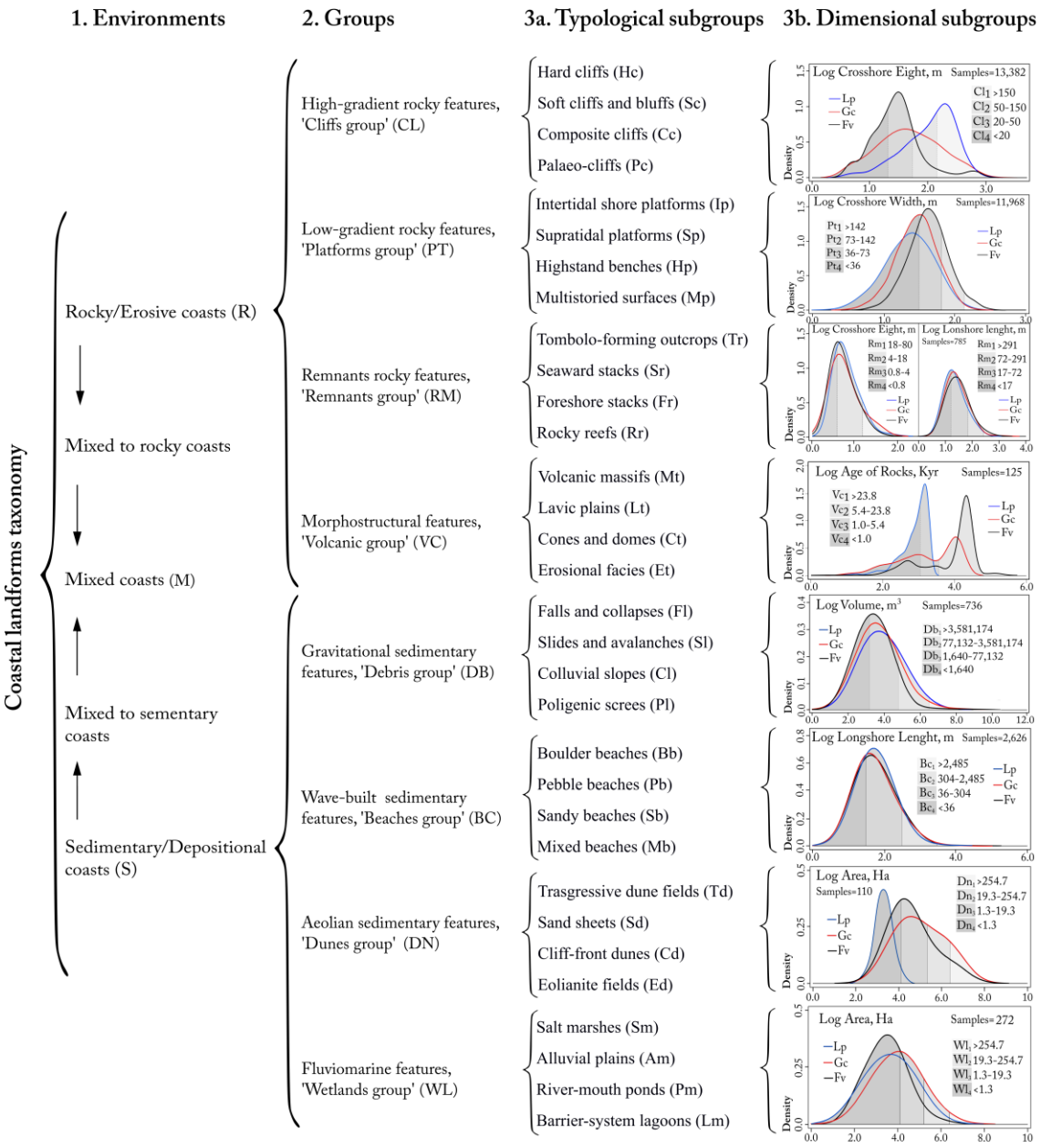

Fig 2. Hierarchical taxonomy designed for coastal geomorphology classification and structural analysis, testing various levels of aggregation or taxonomic orders. In order 3b (size-based classification), the parametric distributions were plotted through kernel density estimation (adjust=1.5) in R-Studio.

3.3. Spatial database and metrics

For computing the presence of the taxonomic classes on coasts, the coastline data-storing (CDS) method was applied (Ferrer-Valero, 2018). This method consists of transferring the planimetric surfaces of features to the coastline in GIS (Figure 3). The coastline vector of each island was divided into *n* segments according to the observed presence [1] or absence [0] of the classes at each taxonomic order, configuring a binary spatial database that results in cascading identifiers (Figure 3). The line of reference for the three islands was level 0 of the Topographic Map 1:5,000 of the Canary Islands (GRAFCAN, S.A.-Government of the Canary Islands).

The CDS method is a consistent cartographic-analytical proxy for computing abundances on coastal environments (Ferrer-Valero, 2018) and enables two different analytical approaches. The

first approach, Non-combinatorial, denoted by the union operator (U), involves the taxonomic classes without their spatial relations. The second approach, Combinatorial, denoted by the intersection operator (∩), involves the spatial relations between taxonomic classes in GIS. All the specific combinations of classes alongshore are computed, so that each final class constitutes a unique combination of same-order classes (coastal morphoassemblage).

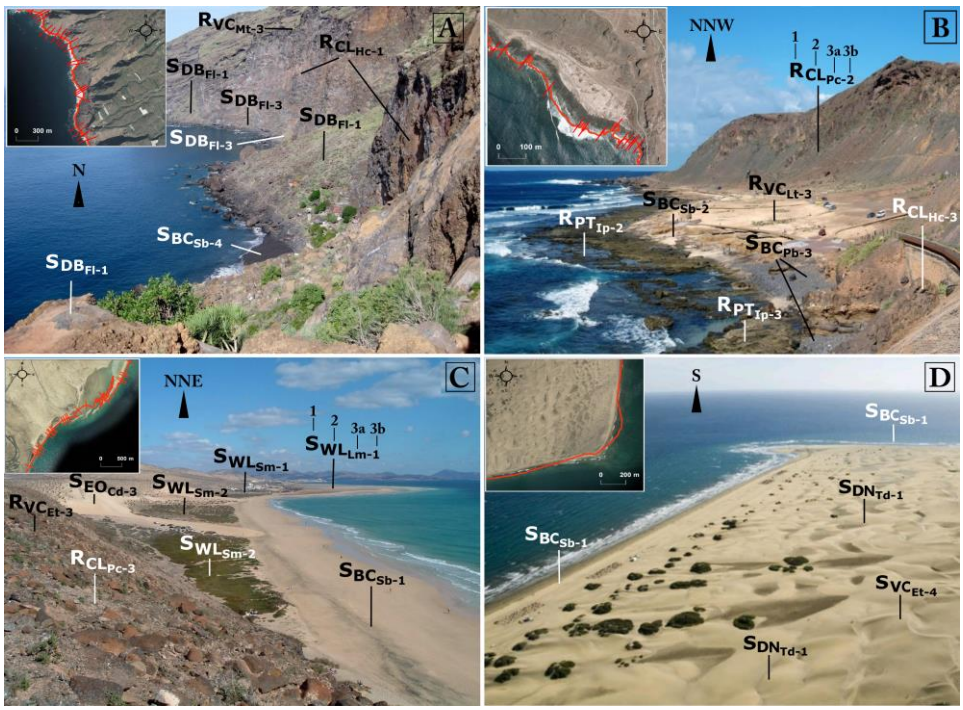

Fig 3. Examples of codes used in the coastal geomorphic database (on photographs) and their projection on the coastline (in each top left corner). The meaning of the codes can be found in Figure 2. A) Playa de la Veta (La Palma), where various large cliff-collapses, huge igneous cliffs and a little black-sand beach are developed in a juvenile volcanic massif context. B) El Confital (Gran Canaria), where some large intertidal shore platforms sculpted in tuffs are backed by narrow-perched biogenic-sand beach, pebble beaches and palaeo-cliffs formed on strombolian cones, in an uplifted terraced area. C) Sotavento (Fuerteventura), where a long beach of bioclastic sands is backed by salt marshes, lagoons, cliff-front dunes and palaeo-cliffs, in a predominantly old erosional area. D) Maspalomas (Gran Canaria), where one of the most notable transgressive dune fields of the archipelago is developed behind a long golden-sand beach overlying an older alluvial fan.

Based on the above, three metrics of geomorphological abundance and four metrics of diversity were applied (Table 1). The first metric applied was the feature longshore frequency (p). It expresses the shoreline perimeter occupied by each taxonomic class in relative terms with respect to the total shoreline (Table 1). With this, we compare the general geomorphic composition of coasts and the typological changes in the dominant geomorphology between islands, from younger to older. The other metrics used are derived from the longshore frequency (p) values.

Two cross-shore abundance metrics were then applied: Whole density (N_U) and Local abundance ($N_\cap$) (Table 1 for the formulas). Whole density (N_U) was estimated normalizing the total longshore frequencies (p) of all classes (Ruban, 2010) to the total coastal perimeter, obtaining a general landform density (km of landforms/km of coast) for each island. Local abundance ($N_\cap$) uses the presence of classes in a combinatorial approach. It indicates the absolute number of landforms that make up the morphoassemblages at each point on the

coastline. Comparing these metrics from younger to older islands, we explored the degree of coastal landforms proliferation from an evolutionary point of view at geological time-scale.

Table 1. Indices used for geomorphological abundance and diversity estimation.

Metric type	Name	Formulation	Parameters
Abundance	Longshore frequency (p)	$= n_{ik}/N$	n_{ik}= abundance of class *i* (km of coastline) at order *k*.
	Local abundance ($N_\cap$)	$= s_k$	
	Whole density (N_U)	$= \sum_{i=1}^{S} n_{ik} \Big/ N$	*N*= coastal perimeter (km).
Diversity (richness)	Normalized Richness (S)	$= S_k / S_{max\ k}$	s_k= number of classes of order *k* at one point on the coast.
	Margalef index (M)	$= (S_k - 1)/\log N$	S_k= number of classes present at order *k*.
Diversity (evenness)	Inverse Simpson index (1-D)	$= 1 - \sum_{i=1}^{S} p_{ik}^2$	$S_{max\ k}$= total number of classes considered at order *k*.
	Shannon index (H')	$= -\sum_{i=1}^{S} p_{ik} \log p_{ik}$	p_{ik}= relative frequency of class *i* at order *k* $= n_{ik}/\mathrm{N}$

Diversity refers to taxonomic heterogeneity. The evolution of geomorphological diversity was explored analyzing four non-parametric measures or 'diversity indices' (Table 1 for the formulas): Normalized Richness (S) and Margalef index (M), for richness comparison; Simpson index (D) and Shannon index (H'), for evenness comparison (Magurran, 1988). These indices have been widely applied in ecology and biodiversity studies (e.g., Izsák and Papp, 2000; Rumohr et al., 2001; Spellerberg and Fedor, 2003), as well as in pedodiversity (Ibáñez et al., 1995, 1998, 2005; Guo et al., 2003; McBratney and Minasny, 2007; Minasny et al., 2010), landscape heterogeneity (Nagendra, 2002; Uuemaa et al., 2011; Malinowska y Szumacher, 2013) and geodiversity issues (Benito-Calvo et al., 2009; Ferrer-Valero et al., 2017).

Richness denotes the total variety of classes and constitutes an over-arching parameter of coastal geomorphic geodiversity (Magurran, 1988). In this study, we used a normalization (S) with respect to the maximum number of taxonomic classes at each order. The Margalef index (M) is a normalization of the number of classes with respect to the natural logarithm of a total statistical population (Margalef, 1958). Evenness indicates the degree of uniformity of the abundances distributions, positively related to diversity (Magurran, 1988), and was estimated through the Simpson (D) and Shannon (H') indices. The Simpson index (D) measures the dominance of classes by calculating the probability of a class repeating itself in a random selection process. It is negatively related to diversity, so it is generally expressed by its inverse value (1-D) (Simpson, 1949). The Shannon index (H') comes from Information Theory and measures the amount of information lost in a system by increasing its complexity, widely used as a measure of diversity (Shannon and Weaver, 1949).

4. Results

A total of 31,512 geomorphological stretches were mapped along the 844 km of coast of the three islands. Based on these, the different patterns in landform composition, abundance and diversity were obtained. The position of the mid value along the island chain leads to three possible patterns: (i) the Mid-Lp pattern, defined by the mid value on La Palma (Lp), the youngest island; (ii) the Mid-Gc pattern, defined by the mid value on Gran Canaria (Gc), the mid-aged island; and (iii) the Mid-Fv pattern, defined by the mid values on Fuerteventura (Fv), the oldest island

(Figure 4). Each mid-value pattern shows as well two possible incremental sequences according to the position of the maximum and minimum values along the island chain. For example, the Mid-Gc pattern may occur as an Lp-Gc-Fv (age-increasing) or Fv-Gc-Lp (age-decreasing) incremental sequence (Figure 4).

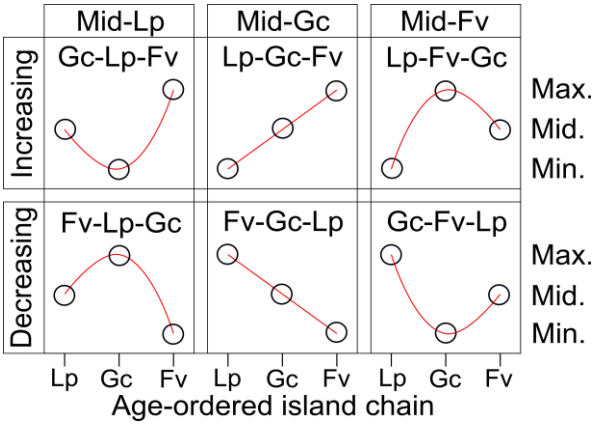

Fig 4. Range of possible chain patterns: three mid-patterns (Lp, Gc, Fv) and six corresponding incremental sequences (Gc-Lp-Fv, Lp-Gc-Fv, Lp-Fv-Gc, Fv-Lp-Gc, Fv-Gc-Lp, Gc-Fv-Lp). Lp, La Palma; Gc, Gran Canaria; Fv, Fuerteventura.

4.1. Geomorphic compositions

The set of longshore frequencies (p) shows the geomorphological composition of coasts of the three islands (Figure 5).

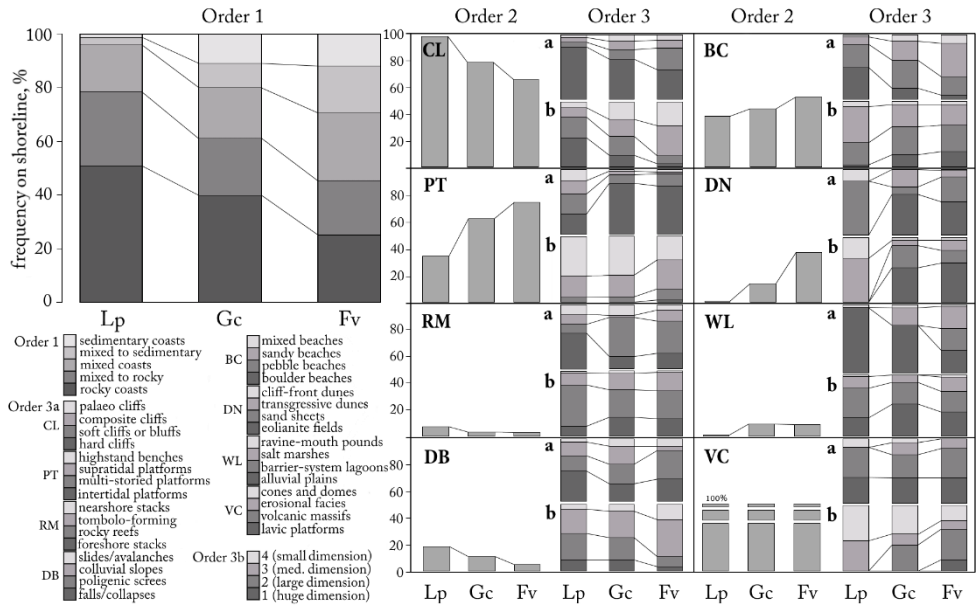

Fig 5. Longshore frequency of each geomorphological class (%) at different taxonomic orders (1, 2, 3a, 3b). The orders 3a and 3b are represented as full bars assuming the frequencies previously expressed at order 2. Note the intermediate longshore frequency of Gran Canaria (Gc) in most series, between La Palma (Lp) and Fuerteventura (Fv), revealing evolutionary features.

At the first taxonomic order, Environments, the Mid-Gc pattern was observed in 3/3 (three of the three) series of longshore frequency, and is the significantly dominant pattern ($p<0.05$) (Table 3). The longshore frequency of the Sedimentary-depositional coasts (S) and Mixed coasts (M) increases, while Rocky-erosive coasts (R) decreases from the youngest to the oldest island (Table 2, Figure 5).

The second taxonomic order, Groups of landforms, replicates the significant dominance of the Mid-Gc pattern in the longshore frequencies ($p<0.05$), which is found in 6/8 series (Table 3). The longshore frequency of the Cliffs (CL), Remnants (RM) and Debris (DB) Groups decreases, while that of the Platforms (PT), Beaches (BC) and Dunes (DN) Groups increases from the youngest to the oldest island (Table 2). Only the Wetland Group (WL) shows a Mid-Fv pattern (Table 3). The coefficient of variation (CV) is >5% in all series (Table 2).

The third taxonomic order of Typological Subgroups (3a) shows the Mid-Gc pattern in 17/32 series of longshore frequency (Table 3), with age-increasing sequences in Soft cliffs and bluffs (Sc), Intertidal shore platforms (Ip), Sandy beaches (Sb), Mixed beaches (Mb), Sand sheets (Sd), Cliff-front dunes (Cd), Eolianite fields (Ed) and Salt marshes (Sm); and age-decreasing sequences in Hard cliffs (Hc), Supratidal platforms (Sp), Lavic plains (Lt), Cones and domes (Ct), Seaward stacks (Sr), Falls and collapses (Fl), Colluvial slopes (Cl), Polygenic screes (Pl) and Boulder beaches (Bb) (Table 2). The Mid-patterns are not random at this order ($p<0.01$), but the dominance of the Mid-Gc pattern is not significant due to the occurrence of the Mid-Fv pattern in another 12/32 series (Table 3). The Mid-Fv pattern shows age-increasing sequences in Composite cliffs (Cc), Paleo-cliffs (Pc), Rocky reefs (Rr) and Erosional facies (Et); and age-decreasing sequences in Highstand benches (Hp), Tombolo-forming outcrops (Tr), Foreshore stacks (Fr) and Volcanic Massifs (Mt) (Table 2). The coefficient of variation (CV) is <5% in only one series (Lt) (Table 2).

Table 2. Variations in longshore frequencies (p) by islands, of any class and taxonomic order, showing the incremental chain pattern for each series. The variations are calculated from the mean frequency of the three islands. CV, coefficient of variation, %. See acronyms in Figure 2.

Order/ Class	Mean	Longshore frequency (p) Variation, Δ%			CV	Incremental sequence	**Order**/ Class	Mean	Longshore frequency (p) Variation, Δ%			CV	Incremental sequence
		Lp	Gc	Fv					Lp	Gc	Fv		
1st							(*bis*)						
R	0.39	34.3	1.7	-36.0	28.7	FvGcLp	Cd	0.005	-89.3	-69.9	159.2	112.8	LpGcFv
M	0.53	-13.9	-4.3	18.2	13.5	LpGcFv	Ed	0.10	-100.0	-3.7	103.7	83.2	LpGcFv
S	0.07	-82.1	22.1	60.0	60.1	LpGcFv	Sm	0.02	-100.0	35.0	65.0	71.8	LpGcFv
2nd							Am	0.05	-45.7	67.0	-21.4	48.4	LpFvGc
CL	0.81	20.9	-27	-18.2	16.1	LpGcFv	Pm	0.002	-63.7	89.9	-26.2	65.4	LpFvGc
PT	0.58	-39.1	9.1	30.0	28.9	LpGcFv	Lm	0.01	-100.0	-100.0	200.0	141.4	None
RM	0.05	59.8	-27.9	-31.9	42.3	FvGcLp	**3rd-b**						
VC	1.00	0.0	0.0	0.0	0.0	None	Cl_1	0.21	110.5	-29.1	-81.3	81.0	FvGcLp
DB	0.12	58.9	-3.2	-55.7	46.9	FvGcLp	Cl_2	0.20	50.4	8.2	-58.6	44.9	FvGcLp
BC	0.45	-14.6	-2.4	16.9	13.0	LpGcFv	Cl_3	0.22	-33.4	-5.0	38.4	29.5	LpGcFv
DN	0.18	-98.5	-15.4	113.9	87.4	LpGcFv	Cl_4	0.18	-49.4	16.1	33.3	35.6	LpGcFv
WL	0.08	-67.7	36.9	30.8	48.0	LpFvGc	Pt_1	0.01	-79.2	-72.8	152.1	107.6	LpGcFv
3rd-a							Pt_2	0.07	-60.4	-23.6	84.0	61.3	LpGcFv
Hc	0.52	49.6	-7.5	-42.1	37.8	FvGcLp	Pt_3	0.21	-48.9	-3.9	52.7	41.6	LpGcFv
Sc	0.14	-44.4	-15.5	59.9	44.0	LpGcFv	Pt_4	0.28	-24.8	30,1	-5.3	22.8	LpFvGc
Cc	0.08	-16.7	20.1	-3.5	15.2	LpFvGc	Rm_1	0.01	16.4	-2.0	-14.4	12.6	LpGcFv
Pc	0.07	-21.1	26.2	-5.1	19.7	LpFvGc	Rm_2	0.02	88.7	-43.4	-45.3	62.7	FvGcLp
Ip	0.38	-71.2	28.0	43.2	50.7	LpGcFv	Rm_3	0.01	33.9	-17.7	-16.2	24.0	GcFvLp
Sp	0.04	68.5	-24.0	-44.6	49.2	FvGcLp	Rm_4	0.002	53.5	-18.7	-34.7	38.4	FvGcLp
Hp	0.05	45.0	-42.7	-2.2	35.8	GcFvLp	Vc_1	0.07	-100.0	-100.0	200.0	141.4	None
Mp	0.11	-1.4	-24.1	25.5	20.3	GcLpFv	Vc_2	0.30	-100.0	47.2	52.8	70.7	LpGcFv
Tr	0.01	87.8	-84.8	-2.9	70.5	GcFvLp	Vc_3	0.26	92.0	-35.1	-56.9	65.6	FvGcLp
Sr	0.01	74.0	-14.0	-60,0	55.6	FvGcLp	Vc_4	0.36	37.7	6.8	-44.5	33.9	FvGcLp
Fr	0.02	120.2	-62.2	-57,9	85.0	GcFvLp	Db_1	0.02	67.1	9.9	-77.0	59.2	FvGcLp
Rr	0.01	-31.9	29.8	2,0	25.2	LpFvGc	Db_2	0.04	88.1	-6.6	-81.5	69.4	FvGcLp
Mt	0.39	9.0	-17.4	8,4	12.3	GcFvLp	Db_3	0.05	43.2	-4.9	-38.2	33.4	FvGcLp
Lt	0.43	0.8	0.4	-1.1	0.8	FvGcLp	Db_4	0.01	6.4	-6.3	-0.1	5.2	GcFvLp
Ct	0.07	91.4	-16.7	-74.7	68.8	FvGcLp	Bc_1	0.07	-80.9	13.0	67.9	61.5	LpGcFv

Et	0.11	-96.3	73.1	23.2	71.1	LpFvGc	Bc_2	0.17	-27.3	5.4	21.9	20.5	LpGcFv
Fl	0.05	91.4	-32.0	-59.4	65.6	FvGcLp	Bc_3	0.18	22.3	-16.4	-5.9	16.3	GcFvLp
Sl	0.01	6.5	31.3	-37.8	28.6	FvLpGc	Bc_4	0.03	9.4	-3.3	-6.1	6.7	FvGcLp
Cl	0.02	57.4	30.5	-87.9	63.1	FvGcLp	Dn_1	0.11	-100.0	-21.4	121.4	91.6	LpGcFv
Pl	0.03	32.3	0.7	-33.0	26.7	FvGcLp	Dn_2	0.04	-100.0	21.6	78.4	74.4	LpGcFv
Bb	0.10	88.0	-24.0	-64.1	64.3	FvGcLp	Dn_3	0.02	-91.6	-47.9	139.4	100.2	LpGcFv
Pb	0.15	-13.5	20.7	-7.2	14.8	LpFvGc	Dn_4	0.01	-86.0	-43.8	129.8	93.4	LpGcFv
Sb	0.14	-72.1	-14.3	86.4	65.5	LpGcFv	Wl_1	0.04	-77.5	59.0	18.5	57.2	LpFvGc
Mb	0.05	-56.4	4.0	52.4	44.5	LpGcFv	Wl_2	0.03	-57.4	38.1	19.3	41.3	LpFvGc
Td	0.03	-100.0	58.8	41.2	71.1	LpFvGc	Wl_3	0.01	-63.7	-17.6	81.3	60.5	LpGcFv
Sd	0.05	-95.7	-66.7	162.4	115.5	LpGcFv	Wl_4	0.002	-59.9	-12.8	72.7	54.9	LpGcFv

At the third taxonomic order of Dimensional Subgroups (3b), the dominance of the Mid-Gc pattern, observed in 25/32 series of longshore frequency, is highly significant ($p<0.01$) (Table 3), with age-increasing sequences in 14 classes (Cl_3, Cl_4, Pt_1, Pt_2, Pt_3, Vc_2, Bc_1, Bc_2, Dn_1, Dn_2, Dn_3, Dn_4, Wl_3 and Wl_4) and age-decreasing sequences in 11 classes (Cl_1, Cl_2, Rm_1, Rm_2, Rm_4, Vc_3, Vc_4, Db_1, Db_2, Db_3 and Bc_4) (Table 2, Figure 2 for acronyms). At this taxonomic order, the Mid-Fv pattern is observed in only 6/32 series (Table 3), as age-increasing sequences in 3 classes (Pt_4, Wl_1 and Wl_2) and age-decreasing sequences in the other 3 classes (Rm_3, Db_4 and Bc_3) (Table 2, Figure 2 for acronyms). From younger to older islands, there is a tendency to decreasing heights of Cliffs (CL) and Remnants (RM), and volumes of Debris (DB); as well as to increasing widths of Platforms (PT), ages of Volcanics (VC), lengths of Beaches (BC) and surfaces of Dunes (DN) and Wetlands (WL). The coefficient of variation (CV) is >5% in all series (Table 2).

Considering all series of longshore frequency, the Mid-Gc pattern sequence was observed in 51/75 classes, with this clearly being the dominant longshore abundance pattern in the landforms distribution throughout the three islands ($p<0.01$) (Table 3). In this sequence, the coasts of Gran Canaria, the mid-aged island, have the mid geomorphological composition, which reveals possible systematic variations in the dominant coastal geomorphic structures with island age.

Table 3. Occurrences number (n) of each mid-pattern in the set of the 75 longshore frequency series; χ^2, Chi-Square Test for mid-pattern configurations.

Taxon.	Mid-pattern occurrences, n						
Order	Lp	Gc	Fv	None	Total	χ^2	p-value
1st	0	3	0	0	3	9.0	<0.05
2nd	0	6	1	1	8	11.0	<0.05
3rd-a	2	17	12	1	32	22.7	<0.01
3rd-b	0	25	6	1	32	50.7	<0.01
Total	2	51	19	3	75	83.6	<0.01

4.2. Geomorphic abundance

The unspecific proliferation in the number of landforms that make up the coasts was analyzed by metrics of Local abundance ($N_\cap$) and Whole density (N_U) at Subgroups order. These metrics show the Mid-Gc pattern in all series in which the mid geomorphological abundance is found in the mid-aged island, Gran Canaria.

Local abundance ($N_\cap$) shows the Mid-Gc pattern in 5/5 (five of the five) series, as a result of the increasing number of landforms that make up the coastal morphoassemblages (Table 4). The shoreline frequency of Single-landform coasts and 2-landforms coasts increases as an Fv-Gc-Lp decreasing-age sequence, while 3-landform coasts, 4-landform coasts and 5-landforms coasts increase as an Lp-Gc-Fv increasing-age sequence (Table 4). As a result, Whole density (N_U) shows an Lp-Gc-Fv incremental sequence, indicating the increase in the overall cross-shore proliferation

of landforms from the youngest to the oldest island (Table 4). The coefficient of variation (CV) is >5% in all series (Table 4).

Table 4. Local abundance (relative frequency on shoreline of each morphoassemblage size) and Whole density by island, expressing their relative variation (Δ%) from the means and coefficients of variation (CV, %). $N_{\cap}$, Local abundance; $N_{\cup}$, Whole density.

Metric	Size, n	Frequency on shoreline			Variation from mean Δ%				Mid-	Incremental
		Lp	Gc	Fv	Lp	Gc	Fv	CV	pattern	sequence
$N_{\cap}$	1	0.21	0.12	0.07	59.0	-13.3	-45.8	43.8	Gc	FvGcLp
	2	0.59	0.55	0.45	10.5	3.9	-14.5	10.6	Gc	FvGcLp
	3	0.19	0.30	0.37	-33.3	3.6	29.7	25.8	Gc	LpGcFv
	4	0.01	0.03	0.10	-76.1	-29.5	105.6	77.1	Gc	LpGcFv
	5	0.000	0.003	0.004	-94.9	28.1	66.8	68.9	Gc	LpGcFv
		Dimensionless			Variation, Δ%					
$N_{\cup}$		2.00	2.27	2.51	-11.5	0.4	11.1	9.2	Gc	LpGcFv

These results support the argument that, combined with characteristic changes in dominant coastal composition, there could be a systematic increment of the general number of landforms on the coasts with island age.

4.3. Geomorphic diversity

The length of the x-axis in the rank-abundances series (Figure 6) shows the absolute richness, and the slopes *m* of lines *y=mx+n*, adjusted by minimum mean square error, indicate the evenness of the distribution through its resemblance to a constant function *y=m*. The slopes are relative to the shorter series (La Palma) to eliminate the effect of richness. These parameters show a systematic increase in the x-length of series (richness) and decreasing slopes (more evenness) according to the Lp-Gc-Fv sequence, from the youngest to the oldest island.

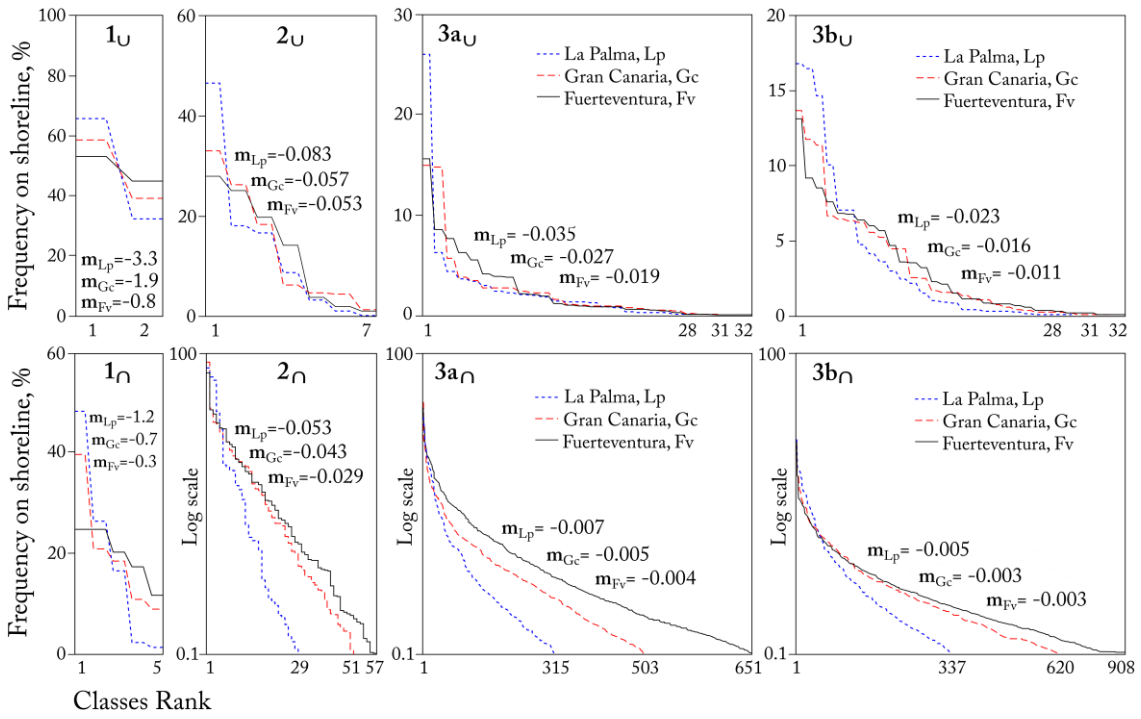

Fig 6. Rank abundance plots for the geomorphological classes at each island (La Palma, Gran Canaria, Fuerteventura), taxonomic order (1, 2, 3a, 3b) and calculation methodology (non-combinatorial, ∪; combinatorial, ∩). The length of the line on the x-axis shows the richness, and the *m* values represent the slopes of rank abundance distributions, indicating evenness.

The diversity indices show variations in the chain patterns (Figure 7). At the first taxonomic order, Environments, in both non-combinatorial and combinatorial, and at the second order, Groups of Landforms, in non-combinatorial, the three islands contain all possible classes. This produces non-differentiation in normalized Richness (S) and inverse-aged sequences of type Fv-Gc-Lp in Margalef index (M) due to the logarithmic coefficient (Figure 7). At the second taxonomic order, richness differentiation becomes evident in combinatorial methodology, showing an increasing Lp-Gc-Fv sequence in both normalized Richness (S) and Margalef index (M) values (Figure 7).

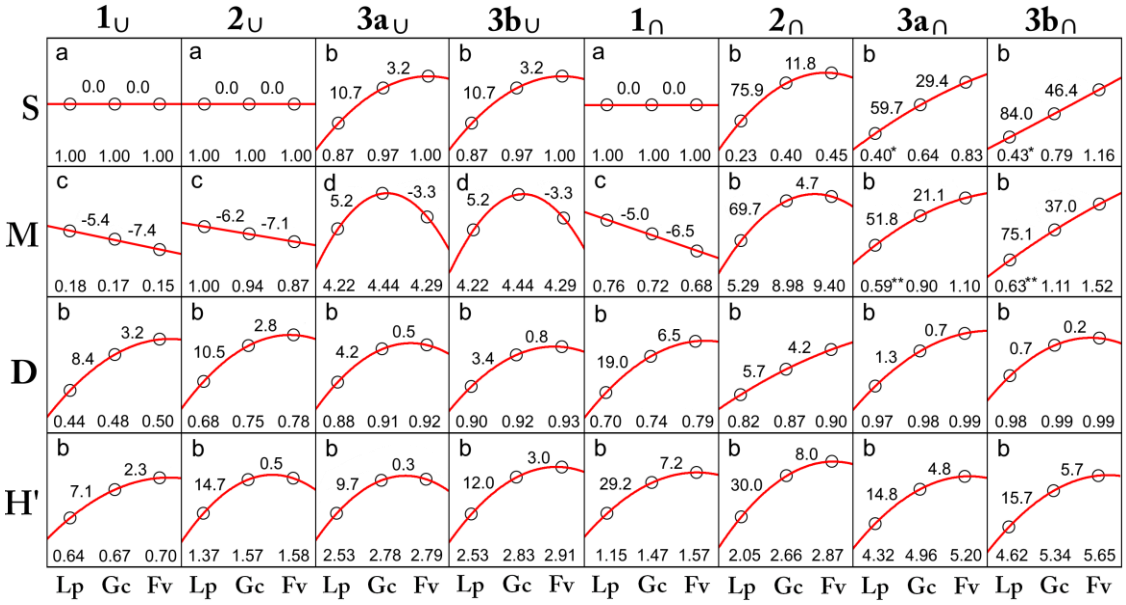

Fig 7. Diversity values (S, Richness; M, Margalef; D, Inverse Simpson; H', Shannon) of the islands (Lp, La Palma; Gc, Gran Canaria; Fv, Fuerteventura), at each taxonomic order (1, 2, 3a, 3b) and methodology (non-combinatorial, U; combinatorial, ∩). Above the x-axis, the diversity values. Along the curves, the proportional variation (Δ%) between diversity values. The scale of the y-axis is not constant for better visualization of the shape of the polynomial curves. In each top left corner, the letters denote the pattern observed: (a) non-differentiation; (b) Lp-Gc-Fv sequence; (c) Fv-Gc-Lp sequence; and (d) Lp-Fv-Gc sequence. *Series expressed in scale of 10^{2}; ** Series expressed in scale of 10^{-2}.

At the third taxonomic orders (3a, 3b), the differentiation in richness is evident in both non-combinatorial and combinatorial classes (Figure 7), due to the absence of 8 classes on La Palma (Td, Ed, Sm, Lm, Dn_1, Dn_2, Vc_1 and Vc_2) and 2 classes on Gran Canaria (Lm and Vc_1) (Figure 2 for acronyms). At these orders, normalized Richness (S) presents Lp-Gc-Fv sequences in all series, while Margalef index (M) shows Lp-Fv-Gc sequences in non-combinatorial, and Lp-Gc-Fv sequences in combinatorial classes. The maximum richness differentiation between islands is attained in the third taxonomic order of Dimensional morphoassemblages, in which the richness of Fuerteventura is almost three times higher than that of La Palma (S_{Lp}=337, S_{Gc}=620, S_{Fv}=908) (Figure 6).

Differentiation between islands in evenness metrics (D, H') is evident at any taxonomic order (1, 2, 3a, 3b) and operative methodology (U, ∩) (Figure 7). This differentiation in evenness metrics is shown as an Lp-Gc-Fv increasing sequence in all series (Figure 7). The maximum evenness differentiation is attained in combinatorial calculations of low-disaggregation orders (1st, 2nd). The inverse Simpson index (D) ranges from a minimum islands differentiation at combinatorial Dimensional Subgroups to a maximum at combinatorial Environments. The Shannon index (H') ranges from a minimum at non-combinatorial Environments to a maximum at combinatorial Groups.

Comparatively, richness metrics (S, M) show higher mean increments and higher variability between taxonomic orders and operative methodologies. The richness differentiation between islands tends to markedly increase with increasing taxonomic disaggregation (from the first to the third order). On the other hand, the evenness metrics (D, H') show more moderate mean increments but less dispersion between taxonomic orders and analytical methods. Unlike richness, evenness differentiation tends to slightly decrease with increasing taxonomic disaggregation. In both groups of metrics, the differentiation increases from non-combinatorial to combinatorial methodologies (Figure 8).

Of the 6 possible chain patterns (Figure 4), only 3 were observed for diversity (Figure 7). Evenness metrics (D, H') are more pattern-consistent. The Lp-Gc-Fv age-island pattern is found in all 16/16 evenness series and is significantly dominant ($p<0.01$) (Table 5). In richness metrics (S, M), more sensitive to taxonomic levels and operative methods, the Lp-Gc-Fv sequence is found in 8/16 richness series. The range of events in the Margalef index (M) does not show significant dominance of any pattern ($p>0.05$) (Table 5). However, the dominance of the Lp-Gc-Fv sequence markedly increases with increasing taxonomic disaggregation (6/8 richness series at 3rd orders) and using combinatorial methodologies (6/8 richness combinatorial series). In total, the Lp-Gc-Fv, age-increasing sequence is found in 24/32 series of diversity, and is the significantly dominant diversity trend ($p<0.01$) (Table 5).

Table 5. Occurrences number (n) of each sequential pattern in the set of 32 diversity series; χ^2, Chi-Square Test for the sequential configurations.

		Incremental sequence occurrences, n									
Diversity metric		None	GcLpFv	FvLpGc	LpGcFv	FvGcLp	LpFvGc	GcFvLp	Total	χ^2	p-value
Richness	S	3	0	0	5	0	0	0	8	21.7	<0.01
	M	0	0	0	3	3	2	0	8	11.2	>0.05
	All	3	0	0	8	3	2	0	16	21.6	<0.01
Evenness	D	0	0	0	8	0	0	0	8	48.0	<0.01
	H'	0	0	0	8	0	0	0	8	48.0	<0.01
	All	0	0	0	16	0	0	0	16	96.0	<0.01
All		3	0	0	24	3	2	0	32	30.9	<0.01

Averaging increments (Δ%) in all diversity indices (S, M, H', D), taxonomic orders (1, 2, 3a, 3b) and operational methodologies (U, ∩) results in a mean increase in coastal geomorphic diversity of 19.0% from La Palma to Gran Canaria, and of 8.5% from Gran Canaria to Fuerteventura. This finding supports the systematic increment of coastal geomorphic diversity (richness and evenness) as compositional changes occur with island age.

5. Discussion

Systematic changes in the dominant coastal landforms from La Palma to Gran Canaria to Fuerteventura were observed. The Mid-Gc pattern was found in 51/75 (fifty-one of the seventy-

five) series of longshore features frequency (68%) (Table 3). The significant dominance of this pattern, in which the mid shoreline frequency of landforms occurs in the mid-aged island (Gran Canaria), supports the argument for the temporal evolution of the dominant coastal geomorphic compositions.

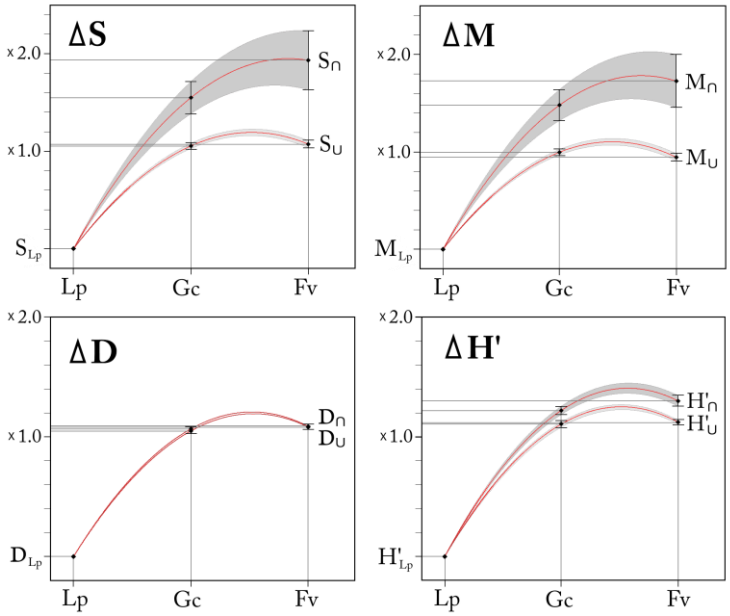

Fig 8. Integrated results showing the increments of index values (ΔS, ΔM, ΔD, ΔH') between islands (Lp, La Palma; Gc, Gran Canaria; Fv, Fuerteventura). Red lines are polynomial curves drawn for better visualization of trends. The grey halos represent the standard deviations between taxonomic orders. The four graphs show positive curves in the La Palma-Gran Canaria-Fuerteventura direction, decaying between Gran Canaria and Fuerteventura.

Associated with the observed compositional evolution in geomorphological structures, two quantitative underlying patterns were detected. First, a systematic increase in geomorphic abundance from La Palma to Gran Canaria to Fuerteventura. The Lp-Gc-Fv sequential pattern, in which there is a general proliferation of coastal landforms with island age, is found in the Whole density series (Table 4). Second, a systematic increase of coastal geomorphic diversity (richness and evenness) from La Palma to Gran Canaria to Fuerteventura. The Lp-Fc-Fv diversity pattern is found in 24/32 series (75%) and is the significantly dominant diversity trend (Table 5), supporting the idea of the systematic increase of coastal geomorphic diversity with island age.

In accordance with the above, (i) the coastal geomorphic composition of La Palma, mostly rocky, has the lowest geomorphic abundance and diversity; (ii) the coast of Gran Canaria shows an intermediate coastal geomorphic composition, with a more environmental mixture, associated with an intermediate geomorphic abundance (Δ13.5% compared to La Palma) and diversity (Δ19.0% compared to La Palma); and (iii) the coasts of Fuerteventura have the most mixed and sedimentary geomorphic composition, with the largest geomorphic abundance (Δ10.6% compared to Gran Canaria) and diversity (Δ8.5% compared to Gran Canaria). Therefore, the Lp-Gc-Fv sequence determines, from younger to older islands, increasing abundance, richness and evenness of the coastal geomorphic structure. Furthermore, the dominance of the parabolic trends indicates a closer general coastal geomorphic structure between Gran Canaria and Fuerteventura, which concurs with the closer age difference between Gran Canaria and Fuerteventura than between Gran Canaria and La Palma.

Assuming a space-for-time reasoning (Picket 1989), these empirical results can be interpreted as a geomorphological evolution over geological time-scales (1.8 to 20.6 My). The evolutionary interpretation involves long-term geomorphic processes in the coastal landscapes of oceanic island chains. First, these data point to classical qualitative morphological transformations based on the concepts of 'youthful' and 'mature' (Johnson, 1919; Shepard, 1937, 1976; Inman and Nordstrom, 1971), with the passage from dominant morphologies to others in the course of coastal and geological processes. In the classic 'marine cycle' of Johnson (1919), the different phases of transformation of coasts are described. It details the differential processes that take place in submergence coasts and emergence coasts in stages of 'youth', and how they tend in phases of 'maturity' towards convergent or equilibrium states (cliffing, sedimentation and linearization of the coast). The last phase, the 'old' stage, would be reached, theoretically, with the total planation of the coastal margin. Inman and Nordstrom (1971) recognized a morphological evolution with a progressive reduction of seismic and volcanic activity, resulting in a decreasing coastal relief and widening continental shelves, drainage networks and coastal sedimentation. In oceanic islands, the volcanic construction dominates during the initial stages, but erosive and sedimentary processes gradually prevail as the volcanic edifice gets older (Ramalho et al., 2013). In this respect, the island of La Palma would represent the characteristic coastal geomorphic structure of a 'young' volcanic island in a state of growth, while Fuerteventura, at the other extreme, would represent the coastal structure configuration of an 'old' volcanic island in a state of erosion.

Our results enable qualitative compositional evolution to be linked with quantitative changes in abundance and diversity in the geomorphology of a coastal landscape over geological time. Accordingly, we put forward the hypothesis that under an apparent purely typological transformation (transition from dominant rocky-erosive coasts to increasingly clastic-depositional coasts), an organizational pattern defined by the increase of the dynamic-structural complexity (abundance and diversity) of the coasts of the hot-spot islands would dominate as they progress from a state of minor to greater temporal development (Figure 9). In line with this, Ibañez et al. (1994) applied measures of richness and entropy (Shannon index) to the distribution and heterogeneity of abiotic and biotic elements in the temporal evolution of a fluvial profile. They managed to relate the increasing processes of fluvial incision during the Plio-Quaternary with the increase of negentropy and complexity of the landscapes.

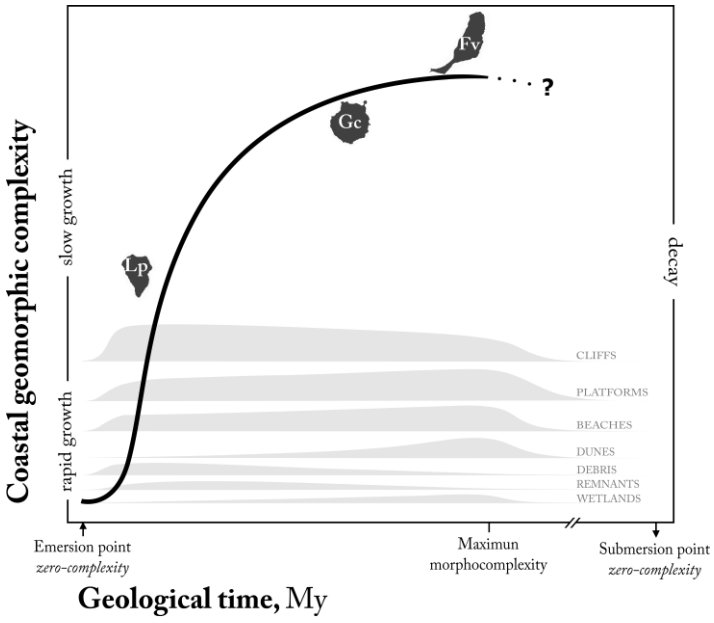

Fig 9. General hypothesis about the roughly parabolic evolution of coastal geomorphic complexity along geological time as entropy progresses in hot-spot volcanic islands. The relative position of the island in the XY plot corresponds to the all mean values of diversity obtained. The gray shapes represent the abundance evolution of the geomorphic Groups.

In view of the fact only three islands have been studied to date, the model shown in Figure 9 illustrates just an evolutionary hypothesis. It contains the deductive assertion that between two *zero-complexity* periods on an island, characteristic of the initial emersion and final submersion in the hot-spot model (Moore, 1987), there must be a rise-fall curve of geomorphological complexity, defined through diversity and abundance. The rise-fall curve spans all the stages of the island, from when it rises above sea level, grows and denudes, to when it ends in a guyot. Although in the Canary Islands it has not been possible to observe any decrease in diversity in the Lp-Gc-Fv direction, the slower increase between Gran Canaria and Fuerteventura could be marking the inflection point after which diversity values decrease to zero with erosion of the island under the sea. A similar bell curve is proposed by Whittaker et al (2008) in relation to the diversification of species in oceanic islands. This model relates the biological processes of colonization, speciation and extinction with the geodynamics that characterize hot-spot islands, predicting a maximum of biological diversity in the central stages of an island's life.

In the model (Figure 9), an initial lag phase in increasing geomorphic complexity represents the constraints of oceanic volcanoes to rise definitively above sea level. There are cases of Surtseyan pyroclastic edifices truncated by marine erosion in a matter of days (Ramalho et al., 2013). The volcanoes can cross the emersion threshold (zero-complexity) several times, until finally emerging by the extrusion of massive lavas (Ramalho et al., 2013). After the initial lag phase, a rapid diversity and abundance growth phase is defined based on the empirical values of La Palma. This island, with 1.8 My, already displays over 70% of the coastal geomorphic diversity of Fuerteventura (~11 times older). After the emersion of an island, the short-term marine forces can produce a great variety of incipient coastal landforms by marine abrasion, mass wasting, cliffing and sedimentation, causing a rapid increase in morphological complexity, thanks, in particular, to an increase of richness from zero. As the shield stage ends (Figure 1), the main volcanic activity ceases, and the terrestrial and marine erosive processes begin to dominate over the constructional volcanic processes. The development of two structures becomes dominant: the drainage network in the subaerial part and the island shelf in the submerged part. Then, the complexity rise-curve experiences a gradual attenuation (empirical values of Gran Canaria) until its maximum point (empirical values of Fuerteventura). The complexity growth in this phase is based on certain increases in richness but, above all, increases in landform abundance, variety of feature sizes (morphometrics) and geomorphological evenness in the coastal system.

In recent decades, the increase in process-based modelling and empirical monitoring studies in the different fields of coastal geomorphology has enabled an understanding of the short-term basic mechanisms of the origin and development of different landforms such as cliffs (Lim et al., 2005; Lee, 2008; Lim et al., 2010), platforms (Stephenson and Kirk, 2000; Trenhaile, 2000, 2005), beaches (Wright and Short, 1984; Gallagher et al., 1998; Buscombe and Masselink; 2006) or dunes (Sherman and Bauer, 1993; Hesp, 2002; Walker and Hesp, 2013). However, the scale-dependence of investigations limits the development of conceptual bridges between fundamental process-response dynamics and long-term processes and controls that govern landform evolution (Walker et al., 2017). Experimental studies show that coastal environments are highly dynamic and changing in the short term, and this work explores tendencies in coastal evolution at landscape scale over millions of years, generating challenges in relating spatiotemporal scales in geomorphology (Schumm and Lichty, 1965; Walker et al., 2017).

The trend we identified in increasing geomorphic complexity over time indicates that, regardless of the rapid short-term local geomorphic transformations, the coastal systems show a general long-term tendency conditioned by larger scale processes. This requires physical

processes that can explain transformations in the broad geomorphic coastal structures over geological time in oceanic islands. The course of time means the occurrence of a greater number of volcanic phases, geodynamic periods, climatic cycles, eustatic oscillations, etc. This implies an increasing abundance and diversity of geologically-inherited geomorphic features and consequently higher landscape complexity. For example, the abundance and variety of dune fields in the eastern Canary Islands have been explained by several climatic cycles and oscillations of the Mio-Plio-Quaternary sea level (Meco et al., 2007). The most important of these cycles took place between the Upper Miocene and the Lower Pliocene (8-4 My), when equatorial climatic conditions (presence of Senegalese equatorial fauna), similar to the current ones in the Cape Verde Islands and the Gulf of Guinea, resulted in abundant marine biological productivity. Later, during the Quaternary glacial cycles, a higher biological productivity in the hotter and more humid interglacial periods (MIS 11.3, 9, 5.5) also generated significant amounts of sediment. These sediments would be exposed to winds during lower sea level phases in colder and drier periods, generating landward aeolian sand transport and the formation of several generations of dune fields.

The increasing abundance of biological and terrigenous sediments in oceanic islands (Ramalho et al., 2013) is a particular factor of the growth pattern in geomorphic complexity found in the Canary Islands. It promotes a progressively greater environmental mixture and landform diversification in the transition from rocky to mixed and sedimentary coastal environments. This process is probably related to the widening of island shelves due to marine erosive processes over geological time. The observable distribution and morphology of the shelves in the Canaries (IEO, 2006) reveals that La Palma has practically no shelf, due to recurring volcanic activity and giant flank collapses during the Quaternary (Carracedo, 1999; Carracedo et al., 1999; Masson et al., 2002). In contrast, Gran Canaria and Fuerteventura, post-erosive islands, are well surrounded by kilometric insular shelves, 50-100 m below sea level. The physical modelling of wave erosion on rocky coasts (Trenhaile, 2000, 2001a, 2001b, 2002), accumulated at different sea levels over the geological periods, suggests the unequivocally erosive origin of insular shelves in many oceanic islands (Trenhaile 2001, Quartau et al., 2010, 2016). The shallow waters of the island shelves contribute to increasing sediment production on the coasts mainly by: (i) dissipation of wave energy, which improves the dynamic conditions for coastal sedimentation; (ii) expansion of the photic zone, which functions as the habitat of marine calcareous organisms (mollusks, calcareous algae and corals) which make up the bioclastic sands; and (iii) retention, on the surrounding marine bottoms, of terrigenous sediments derived from the coastal and subaerial erosion of the volcanic edifice.

On the other hand, the drainage network is also expanding and deepening over geological time in oceanic islands (Woodroffe, 2014), as can be seen in the Canaries and, in particular, in the island sequence studied. The progressive subaerial dissection generates greater topo-morphological complexity of the volcanic edifice (Ibañez et al., 1994; Whittaker et al., 2008). On the coast, this process generates low-lying alluvial plains by erosion and fragmentation of the sea-cliff fronts, favoring environmental heterogeneity. Gradual transformation of steep coasts into low-lying coastal sedimentary environments leads to the development of plains and depressions along the coast, and so to the proliferation of landforms such as coastal lagoons or salt marshes, which contribute to the observed increase of coastal geomorphic complexity.

Therefore, the long-term combined processes of erosion and sedimentation on the volcanic edifice, are the main driver mechanisms of the physical transformations of the studied coastal landscapes toward increasing geomorphic complexity in the coastal structure throughout geological time. As the forces of marine agents truncate the edifice laterally (marine abrasion) and subaerial agents (terrestrial erosion) reduce it vertically, a structural co-evolution between geomorphic composition, abundance and diversity is observed in the form of a rise-fall curve of coastal geomorphic complexity between the periods of emersion and submersion of an island. Given the correlation between geodiversity and biodiversity (Hjort et al., 2012; Tukiainen et al., 2017), the transforming coastal landscape towards morphological complexity opens new insights

about the development of habitat heterogeneity for biological communities over time in hot-spot oceanic islands.

6. Conclusions

The coastal geomorphic structure is described and quantitatively compared for three independent insular edifices of the same hot-spot archipelago (Canary Islands), with different ages and development stages: La Palma (1.8 My), Gran Canaria (14.5 My) and Fuerteventura (20.6 My). The lack of tectonic subsidence and the long periods of emergence of the Canary Islands enable a study of coastal evolution at a geological time-scale of over 20 My. A volcanic edifices predominantly composed of piled basaltic lavas, absence of surrounding coral reefs, medium-energy wave, meso-tidal regime and coastal aridity are the common boundary conditions of the coastal dynamics throughout the study area which allowed us to isolate the time dimension.
A clear pattern of increasing coastal geomorphic abundance and diversity has been observed from La Palma to Gran Canaria to Fuerteventura. This pattern is associated with observed systematic changes in the geomorphic typological characteristics (composition) of the coastal systems. The results, obtained on the basis of a systematic analysis of classified coastal geomorphic features, have been interpreted at a geological temporal scale (Figure 9), supporting an evolutionary pattern characterized by an increase with island age of the geomorphic structural complexity of the physical coastal landscapes. This provides new insights about long-term coastal evolution at landscape scale and opens new perspectives in the study of the relations between geomorphological diversity and biodiversity in the coastal environments of hot-spot oceanic islands.

Acknowledgments

This work is a contribution to the CSO2013-43256-R and CSO2016-79673-R projects of the Spanish National Plan for R+D+i (innovation), co-financed with ERDF funds, and was supported by an FPI-PhD grant from the Universidad de Las Palmas de Gran Canaria (E-35-2014-0231941). It was completed while N. Ferrer-Valero was a Ph.D. student in the IOCAG Ph.D. Program in Oceanography and Global Change. Special thanks are expressed to the Professors Stuart N. Lane and Kenneth F. Rijsdijk as well as the anonymous reviewers whose recommendations have helped to improve the quality of manuscript.

ANNEX. Short definitions of the coastal landforms taxonomy designed for the geomorphic structure analysis.

1. Environments	2. Groups of landforms	3a. Landforms	3b. Dimensional classes
1.1. Rocky/erosive Coasts (R) Active rocky/erosive coastal landforms. 1.2. Mixed to rocky/erosive coasts Active rocky landforms combined with some relict sedimentary landforms. 1.3. Mixed coasts (M) Both active rocky and sedimentary landforms combined. 1.4. Mixed to sedimentary coasts Active sedimentary landforms combined with some relict rocky/erosive landforms. 1.5. Sedimentary/ depositional coasts (S) Active sedimentary coastal landforms	2.1. High-gradient rocky features (CL) Or 'Cliffs Group': plunging and backshore scarps and other lower gradient coastal slopes, higher than 3 m, caused by marine activity. Sources. LiDAR altimetry Geologic map	3a.1. Hard cliffs (Hc) Near-vertical slopes under the effect of waves, mainly composed of highly resistant igneous materials: lavas and intrusions. 3a.2. Soft cliffs and bluffs (Sc) Near-vertical and lower-gradient slopes under the effect of waves, mainly composed of epiclastic sediments or fragmental volcanic materials (tephra). 3a.3. Composite cliffs (Cc) Complex-profile slopes under the effect of waves, composed of sections of hard and soft materials. 3a.4. Palaeo-cliffs (Pc) Backshore relict slopes originally eroded by the sea, abandoned permanently by marine activity.	Metric. Cross-shore height, m Samples. 13,382 Breaks. Quantiles Classes. Cl_4 (<20) Cl_3 (20-50) Cl_2 (50-150) Cl_1 (>150)
	2.2. Low-gradient rocky features (PT) Or 'Platforms group': shore platforms and other low-lying rocky areas, caused by mechanical action of waves, subaerial watering or cementation of sediments (beachrocks). Sources. Orthophotos 2002-15 Aerial photos 60's LiDAR altimetry	3a.5. Intertidal shore platforms (Ip) A and B shore platforms, up to 2.5 m AMSL, repeatedly flooded and exposed to combined action of tides and modal waves. 3a.6. Supratidal platforms (Sp) Shore platforms, between 2.5-5 m AMSL, not flooded by tides but reachable by storm waves or strong swells. 3a.7. Highstand benches (Hp) Platforms perched 5 m AMSL, probably related to paleo relative sea-level positions. 3a.8. Multistoried surfaces (Mp) Highly rugged platforms or cross-shore multi-level platforms.	Metric. Cross-shore width, m Samples. 11,968 Breaks. Natural breaks Classes. Pt_4 (<36) Pt_3 (36-73) Pt_2 (73-142) Pt_1 (>142)
	2.3. Remnant rocky features (RM) Or 'Remnants Group': rocky outcroppings isolated as a result of differential erosion or processes of lithification at the nearshore environment. Sources. Orthophotos 2002-15 LiDAR altimetry	3a.9. Foreshore stacks (Fr) Over 5 m high remnants located at the intertidal zone. 3a.10. Seaward stacks (Sr) Over 2.5 m high pinnacles, stacks and islets located offshore. 3a.11. Tombolo-forming outcrops (Tr) Stacks, pinnacles or platforms connected to the land via sandy or gravel bars. 3a.12. Rocky reefs (Rr) Bars of rock in nearshore that rises from the bed of the water to near the surface, under 2.5 m AMSL.	Metric. Height, m Longshore length, m Samples. 785 Breaks. Geometric intervals Classes. Rm_4 (<0.7) (<17) Rm_3 (0.8-3.9) (17-71) Rm_2 (4-17.8) (71-277) Rm_1 (>18) (>277)
	2.4. Morphostructural features (VC) Or 'Volcanic Group': the main landforms related to the structural evolution of oceanic volcanoes, upon which the modern coastal morphogenetic processes develop. Sources. Geologic map LiDAR altimetry	3a.13. Volcanic massifs (Mt) Developing shield volcanoes or remains of older shield volcanoes and stratovolcanoes. 3a.14. Lavic plains (Lt) Platform-forming lavas: lava-deltas, denudational lava-plains or isostatic igneous terraces. 3a.15. Strombolian cones and felsic domes (Ct) Minor volcanic edifices: cinder cones, tuff rings, littoral cones or felsic domes. 3a.16. Erosional facies (Et) Areas mainly constituted by sediments originated during old erosive episodes or erosional gaps in the volcanic buildings.	Metric. Age of rocks, My Samples. 125 Breaks. Geometric intervals Classes. Vc_4 (<1) Vc_3 (1-5.4) Vc_2 (5.4-23.8) Vc_1 (>23.8)
	2.5. Gravitational sedimentary features (DB) Or 'debris Group': onshore sedimentary deposits generated by the marine-induced displacement of rocks from coastal slopes driven by gravitational stress. Sources. Orthophotos 2002-15 LiDAR altimetry	3a.17. Falls and collapses (Fl) Very coarse, semicone-shaped, detritic deposits, plucked from a partial or total section of vertical cliffs. 3a.18. Slides and avalanches (Sl) Chaotic, concave ramp-lobe shaped, detritic deposits, commonly affecting the total profile along a cutting plane. 3a.19. Colluvial slopes (Cl) Fine-grain rich concave-talus formed by progressive inputs of material during long periods. 3a.20. Polygenic screes (Pl) Highly heterometric talus at the base of active cliffs resulting from successive mass-wasting episodes.	Metric. Volume, m^3 Samples. 736 Breaks. Geometric intervals Classes. Db_4 (<1,640) Db_3 (1,640-77,132) Db_2 (77,132-3,581,174) Db_1 (>3,581,174)
	2.6. Wave-built sedimentary features (BC) Or 'Beaches Group': shore-parallel structures generated by the sedimentary combined action of waves and currents, perched on a platform or composed of emerged and submerged bodies.	3a.21. Boulder beaches (Bb) Modern accumulations of boulder dominant grain size, usually forming supratidal ridges. 3a.22. Pebble beaches (Pb) Modern accumulations of pebble-dominant grain size, usually forming supratidal ridges. 3a.23. Sandy beaches (Sb)	Metric. Longshore length, m Samples. 2,626 Breaks. Geometric intervals

	Sources. Orthophotos 2002-15 Aerial photos 60's LiDAR altimetry Field observations	Modern accumulations of sand-dominant grain size, usually composed of both emerged and submerged bodies. 3a.24. Mixed beaches (Mb) Heterometrical cross-shore combination, usually sandy in the intertidal zone and gravelly in the supratidal zone.	Classes. Bc_4 (<36) Bc_3 (36-304) Bc_2 (304-2,485) Bc_1 (>2,485)
	2.7. Aeolian sedimentary features (DN) Or 'Dunes Group': backshore deposits created by the action of wind over sandy beach sediments and transported landward over coastal plains. Sources. Orthophotos 2002-15 Aerial photos 60's Field observations	3a.25. Transgressive dune fields (Td) Modern backshore deposits of landward free dunes (barchans) evolving large accumulations of aeolian sands. 3a.26. Sand sheets (Sd) Sedimentary plains formed by thin layers of mobile, semi-mobile or stabilized sands, which may have associated nebkhas. 3a.27. Cliff-front dunes (Cd) Dune formations attached to cliffs: climbing-dunes, falling-dunes and echo-dunes. 3a.28. Eolianite fields (Ed) Relict deposits of dunes or sand plains subjects of natural cementation processes.	Metric. Area, hm² Samples. 110 Breaks. Geometric intervals Classes. Dn_4 (<1.4) Dn_3 (1.4-19.3) Dn_2 (19.3-254.7) Dn_1 (>254.7)
	2.8. Fluviomarine features (WL) Or 'Wetlands Group': backshore wetlands mainly with dual alluvial and marine origin. Sources. Orthophotos 2002-15 Geologic map Vegetation map	3a.29. Alluvial plains (Am) River mouths forming low-lying areas with continuous or sporadic fresh-water flows and salt-water flooding. 3a.30. Salt marshes (Sm) Backshore depressions where halophilous plant communities are developed, locally known as *saladares*. 3a.31. River-mouth ponds (Pm) Backshore permanent water bodies clearly confined to ravine mouths, seaward enclosed by a sandy or gravel beaches. 3a.32. Barrier-system lagoons (Lm) Shallow salt-water bodies affecting by tides, not confined to ravine mouths, seaward enclosed by a sandy or calcarenitic barriers.	Metric. Area, hm² Samples. 272 Breaks. Geometric intervals Classes. Wl_4 (<0.11) Wl_3 (0.11-1.5) Wl_2 (1.5-19.6) Wl_1 (>19.6)

Crono-secuencias geomorfológicas en las costas de Cabo Verde

(No publicado)

Cape Verde coastal geomorphic chronosequences

(Not published)

Contenidos

1. Objetivo

Este trabajo se propone estudiar, mediante "sustitución espacio por tiempo" (*space-for-time substitution*), la evolución a escala geológica de la estructura geomorfológica de las costas de Cabo Verde, y en concreto, de su composición, abundancia y diversidad. Para ello se cuenta con los precedentes metodológicos y conceptuales de trabajos elaborados en el archipiélago canario (Ferrer-Valero, 2018; Ferrer-Valero et al., 2018), que dieron lugar a diferentes hipótesis sobre la evolución costera en archipiélagos de punto caliente, que se pretenden explorar ahora con nuevos casos.

2. Métodos

2.1. Selección de islas de Cabo Verde

El archipiélago de Cabo Verde se sitúa en el Atlántico Norte, entre 14º-17º norte y 21º-25º oeste, a una distancia entre 550 y 830 km de la costa occidental del continente africano (Fig. 1). El origen del archipiélago se asocia a la actividad eruptiva de un punto caliente (*Cape Verde Rise*) sobre la litosfera oceánica de la placa africana, desde el Oligoceno-Mioceno (Ramalho, 2011). Al igual que en la islas Canarias, la corteza es antigua (jurásico-cretácica), gruesa y de lento movimiento, lo que explica la configuración espaciotemporal del archipiélago. Se compone de 10 islas principales dispuestas en dos cadenas, norte (E-O: São Nicolau, Santa Luzia, São Vicente y Santo Antão) y sur (NE-SO: Sal, Boa Vista, Maio, Santiago, Fogo y Brava) (Fig. 1), establecidas a partir de los mapas batimétricos (Amante y Eakins, 2009).

El razonamiento "espacio por tiempo" (Pickett, 1989) se aplica a lo largo del gradiente temporal y morfológico en sentido E-O. Las islas orientales, más antiguas (miocenas) y erosionadas, son bajas y planas, con elevaciones máximas por debajo de 500 msnm. Por el contrario, las islas occidentales, más jóvenes (plio-cuaternarias), presentan mayores relieves y morfologías volcánicas mejor conservadas. Este gradiente es especialmente notorio en la cadena sur. La cadena norte parece haber surgido de forma prácticamente simultánea (Holm et al., 2008), aunque la isla de Santo Antão es la que mejor conserva la morfología de un escudo volcánico joven (Ramalho, 2011).

Siguiendo un criterio de estado evolutivo y tamaño, se han seleccionado para este estudio 4 islas representativas (Fig. 1):

1. Fogo se sitúa en el extremo suroccidental de la alineación sur. Tiene una superficie de 476 km^2, un perímetro circular de 105 km y una altitud máxima de 2.829 msnm, por lo que es punto más alto del archipiélago. Constituye un estratovolcán activo, con una breve historia geológica (<1 ma) (Ramalho, 2011), cuya morfología conserva, como ningún otro caso en Cabo Verde, la estructura de un volcán oceánico joven, de elevada pendiente y relativamente poco afectado por procesos erosivos.
2. Santiago se sitúa en la alineación sur, a 55 km al este de Fogo, aunque separada por profundidades oceánicas de 2,500 a 3,000 m. Cuenta con una superficie de 991 km^2, un perímetro de 244 km y una altitud máxima de 1,394 msnm. Su desarrollo subaéreo (complejo volcánico "Pico da Antonia", Serralheiro, 1976) data de hace tan solo ~3.5 ma, (Holm et al., 2008). Santiago es representativa de un volcán oceánico en estado posterosivo temprano, donde la morfología en escudo es todavía evidente pero la superficie se encuentra fuertemente erosionada por una red de profundos barrancos.

3. São Vicente se sitúa en la alineación norte, entre las islas de Santo Antão y Santa Luzia. Forma una superficie de 227 km^2, con un perímetro de ~98 km y 725 m de altitud máxima. Constituye un escudo volcánico maduro, de aproximadamente ~7 ma. de antigüedad (Holm et al., 2008; Ancochea et al., 2010), fuertemente erosionado, en cuya depresión central afloran rocas del complejo basal. Representa un estadio posterosivo más avanzado que Santiago o Santo Antão, donde el desmantelamiento del edificio es muy acusado y donde son muy evidentes los procesos de reactivación volcánica en áreas periféricas.
4. Boa Vista forma parte del grupo oriental de la alineación sur. Cuenta con una superficie de 620 km^2, un perímetro de 130 km y apenas 378 m de altitud máxima. Con una antigüedad superior a 16 ma y ausencia de actividad volcánica cuaternaria (Dyhr y Holm, 2010), representa una fase de arrasamiento casi total de un volcán oceánico.

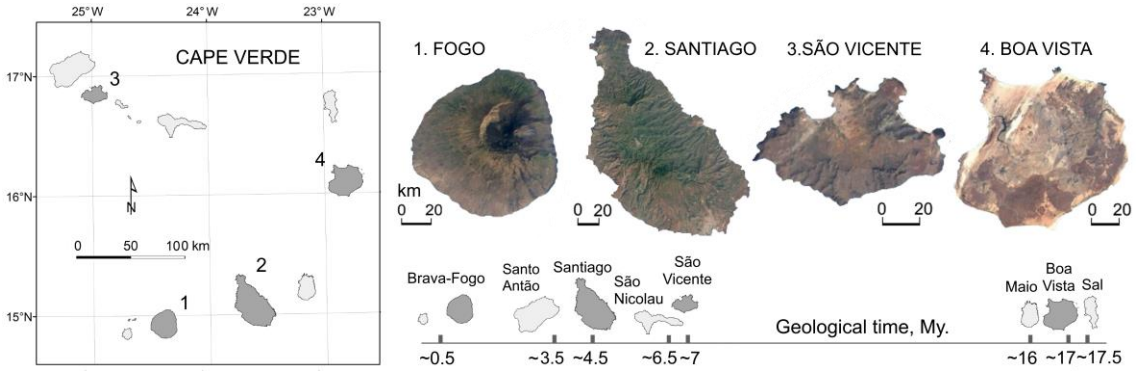

Fig. 1. Islas seleccionadas para el estudio. Cada isla representa un estadio diferenciado de la evolución de una isla oceánica. En la imagen satelital se puede observar el gradiente temporal en la fisiografía general. Las edades geológicas están recogidas de Ramalho (2011) para el inicio de la formación de los escudos volcánicos de Cabo Verde.

2.2. Muestreo

El estudio íntegro del perímetro costero (Ferrer-Valero et al., 2017; Ferrer-Valero, 2018; Ferrer-Valero et al., 2018) es sustituido por el análisis geomorfológico en puntos muestrales. El tamaño muestral mínimo para estimar la diversidad con un error aceptable se calculó mediante curvas de rarefacción sobre las cartografías geomorfológicas de las islas canarias de La Palma, Gran Canaria y Fuerteventura (Ferrer-Valero et al., 2018). Dichas curvas fueron obtenidas empíricamente mediante un método Bootstrap (Efron y Tibshirani, 1993) en R-Studio, con 5,000 remuestreos aleatorios, sin reemplazo, en cada aumento muestral de 5, 15, 25, 50, 75,...1,000. A partir de 250 puntos se obtuvieron errores por debajo del 5% (IC=95%) en los valores de entropía de Shannon (H') y Simpson (D), y errores en torno al 15% (IC=95%) en la riqueza (S). El tamaño muestral se fijó finalmente en 300 puntos (Fig. 2).

Con ello, se procedió a proyectar 300 puntos aleatorios, sin reemplazo, a lo largo de la costa de cada una de las 4 islas objeto de estudio. A estos puntos de se les asignó un radio de 25 m para construir tramos costeros de 50 m (1 punto=50 m de línea costera), donde se registró, hacia el mar y hacia tierra (*cross-shore*), la presencia [1] o ausencia [0] de cada clase taxonómica y sus parámetros dimensionales.

Para compensar en lo posible el error de muestreo en la riqueza geomorfológica (en torno al 15% en los remuestreos de 300 puntos, con la consiguiente probabilidad de solapamiento de valores entre islas, se implementó posteriormente una búsqueda general de las clases *a priori* inexistentes (no capturadas en el muestreo), que dio lugar a la incorporación manual de dos

puntos adicionales en la isla de Santiago (+2 clases de segundo orden) y un punto en la isla de São Vicente (+1 clase de segundo orden).

```
BOOTSTRAP=function(tamaño,B=5000){
  indices=NULL
  for(i in 1:B){
    MUESTREO=sample(1:nrow(datos),tamaño,replace=FALSE)
    MUESTRA=datos[MUESTREO,15:50]
    numGeo=colSums(MUESTRA)
    probGeo=numGeo/tamaño
    Riqueza=sum(ifelse(probGeo>0,1,0))
    Shannon=-sum(ifelse(probGeo==0,0,probGeo*log(probGeo)))
    indices=rbind(indices,c(Riqueza=Riqueza,Shannon=Shannon,probGeo))
  }
  medias=colMeans(indices)
  cuantiles=apply(indices,2,quantile,probs=c(0.025,0.975))
  errores=(cuantiles[2,]-cuantiles[1,])/2
  data.frame(media=medias,error=errores)
}
```

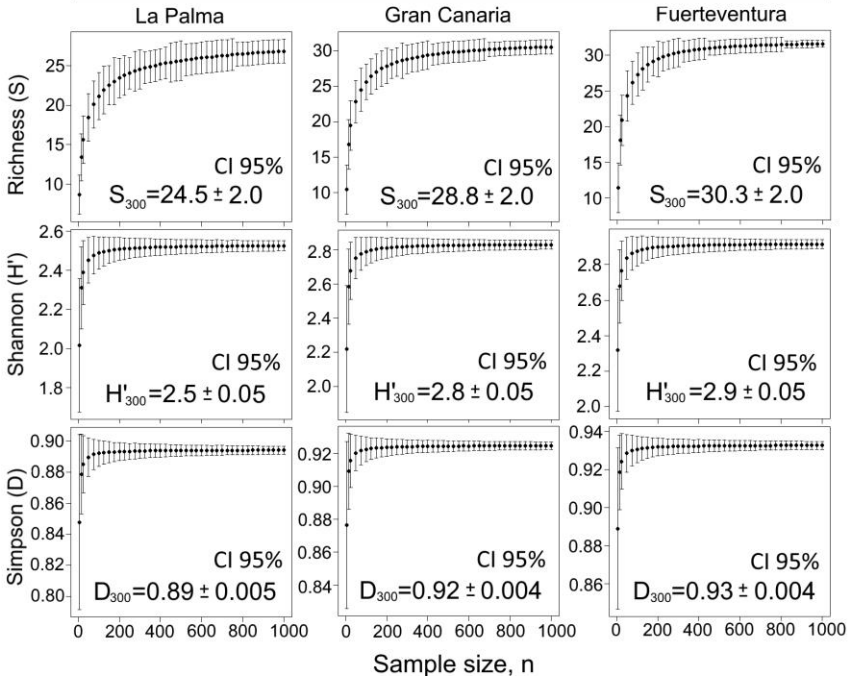

Fig. 2. Código en R y curvas resultantes de la aplicación de un *bootstrap* a la diversidad geomorfológica de las costas de La Palma, Gran Canaria y Fuerteventura. Los resultados numéricos corresponden con las medias y errores para una muestra de 300 puntos al 95% de confianza.

2.3. Taxonomía y fuentes

La estructura geomorfológica costera se analiza a través de la taxonomía para áreas con baja disponibilidad de fuentes propuesta por Ferrer-Valero (2018).

En Cabo Verde, las fuentes abiertas para el conjunto del archipiélago son principalmente topografías de escala 1:10,000 (IDE de Cabo Verde, Gobierno de Cabo Verde), 4 series de ortofotos digitales (2003-actualidad) con resoluciones entre 50 y 12.5 cm/pixel (Infraestructura de Datos Espaciales, IDE, de Cabo Verde, Gobierno de Cabo Verde) y 10 imágenes satelitales (2002-2018) de Landsat/Copernicus, CNES/Airbus y Digital Globe, incorporadas en la plataforma 3D de *Google Earth*. Además, la interpretación se apoya en los estudios geológicos y geomorfológicos publicados de la isla de Fogo (Machado y Asunção, 1965), Santiago (Serralheiro, 1976), São Vicente (Ancochea et al., 2010) y Boa Vista (Dyhr y Holm, 2010; Hernández-Calvento et al., 2017). El trabajo de campo se realizó en las tres primeras semanas de noviembre de 2017, habiéndose reconocido *in situ* 200 puntos de muestreo (16% del total).

Respecto a la propuesta taxonómica de Ferrer-Valero (2018), este trabajo introduce las siguientes novedades:

(i) En el segundo orden taxonómico se homogeniza toda la información a medidas unidimensionales de longitud, referidas al punto de muestreo, prescindiendo de medidas bidimensionales (áreas), tridimensionales (volúmenes) y lineales *longshore*. Los parámetros pasan todos a dimensiones lineales *cross-shore* en el punto de muestreo.

(ii) Se incorpora el Grupo "Plataforma insular" (SH), con tres Subgrupos de "anchura" (SH_1, SH_2, SH_3). Se ha utilizado para ello el límite convencional de la curva batimétrica -50 m de la Carta Náutica de Cabo Verde.

(iii) Se incorporan 6 Grupos y 18 Subgrupos relacionados con la forma en planta de la línea de costa.

La morfología en planta de la costa debe considerarse en una descripción completa de la estructura geomorfológica, por lo que se incorpora en este trabajo. El interés por estimar y caracterizar la irregularidad de la costa, también llamada complejidad costera (*coastal complexity*), ha llevado al empleo de procedimientos basados en dimensiones fractales (e.g. Jiang y Plotnick, 1998; Dai et al., 2004; D'Alessandro et al., 2006) y ángulos (e.g. Andrle, 1994; Bartley et al., 2001; Porther-Smith y McKinlay, 2012). Ninguno de estos procedimientos, sin embargo, se adecúa a la estructura analítica de esta investigación, que exige, por un lado, el uso de categorías en primer orden taxonómico, y por otro, determinar la irregularidad como propiedad de cualquier punto de muestreo y no como valor general.

La forma y longitud sobre el plano de una línea de costa es fractal (Mandelbrot, 1967), es decir, dependiente de la escala. Puede describirse como una sucesión de trayectorias ondulatorias a determinada escala, contenidas en otras mayores que se expresan al disminuirla, y recorridas por otras más pequeñas que se expresan al aumentarla. Un pequeño saliente de la costa puede estar inserto en una bahía más grande que a su vez se inserte en un promontorio de escala mayor (la sucesión escalar puede ser casi-infinita). Así, un punto de muestreo puede formar parte de varias geoformas planimétricas en función de la escala (Fig. 3). Una bahía se percibe geométricamente por los promontorios que la comprenden, y los promontorios se entienden en relación a la bahía.

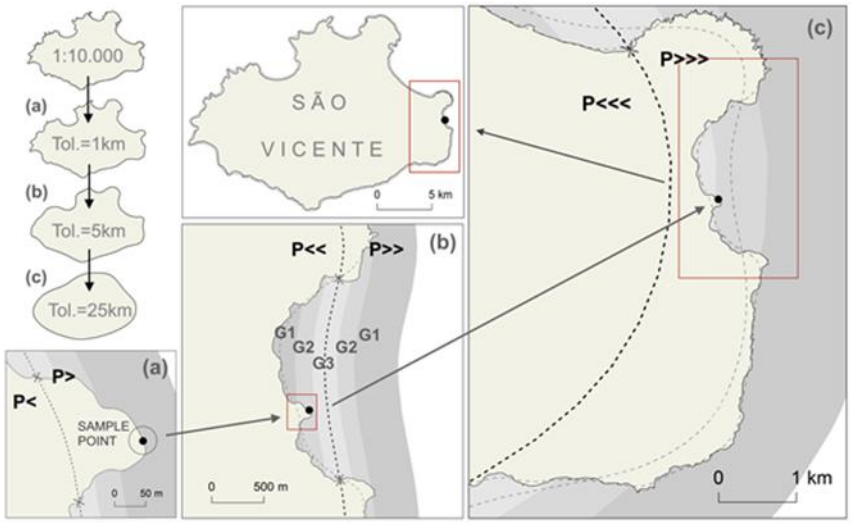

Fig. 3. Ejemplo de un punto de muestreo en la costa oriental de la isla de São Vicente, situado en el promontorio (a) de una bahía (b) de un promontorio (c). La geometría costera en ese punto se denota como $P>_1<_2>_2$. Las líneas punteadas son las líneas de referencia generadas por el algoritmo PAEK.

En este trabajo se ensaya el análisis de la forma de la línea de costa como un espectro de onda a tres escalas. Se generan tres líneas de referencia, una para cada escala, cuya intersección con la línea original, de escala 1:10.000, marca el "nivel 0" o eje del plano x, permitiendo la diferenciación categorial y sistemática de salientes y entrantes. Las crestas son salientes costeros (*forelands*) y los senos entrantes (*inlets*). Estas líneas son generadas cartográficamente a través de ajuste polinomial con núcleo exponencial (*PAEK algorithm*, Bodansky et al., 2002), con tolerancias constantes para el conjunto de las islas (T=1 km, T=5 km y T=25 km). A menor generalización, menor tamaño de onda discernido (pequeños entrantes o salientes en la costa); a mayor generalización, mayor tamaño de onda discernido (grandes salientes y entrantes) (Fig. 3). Una vez diferenciados entrantes y salientes a las tres escalas, y siguiendo la estructura de información, se recoge la distancia euclidiana del punto de muestreo a la línea de referencia, estableciendo así tres Subgrupos por cada clase, mediante cortes naturales (Jenks, 1967), que permiten diferenciar dimensiones en las morfologías categoriales.

Prescindiendo de la terminología convencional no sistemática (bahías, promontorios, salientes, entrantes, cabos, golfos, etc.), se adopta una notación particular basada en símbolos angulares precedidos de la letra P (de "*Planform*"). El ángulo a derecha "<" denota la categoría "entrante" y el ángulo a izquierda ">" la categoría "saliente". La posición del símbolo indica la escala de la "onda", y el subíndice la distancia a la línea de referencia. Un punto, por ejemplo:

$P>_1<_2>_2$, se sitúa en la punta de un promontorio, de una zona de media bahía, en una zona media, casi interior, de un promontorio (Fig. 3).

2.4. Métricas

Siguiendo los precedentes metodológicos (Ferrer-Valero, 2018; Ferrer-Valero et al., 2018), se analiza y compara la composición, abundancia y diversidad de la estructura geomorfológica de las costas de las cuatro islas objeto de estudio, por medio de diferentes métricas.

La composición resulta de la presencia /ausencia de las clases taxonómicas y de su frecuencia relativa (p) a lo largo de la costa, que es calculada sobre el total de puntos de muestreo. A partir de ello se caracterizan las zonas costeras de cada isla y se comparan desde el punto de vista de su similitud, con el objetivo de encontrar parentescos relacionados con la edad geológica y el estado evolutivo. Para ello se ensaya el cálculo, por pares de islas, del índice diversidad-beta de Whittaker (βw) y del índice de similitud de Sorensen (Cs) (tabla 1). A mayor valor en βw [1,2], mayor contraste en la estructura geomorfológica entre las islas que se comparan, y por lo tanto, menor similitud; y a mayor valor en Cs [0,1], mayor similitud entre las "poblaciones" geomorfológicas comparadas (Magurran, 2004).

A través del análisis de asociaciones (*coastal morphoassemblages*) se analiza la forma de combinarse de las georformas que componen la costa. Con ello se mide la redundancia geomorfológica y la densidad geomorfológica (tabla 1). La redundancia informa acerca del grado de repetición de las asociaciones geomorfológicas. Cuanto mayor es la redundancia, más homogénea es la costa y menor es la heterogeneidad *longshore*. La densidad es el número promedio de geoformas que componen las asociaciones geomorfológicas (tabla 1). Un número promedio mayor indica una mayor abundancia o proliferación de geoformas a través de una mayor densidad geomorfológica por km de costa.

La diversidad se analiza a través de la variación media entre islas, de 6 índices de diversidad-alfa no paramétricos. La riqueza (S) informa de la variedad absoluta de clases taxonómicas presentes, y el índice de Menhinick (D_{MN}) compensa esa riqueza con el número total de "individuos". Los índices de Shannon (H'), Simpson (D), Berger-Parker (d) y Billouin (HB) son índices de equidad-dominancia (Tabla 1). En estos dos últimos se calculan los complementarios 1-*D* y 1-*d* (Magurran, 2004). La variación, o diversidad beta, a lo largo de los gradientes cronológicos se estimó como tasa de variación de los índices, del tipo $(t_1 - t_0)/t_0$, donde t_0 es el valor inicial o de referencia, y t_1, el valor final o comparado.

Tabla 1. Índices y métricas utilizados, y sus formulaciones.

Composición y abundancia	
Whittaker*	$\beta_w = S/\overline{s}$
Sorensen**	$C_s = 2a/2a + b + c$
Nestedness	$NODF = \sum N_{paired} / N_{col}$
Geom. redundancy***	$R_g = S_m/N$
Geom. density	$D_g = \overline{S_m}$
Diversidad	
Menhinick	$D_{Mn} = S/\sqrt{N}$
Simpson	$D = 1 - \sum p_1^2$
Shannon	$H' = -\sum p_i \log p_i$
Berger-Parker	$d = 1 - N_{max}/N$
Brillouin	$HB = \ln N! - \sum \ln n_i\,! /N$

*$\overline{s}$= riqueza media de las muestras.

**a=geoformas comunes, b= ganadas, c=perdidas.

***S_m= tamaño (riqueza) de la asociación geomórfica.

3. Resultados

3.1. Composiciones

La distribución de las 21 clases de primer orden en las cuatro islas permite observar una mayor prevalencia de los Grupos rocoso-erosivos en las islas de Fogo (FG) y Santiago (ST), frente a las islas de São Vicente (SV) y Boa Vista (BV), donde se observa una tendencia al aumento de los Grupos clástico-acrectivos (Fig. 3).

El patrón cronológico en los valores de frecuencia (*p*) se produce cuando hay una tendencia constante a lo largo de la serie FG-ST-SV-BV, con mínimo y máximo en los extremos de la cadena. Esta se produce en forma creciente en los Grupos PDn (m=0.16, r^2=0.79; p<0.05), FM (m=0.07, r^2=0.99; p<0.05) y LG (m=0.06, r^2=0.78; p<0.05), y en forma decreciente en CL (m=-0.22, r^2=0.87, p<0.05) (Fig. 3).

El patrón semi-cronológico se produce cuando un valor *p* altera la secuencia cronológica, de forma que el mínimo/máximo primario recae en algún extremo de la serie FG-ST-SV-BV y el mínimo/máximo secundario en alguno de los elementos centrales. Se da en modo creciente en DN (m=0.24, r^2=0.70; p<0.05) y SB (m=0.16, r^2=0.61; p>0.05), y en modo decreciente en PCl (m=0.08, r^2=0.26; p>0.05), GB (m=-0.05, r^2=0.84, p>0.05) y RM (m=-0.03, r^2=0.87; p>0.05) (Fig. 3).

Con el mínimo/máximo, primario y secundario, en los elementos centrales, el patrón es parabólico, de modo que *p* aumenta y decae, como en PT (m=0.06, r^2=0.10; p>0.05) y P> (m=-0.01, r^2=0.01; p>0.05), o decae y aumenta, como en P< (m=0.01, r^2=0.11; p>0.05). Finalmente, bajo alternancia constante de valores, el patrón es sinusoide, en forma creciente, como en MT (m=0.26, r^2=0.54; p>0.05) y P<< (m=0.04, r^2=0.73; p>0.05), o decreciente, como en LD (m=-0.08, r^2=0.31, p>0.05), DB (m=-0.04, r^2=0.50, p>0.05), P>> (m=-0.04, r^2=0.07; p>0.05), P>>> (m=-0.01, r^2=0.01; p>0.05), P<<< (m=-0.01, r^2=0.01; p>0.05) y RF (m=-0.004, r^2=0.02, p>0.05) (Fig. 3).

En segundo orden taxonómico aparecen las siguientes distribuciones (Fig. 4). Los Grupos PCl, RF, SH, DN, PDn, FM y LG muestran un dimensionamiento cronológico, decreciente en PCl y creciente en el resto. Como resultado, en Fogo no se observan los Subgrupos RF_1 (>150 m), SH_1 (>5,000 m), RF_2 (60-150 m), SH_2 (1,850-5,000 m), DN_2 (1,450-4,825), DN_1 (>4,825 m), FM_1 (372-1,030 m), FM_2 (>1,030) LG_2 (130-390 m) y LG_1 (>390 m). En Santiago, tampoco se observan RF_1 (>150 m), SH_1 (>5,000 m), DN_2 (1,450-4,825), DN_1 (>4,825 m), PDn_1 (>2,910 m), LG_2 (130-390 m)

y LG_1 (>390 m); y en São Vicente, tampoco se observa LG_1. Las anchuras de GB y SB siguen patrones semi-cronológicos, decrecientes en GB (Q2 {m=-0.80, r^2=0.64; p>0.05}) y crecientes en SB (Q2 {m=4.65, r^2=0.36; p>0.05}).

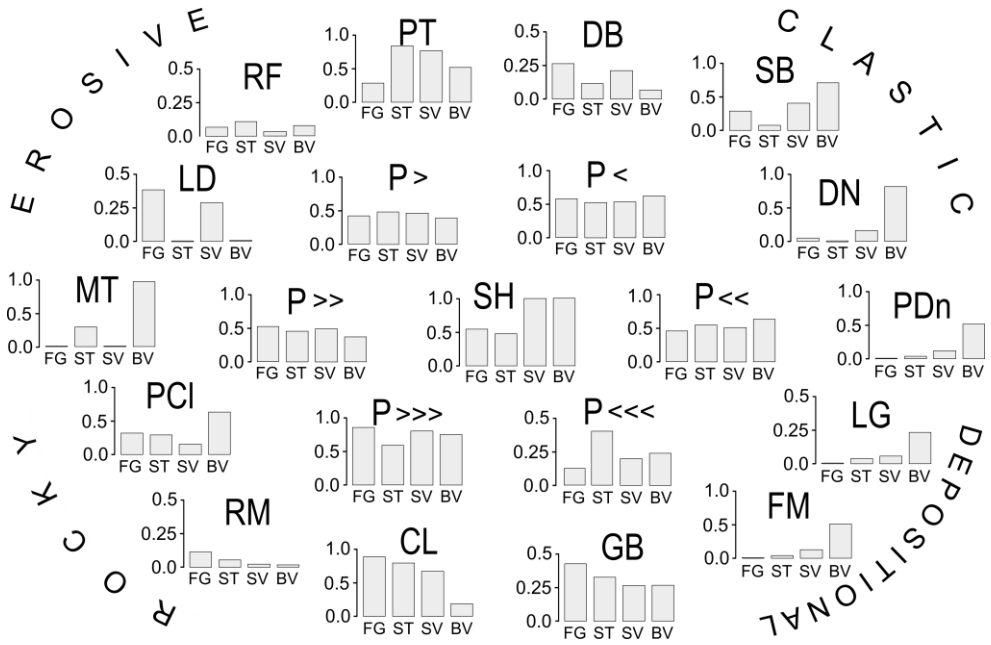

Fig. 3. Frecuencias (p) de los Grupos geomorfológicos del primer orden taxonómico, por islas. FG, Fogo; ST, Santiago; SV, São Vicente; BV, Boa Vista. CL, "*Cliffs group*"; PCl, "*Paleo-cliffs group*"; RM, "*Remnants group*"; RF, "*Reefs group*"; MT, "*Marine terraces group*"; LD, "*Lava-delta group*"; SH, "*Shelf group*"; DB, "*Debris group*"; GB, "*Gravel beaches group*"; SB, "*Sandy beaches group*"; DN, "*Dunes group*"; PDn, "*Paleo-dunes group*"; FM, "*Fluvio-marines group*"; LG, "*Lagoons group*"; P>, "*Foreland scale 1*"; P>>, " *Foreland scale 3*"; P>>>, " *Foreland scale 3*"; P<, "*Inlet scale 1*"; P<<, "*Inlet scale 2*"; P<<<, "*Inlet scale 3*".

Las alturas en CL y DB presentan un patrón parabólico de crecimiento y caída en la serie FG-ST-SV-BV, con máximo en São Vicente, y con ausencia de CL_1 (>225 m) en Boa Vista, y de DB_1 (>110 m) en los extremos de la secuencia: Fogo y Boa Vista. La distribución secuencial de anchuras es sinusoide con tendencia creciente en PT (Max. {m=6.9, r^2=0.54; p>0.05}), MT (Max. {m=2,039, r^2=0.57; p>0.05}) y LD (Max. {m=55.5, r^2=0.00; p>0.05; para máximos}). MT_1 (>4,146 m) no se encuentra en Santiago, ni LD_1 (>1,560 m) en Fogo. Los Grupos MT y LD se encuentran ausentes, respectivamente, en Fogo/São Vicente y en Santiago/Boa Vista.

Las morfologías planimétricas tienden a maximizar su proyección en las islas centrales de la secuencia cronológica, en las irregularidades de menor (P<, P>) y media escala (P<<, P>>), y a presentar una proyección cronológico-creciente, con máximo en Boa Vista, en las irregularidades de mayor escala (P>>>). Todos los Subgrupos en las tres escalas de salientes (P>, P>>, P>>>) están presentes en las cuatro islas, pero los entrantes de escala $P<_1$ (>73 m), $P<<_1$ (>283 m), $P<<<_2$ (583-1,241 m) y $P<<<_1$ (>1,241 m), están ausentes en Fogo (Fig. 4).

Asumiendo equiprobabilidad, la ocurrencia esperada de la secuencia cronológica FG-ST-SV-BV, en modo creciente o decreciente, es de 2/24=0.08 (n!). Teniendo en cuenta que la ocurrencia observada es 4/20=0.20, en primer orden, y 7/21=0.33, en segundo orden, se puede determinar una tendencia de los datos recogidos a configurarse cronológicamente. Por otro lado, los valores *p* covarían significativamente con los valores dimensionales medianos (r=0.40, p<0.01) y máximos (r=0.58, p<0.01), normalizados, lo que quiere decir que las geoformas tienden a aumentar su frecuencia *longshore* a la vez que su dimensión *cross-shore.*

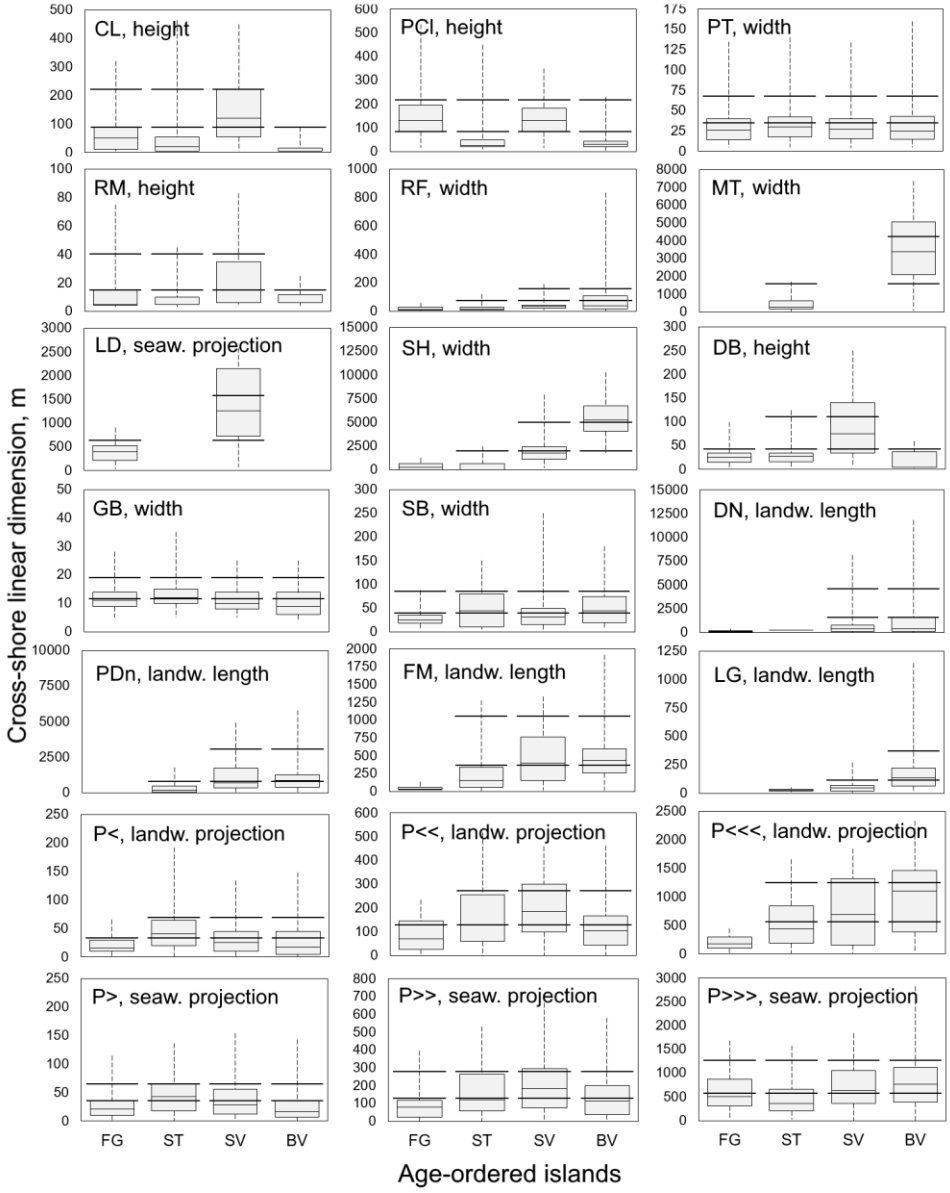

Fig. 4. Distribución de los mínimos, maximos y cuantiles de las series dimensionales de cada Grupo de geoformas, con las líneas negras horizontales marcando los cortes naturales de las series. FG, Fogo; ST, Santiago; SV, São Vicente; BV, Boa Vista. CL, "*Cliffs group*"; PCl, "*Paleo-cliffs group*"; RM, "*Remnants group*"; RF, "*Reefs group*"; MT, "*Marine terraces group*"; LD, "*Lava-delta group*"; SH, "*Shelf group*"; DB, "*Debris group*"; GB, "*Gravel beaches group*"; SB, "*Sandy beaches group*"; DN, "*Dunes group*"; PDn, "*Paleo-dunes group*"; FM, "*Fluvio-marines group*"; LG, "*Lagoons group*"; P>, "*Minor foreland scale*"; P>>, "*Mid foreland scale*"; P>>>, "*Major foreland scale*"; P<, "*Minor inlet scale*"; P<<, "*Mid inlet scale*"; P<<<, "*Major Inlet scale*".

Los resultados de los índices de disimilitud de Whittaker, βw, y de similitud de Sorensen, Cs (Fig. 5), indican que la mayor proximidad en las estructuras geomorfológicas costeras se produce entre islas cronológicamente contiguas de la cadena FG-ST-SV-BV. Cuando los índices se contrastan por pares desde los extremos de la serie (Fogo o Boa Vista), se obtiene la secuencia cronológica (Fig. 5). La única distorsión del patrón se produce al aplicar los índices respecto a la isla de Santiago. Entonces, Santiago aparece más emparentada con Boa Vista que con Fogo, su adyacente, debido al afecto de las clases MT, que aparece solo en estas islas, y LD, que no aparece en ninguna de ellas. Cabe subrayar, sin embargo, que MT y LD son las dos clases menos relacionadas con procesos costeros y más con procesos volcánicos y tectónicos. Pero al calcular las medias, se vuelve a obtener el patrón cronológico. Para βw, las medias de disimilitud son más

altas en los extremos de la cadena de islas (Fogo y Boa Vista), y para Cs, las medias de similitud son más altas en los elementos centrales (Santiago y São Vicente). Además, las medias indican que Fogo es la isla geomorfológicamente más "diferente" al resto (Fig. 5).

Con esto, queda verificado el "patrón cronológico" de cambio en las estructuras geomorfológicas costeras de la cadena de islas FG-ST-SV-BV.

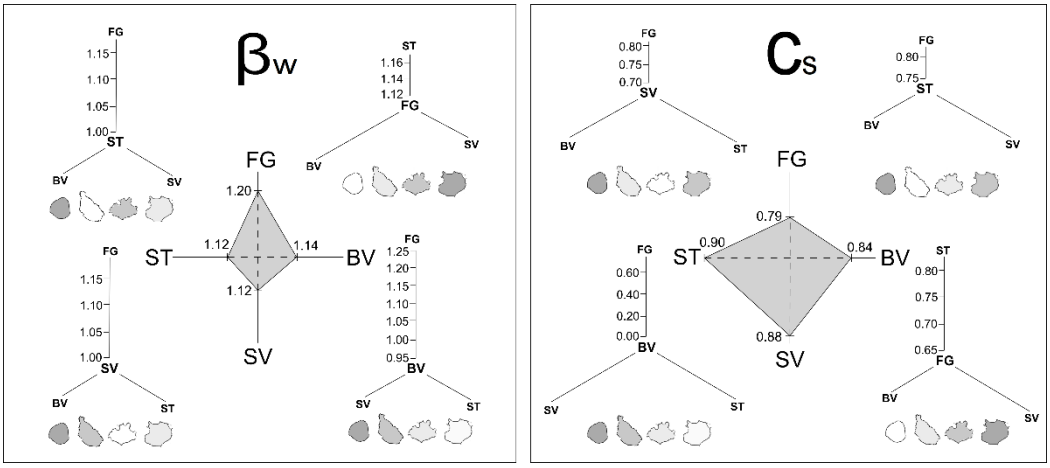

Fig. 5. Indices de Whittaker (βw) y Sorensen (Cs), aplicados por pares de islas. En el centro de los gráficos, las medias de los dos índices, indicando, respectivamente mayor dismilitud y mayor similitud entre el conjunto de islas. FG, Fogo; ST, Santiago; SV, São Vicente; BV, Boa Vista.

El patrón de distribución de las clases taxonómicas podría además indicar un fenómeno de anidamiento (*nestedness*) a lo largo de la cadena temporal FG-ST-SV-BV (Fig. 6). El anidamiento significa que las clases presentes en una isla "joven" forman un subconjunto dentro del conjunto de clases de la isla inmediatamente más "vieja", y así sucesivamente. El 100% de las clases presentes en Fogo, están en Santiago. El 94% de las clases de Santiago, se registran tambien en São Vicente, y el 92% de las clases de São Vicente, están en Boa Vista. El valor final de anidamiento según el modelo NODF (Almeida-Neto et al., 2008) es 79, lo que permite confirmar la existencia de este patrón de transformación entre islas.

	FG	ST	SV	BV		FG	ST	SV	BV		FG	ST	SV	BV
SH_3	1	1	1	1	RM_3	1	1	1	1	$P_{<<<2}$	0	1	1	1
CL_3	1	1	1	1	PCl_3	1	1	1	1	$P_{<1}$	0	1	1	1
$P_{>>3}$	1	1	1	1	LD_2	1	0	1	0	LG_3	0	1	1	1
$P_{<3}$	1	1	1	1	PT_2	1	1	1	1	$P_{<<<1}$	0	1	1	1
$P_{>3}$	1	1	1	1	RF_3	1	1	1	1	FM_2	0	1	1	1
$P_{>>2}$	1	1	1	1	SB_2	1	1	1	1	PDn_3	0	1	1	1
$P_{<3}$	1	1	1	1	PCl_1	1	1	1	1	RF_2	0	1	1	1
LD_3	1	0	1	0	DB_2	1	1	1	1	PDn_2	0	1	1	1
$P_{>3}$	1	1	1	1	DN_3	1	1	1	1	SH_2	0	1	1	1
GB_3	1	1	1	1	CL_1	1	1	1	0	MT_2	0	1	0	1
SB_3	1	1	1	1	$P_{>>>1}$	1	1	1	1	DB_1	0	1	1	0
CL_2	1	1	1	1	PT_1	1	1	1	1	FM_1	0	1	1	1
DB_3	1	1	1	1	FM_3	1	1	1	1	LD_1	0	0	1	0
GB_2	1	1	1	1	RM_1	1	1	1	1	SH_1	0	0	1	1
PT_3	1	1	1	1	GB_1	1	1	1	1	DN_1	0	0	1	1
PCl_2	1	1	1	1	$P_{>1}$	1	1	1	1	PDn_1	0	0	1	1
$P_{<2}$	1	1	1	1	RM_2	1	1	1	1	LG_2	0	0	1	1
$P_{<<2}$	1	1	1	1	$P_{>>1}$	1	1	1	1	RF_1	0	0	1	1
$P_{<<<3}$	1	1	1	1	SB_1	1	1	1	1	DN_2	0	0	1	1
$P_{>2}$	1	1	1	1	MT_3	0	1	0	1	MT_1	0	0	0	1
$P_{>>2}$	1	1	1	1	$E_{<<1}$	0	1	1	1	LG_1	0	0	0	1

Fig. 6. Tabla de presencias (1-cuadros grises) y ausencias (0-cuadros blancos) para las 63 clases de segundo orden. El valor de anidamiento para la configuración cronológica es NOFD=79. FG, Fogo; ST, Santiago; SV, São Vicente; BV, Boa Vista.

3.2. Asociación ('assembling')

Se denomina *coastal morphoassemblage* (Ferrer-Valero, 2018; Ferrer-Valero et al., 2018) a una asociación de n geoformas que coexisten en un punto de la costa (Fig. 7).

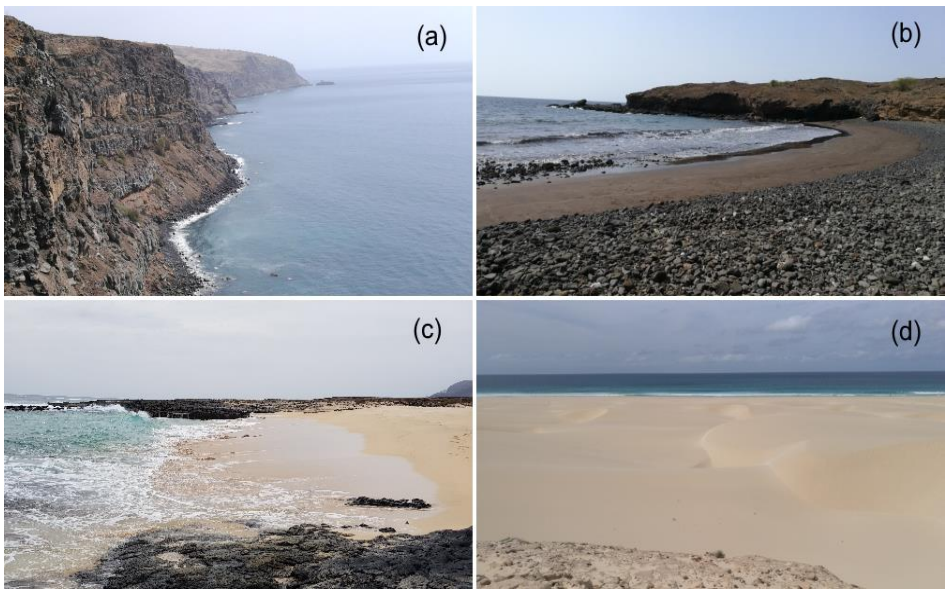

Fig 7. Ejemplos de *morphoassemblages* costeros en las islas de Cabo Verde. (a) Asociacion de acantilados (CL_2) con depósitos de ladera (DB_2) y playas de bolos (GB_3). Es la asociación geomorfológica más frecuente en la isla de Fogo. (b) Playa mixta con arena (SB_3) en el intermareal, y cantos (GB_3) en el supramareal. Al fondo se puede ver un pequeño acantilado (CL_3) con plataforma intermareal (PT_2), que constituye la asociación más frecuente en la isla de Santiago. (c) Costa baja con asociacion de playa de arena organógena (SB_2) y plataforma lávica intermareal (PT_2), característica de la costa este de São Vicente. (d) Asociación de playas de arena (SB_2) y cordones dunares transgresivos (DN_2) de la costa oeste de Boa Vista, vistos desde un nivel de terraza marina (MT_1).

La *redundancia geomorfológica*, como medida derivada de la riqueza de asociaciones, informa acerca del grado de repetición de los *morphoassemblages* costeros y, por lo tanto, de la heterogeneidad paisajística a lo largo de las costas de las cuatro islas. Los resultados en este parámetro indican que existe una tendencia al aumento de riqueza y a la disminución de la redundancia geomorfológica a lo largo de la cadena de islas FG-ST-SV-BV, tanto en primero, como en segundo orden taxonómico (Tabla 2). Nos obstante, la tendencia no es limpia, pues São Vicente presenta valores intermedios entre Fogo y Santiago, no entre Santiago y Boa Vista. En São Vicente existe, por lo tanto, un abanico menor de "mezclas" de geoformas que en Santiago.

Tabla 2. Valores de redundancia y densidad geomorfológica derivados del análisis cuantitativo de las asociaciones geomorfológicas (*morpho-assembling*).

	Islands	Variation, %

	Tax. order	FG	ST	SV	BV	FG-ST	ST-SV	SV-BV
Morphoassemblages	1	143	152	144	193	*6.3*	*-5.3*	*34.0*
richness	2	263	287	270	278	*9.1*	*-5.9*	*3.0*
Geomorphic	1	0.52	0.49	0.52	0.35	*-5.1*	*5.0*	*-31.6*
redundance	2	0.12	0.05	0.10	0.07	*-59.7*	*107.4*	*-28.8*
Geom. density	1/2	4.94	5.45	5.89	7.60	*10.2*	*8.2*	*29.0*

La densidad geomorfológica, o número medio de geoformas que componen las asociaciones geomorfológicas, crece limpiamente en la secuencia cronológica FG-ST-SV-BV (Tabla 2). Las frecuencias de los tamaños de las asociaciones forman curvas normales que tienden a desplazar su valor medio a lo largo del eje de abscisas (Fig. 8). Este comportamiento en la densidad y la distribución de frecuencias indica un patrón cronológico en la abundancia geomorfológica de las costas. La proliferación general de geoformas costeras es, según estos datos, creciente en la secuencia FG-ST-SV-BV.

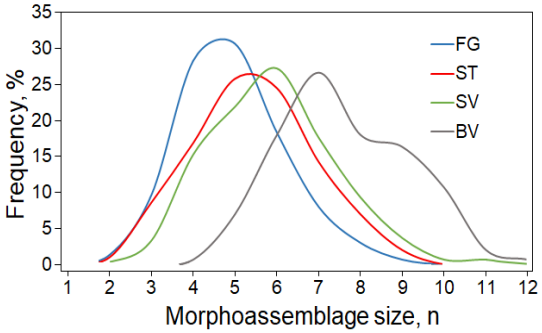

Fig. 8. Distribución de las frecuencias de los tamaños, n, de las asociaciones geomorfológicas en cada uno de los puntos costeros analizados. FG, Fogo; ST, Santiago; SV, São Vicente; BV, Boa Vista.

3.3. Diversidad

La longitud del eje x en las series de rango-abundancia (Fig. 9) muestra la riqueza absoluta de clases (S), y las pendientes m de las rectas $y = mx + n$, ajustadas por mínimo error cuadrático medio, indica la uniformidad (horizontalidad) de la distribución de frecuencias a través de su parecido con una función constante $y = m$. Las pendientes son relativas a serie más corta (Fogo) para neutralizar el posible efecto de la riqueza. La longitud x de la serie (riqueza) muestra indiferenciación general en primer orden y aumento sistemático en la secuencia cronológica FG-ST-SV-BV, en segundo orden (Fig. 9). Las pendientes *m* muestran una horizontalidad creciente en la secuencia FG-ST-SV-BV, ligeramente alterada por los valores de São Vicente, que muestran menor pendiente (mayor uniformidad) que Boa Vista, en primer y segundo orden (Fig. 9).

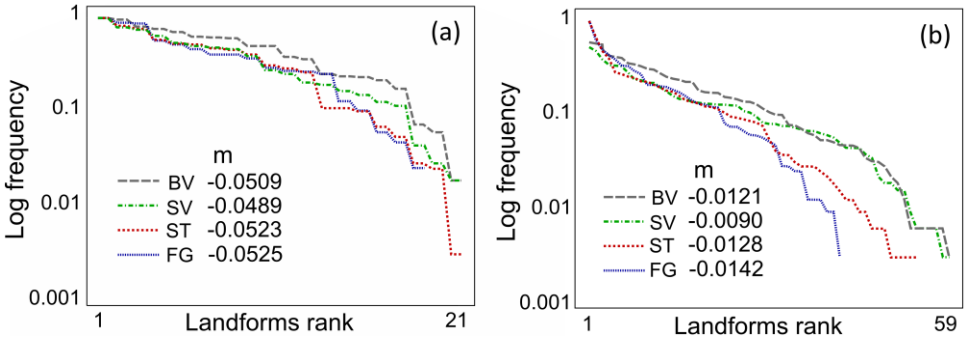

Fig. 9. Curvas de rango-abundancia en primer orden (a) y segundo orden taxonómico (b). *m*, pendiente de la recta, ajustada por mínimo error cuadrático medio, normalizada a la longitud de la serie más corta. FG, Fogo; ST, Santiago; SV, São Vicente; BV, Boa Vista.

Los 6 índices de diversidad aplicados para estimar el comportamiento de la diversidad geomorfológica a lo largo de la cadena de islas FG-ST-SV-BV, muestran la misma configuración secuencial: la diversidad aumenta entre Fogo y Santiago, vuelve a aumentar de Santiago a São Vicente, para disminuir finalmente entre São Vicente y Boa Vista, donde, a excepción del índice de Menhinick (DMN), los valores son más altos que en Santiago (Tabla 3).

Tabla 3. Valores de los índices de diversidad e incrementos porcentuales por pares de islas a lo largo de la secuencia cronológica FG-ST-SV-BV.

	α-diversity (index value)				β-diversity (variation, %)			Incremental
	FG	ST	SV	BV	FG-ST	ST-SV	SV-BV	pattern
Richness (S)	40	52	59	58	*30*	*13.46*	*-1.69*	FG-ST-BV-SV
Menhinick (DMN)	0.87	1.13	1.27	1.11	*30.0*	*11.75*	*-12.58*	FG-ST-BV-SV
Simpson (1-D)	0.94	0.95	0.97	0.97	*0.34*	*2.13*	*-0.04*	FG-ST-BV-SV
Shannon (H')	3.18	3.31	3.64	3.61	*3.85*	*10.15*	*-0.92*	FG-ST-BV-SV
Berger-Parker (1-d)	0.86	0.86	0.93	0.94	*0.00*	*8.01*	*0.96*	FG-ST-SV-BV
Brillouin (HB)	0.32	0.33	0.41	0.36	*5.31*	*21.66*	*-10.62*	FG-ST-BV-SV

Dados los contrastes de magnitud entre los valores absolutos de los índices, se normalizan las variaciones a incrementos porcentuales entre pares de islas (Tabla 3). Aunque dentro del patrón señalado, los incrementos vuelven a mostrar contrastes importantes. La variación mínima entre Fogo y Santiago es de 0.0%, en Berger-Parker (1-d), y la máxima de 30.0%, en Riqueza (S). Entre Santiago y São Vicente, el mínimo es de 2.1%, en Simpson (1-D), y la máxima de 21.7%, en Brillouin (HB). Entre São Vicente y Boa Vista, la mínima variación es de -0.04%, en Simpson (1-D), y máxima de 12.6%, en Menhinick (DMN).

La variación promedio muestra finalmente ese patrón parabólico (Fig. 10), con rangos de desviación significativos, donde la diversidad geomorfológica aumenta de forma inequívoca a lo largo de la cadena de islas FG-ST-SV, y decae ligeramente al final, entre SV-BV.

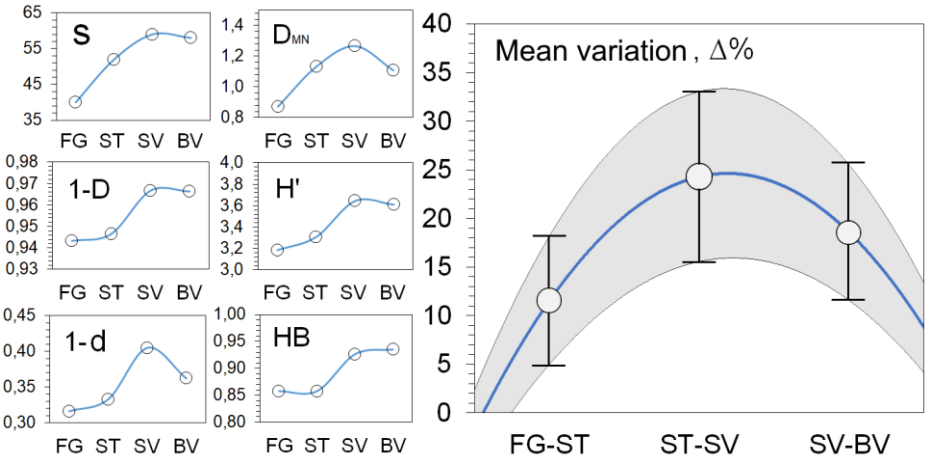

Fig. 10. Valores de los índices de diversidad a lo largo de la cadena de islas FG-ST-SV-BV, y patrón parabólico, de crecimiento-caída, en la estimación promedio y desviación típica de la variación intermuestral.

4. Discusión y conclusiones

Utilizando una taxonomía geomorfológica *ad hoc*, compuesta de 21 Grupos categoriales y 63 Subgrupos dimensionales, analizada en 300 puntos de muestreo aleatorios, en las costas de cuatro islas del archipiélago de Cabo Verde, con diferentes edades y estados evolutivos, se ha obtenido que:

1. Como fue observado en Canarias (Ferrer-Valero et al., 2018), la estructura geomorfológica de las costas sigue un patrón predominantemente cronológico y las composiciones generales en la cadena señalan que el parentesco es inequívocamente mayor entre islas cronológicamente más próximas, que entre islas cronológicamente más alejadas. Además, según lo observado, la transformación tipológica sigue un patrón de anidamiento (*nestedness*).
2. Como también fue observado en Canarias (Ferrer-Valero et al., 2018), la abundancia geomorfológica, entendida como grado general de proliferación de geoformas costeras, es mayor cuanto mayor es la edad geológica de la isla y más avanzado es su estado evolutivo. Por lo tanto, crece cronológicamente de forma inequívoca a lo largo de la muestra analizada.
3. De forma muy semejante a lo observado en Canarias (Ferrer-Valero et al., 2018), la diversidad, en sus parámetros de riqueza y equiabundancia, señalan un patrón parabólico, marcado por un crecimiento constante entre Fogo (0.5 ma.), Santiago (3.5 ma.) y São Vicente (7 ma.), matizado al final por una caída de los valores en Boa Vista (17 ma.). La diferencia principal es que en Canarias se observa una disminución del crecimiento entre Gran Canaria y Fuerteventura, no una caída neta de los valores.

Siguiendo un razonamiento espacio por tiempo, estos resultados confirman una coevolución tipológico-cuantitativa de los paisajes costeros de islas oceánicas, donde las estructuras geomorfológicas evolucionarían a una mayor diversidad y abundancia, dirigidas por un patrón de anidamiento. Este patrón indicaría que las islas conservan rasgos estructurales de estadios anteriores, incorporando nuevos rasgos en un proceso evolutivo de tipo acumulativo.

Estos resultados nos llevan a reforzar las observaciones previamente hechas en Canarias (Ferrer-Valero et al., 2018) y reafirmar la hipótesis general de esta investigación.

Conclusiones generales

Este trabajo ha supuesto la apertura de una línea de investigación novedosa. Durante la misma, se ha pretendido explorar nuevos aspectos evolutivos de la geomorfología costera de islas oceánicas desde las métricas estructurales de paisaje, prestando una atención particular a la estimación de la diversidad y la complejidad.

Los primeros artículos de esta tesis (Ferrer-Valero et al., 2017; Ferrer-Valero, 2018) suponen los ensayos iniciales del desarrollo de una metodología adecuada para la consecución del objetivo principal expuesto en los dos siguientes: analizar la evolución costera a escala geológica, en islas oceánicas, desde la perspectiva de la composición y complejidad de su configuración geomorfológica.

En el primero de ellos (Ferrer-Valero, 2017), se utilizó Gran Canaria como isla "piloto". En ella se ensayó por primera vez la forma de computación en línea de costa (CDS). Se cartografiaron 9 tipos de geoformas costeras y se analizó su evolución, o estado de conservación, desde la década de 1960 hasta la actualidad, para obtener una imagen global de los impactos históricos en las costas de la isla. Gran Canaria es una isla con alta presión sobre sus entornos costeros, intensificada en las últimas décadas por el desarrollo urbano derivado del crecimiento demográfico, del desarrollo industrial y comercial, y sobre todo, de la actividad turística. El turismo, actividad vertebral de la economía de Gran Canaria, esta principalmente ligado a las cualidades naturales de la isla, y en especial, a las características geomorfológicas de sus costas (las dunas de Maspalomas son su principal reclamo). Y de aquí nace el conflicto, pues el turismo de "sol y playa" consume, degrada y pone en peligro precisamente el recurso que lo sostiene. Ante la necesidad de un inventario y valoración globales de la evolución histórica de los sistemas geomorfológicos de la costa de Gran Canaria, se elaboró este levantamiento geomorfológico, cuyo grado de detalle, propio de una escala local, abarca todo el perímetro costero de la isla. Se trata de un trabajo, por lo tanto, pionero como análisis integrado de la evolución histórica de costas sedimentarias y rocosas a escala regional. Los resultados indicaron que el 43% de las formas de relieve costeras se habían visto afectadas por impactos humanos en mayor o menor grado. De ellas, las geoformas sedimentarias, más escasas, dunas costeras, paleo-dunas, playas y humedales, resultaron ser las más gravemente afectadas. La pérdida de diversidad geomorfológica estimada fue de −15.2%, según el índice de entropía de Shannon (H ’), y de −32.1% según el índice *Proportional Losses index* (PLi), propuesto en este trabajo. El índice PLi es

particularmente sensible a la singularidad (escasez) de los elementos. Dados los resultados en Gran Canaria, se planteó el potencial de extender esta metodología a otras islas del mundo.

El segundo artículo (Ferrer-Valero, 2018) constituye el esfuerzo por consolidar una metodología para la comparación geomorfológica de islas. En él se desarrollaron y aplicaron procedimientos cartográficos, taxonómicos y numéricos para la estimación de la diversidad geomorfológica costera. Estos procedimientos muestran una perspectiva distinta a la que caracteriza los estudios de geodiversidad, configurados desde una perspectiva *particularista* y *holística*. *Particularista* porque, al querer construirla sobre nuevos conceptos y formas de estimación, ignorando los antecedentes conceptuales y metodológicos, se le da a la geodiversidad un estatus injustificado de "caso" particular e independiente, no sujeto a las mismas reglas, de diversidad natural. Y *holística*, debido a la ambición constante por integrar los diferentes elementos de la geodiversidad (suelos, geología, geomorfología, hidrología, etc.) en cada estudio, despreciando la posibilidad y el potencial de los enfoques específicos. Por lo tanto, la propuesta metodológica de este trabajo es, en contra de las tendencias imperantes, *exclusiva*, porque se centra y profundiza específicamente en la diversidad geomorfológica, y *generalista*, porque emplea el potencial conceptual y metodológico de la diversidad entendida como idea universal. Además, el estudio se desarrolló un ámbito particular, las costas de islas oceánicas, donde no existían estudios de geodiversidad relevantes. Con fines comparativos, el análisis abarcó los 459 km de costa volcánica de las islas de Gran Canaria y La Palma (Islas Canarias). El levantamiento geomorfológico se hizo conforme a una taxonomía ampliada de 14 grupos y 42 subgrupos. El método cartográfico-analítico CDS, basado en el almacenamiento de información binaria en el vector cartográfico, permitió el cálculo de las probabilidades de ocurrencia a lo largo de la costa, previa diferenciación de 17,500 secciones. Con ello, se estimaron tres componentes de la diversidad (riqueza, equi-abundancia y disimilitud), a través de índices de riqueza (R), entropía de Shannon (H') y entropía cuadrática de Rao (Q). Los datos revelaron que la diversidad geomorfológica costera es entre 11,1% y 48,2% más alta en Gran Canaria que en La Palma. Tras someterlos a una prueba de estrés fractal y rarefacción por ventana móvil, la variabilidad obtenida permitió determinar un error aceptable por deformación escalar y confirmar el contraste de diversidad una vez homogeneizada la muestra. Una vez comprobado que pueden verificarse contrastes en la diversidad geomorfología costera, se validó el procedimiento comparativo que serviría después para progresar en el objetivo de contrastar las hipótesis evolutivas.

El tercer (Ferrer-Valero et al., 2018) y cuarto artículo (no publicado) versan ya sobre la búsqueda de patrones evolutivos en las estructuras geomorfológicas, a escala geológica, y del contraste de la hipótesis inicial. A partir de los antecedentes metodológicos expuestos, y

aplicando un razonamiento espacio por tiempo, en el tercer artículo (Ferrer-Valero et al., 2018) se presenta la comparación de tres islas oceánicas de las islas Canarias en diferentes fases de desarrollo: La Palma (1.8 ma.), Gran Canaria (14.5 ma.) y Fuerteventura (22.6 ma.). En este trabajo se utilizó una taxonomía ampliada a tres niveles jerárquicos (3 clases, 8 subclases y 64 sub-subclases), aplicada sin unidad mínima cartografiable, a lo largo de 840 km de costa. Además se amplió el espectro de análisis a tres aspectos diferentes de la estructura geomorfológica de las islas: (i) composición, (ii) abundancia y (iii) diversidad, añadiendo la perspectiva combinatoria basada en el análisis de las asociaciones geomorfológicas. En el cuarto artículo (no publicado), se presenta la comparación de cuatro islas en el archipiélago de Cabo Verde, también en estados evolutivos diferenciados: Fogo (0.5 ma.), Santiago (3.5 ma.), São Vicente (7 ma.) y Boa Vista (17 ma.). En este caso se adoptó una versión ampliada de la taxonomía expuesta en Ferrer-Valero (2018), compuesta de 21 clases y 63 subclases dimensionales, habiéndose aplicado al análisis geomorfológico de 300 puntos de muestreo en cada isla. Una vez más, se examinaron, a través de varias métricas e índices, los patrones de composición, abundancia y diversidad.

Los resultados obtenidos en Canarias (Ferrer-Valero et al., 2018) y Cabo Verde (no publicado) muestran un patrón evolutivo de largo plazo en la geomorfología de las costas de islas oceánicas. Este patrón vendría marcado, según los datos empíricos obtenidos, por un aumento de la diversidad y de la abundancia geomorfológica (complejidad) con la edad geológica, ligadas a la transformación sistemática de la estructura geomorfológica a lo largo del tiempo. Esta transformación sistemática ha sido verificada estadísticamente por medio de pruebas de aleatoriedad secuencial e índices de similitud beta. Estos cambios sistemáticos son claves para entender que, de existir un aumento de la complejidad geomorfológica con el tiempo, este es consistente y consustancial a un patrón de cambio tipológico que no es aleatorio, sino evolutivo o secuencial. Este patrón de transformación vendría determinado por la transición ambiental desde sistemas más rocosos a más sedimentarios, y controlado en último término por la actividad erosiva y sedimentaria a lo largo de millones de años. En este proceso de transición ambiental, se produciría un aumento de la riqueza, conforme a un fenómeno de anidamiento en la composición geomorfológica del sistema, así como una tendencia a equilibrar las abundancias y mostrar una mayor variedad genética de formas, maximizando la entropía del sistema. Esta teoría se encuadra dentro de la hipótesis afirmativa planteada al inicio de la investigación, en la cual se exponía la posibilidad de un patrón evolutivo de la diversidad-complejidad costera, enmarcado en el ciclo de vida de una isla oceánica y, por lo tanto, inscrito en una trayectoria parabólica de crecimiento y caída. En Canarias, solo se obtuvieron aumentos, aunque decelerados, mientras que, en Cabo Verde, se observó una inflexión con decaimiento de los valores de diversidad geomorfológica, ajustables a una trayectoria parabólica.

Perspectivas

La línea de investigación iniciada en esta tesis no queda agotada en ella. De forma sumaria, se exponen a continuación algunos puntos relevantes de las futuras investigaciones:

- Ampliación de las observaciones a nuevas islas en el mundo. Se considera necesario, desde el punto de vista de la hipótesis de investigación, ampliar los estudios a un número significativo y relevante de casos a nivel mundial. En 2017 ya se realizaron las primeras visitas a las islas de Madeira y Porto Santo (archipiélago de Madeira), y se ha proyectado la posibilidad de realizar campañas en Hawái durante 2019-2020. Otros archipiélagos de punto caliente, como Mauricio-Reunión, Galápagos o Polinesia Francesa, podrían ser objetivo también de futuros trabajos.

- Ampliación de las variables y métricas de análisis. Hasta ahora se han investigado tres variables relevantes de la estructura geomorfológica de los paisajes costeros: composición, abundancia y diversidad; pero el método CDS tiene potencial para incorporar nuevas variables que también puedan ser puestas en el esquema evolutivo, como por ejemplo, fragmentación, dispersión y fractalidad. Asimismo, en un futuro se plantea el ensayo de modelos paramétricos de diversidad y la aplicación de medidas de diversidad gamma para comparaciones de tipo regional a partir de datos de diferentes archipiélagos del mundo.

- Búsqueda de modelos explicativos que puedan consolidar la teoría evolutiva, surgida de la observación. El reto en un futuro es poder explicar lo observado. Esto implica: (i) poner en relación estadística los datos obtenidos frente a diferentes variables explicativas; (ii) buscar las conexiones del modelo de evolución a largo plazo con modelos morfodinámicos a corto plazo que puedan sustentarlo (es decir, encontrar la interconexión de escalas); e (iii) integrar los ciclos iso-esutaticos y volcánicos a escala geológica en un esquema global de comprensión. La observación de nuevos casos ayudará a la construcción de este sistema explicativo.

- Investigar las relaciones de la diversidad geomorfológica con otros componentes de la geodiversidad (suelos, litología, etc), así como su influencia sobre los patrones de biodiversidad en el territorio.

- Investigar cómo la diversidad geomorfológica puede informar en el proceso de selección de lugares de interés geopatrimonial.

- A nivel técnico, se plantea la necesidad de automatización geomática del procedimiento CDS. La informatización permitiría (i) la optimización de los esfuerzos, (ii) la obtención de resultados exactos dotados de estimaciones de errores asociados al método de proyección, a la fractalidad y al tamaño muestral, y (iii) en definitiva, la homogeneización y reproducibilidad de los experimentos por la comunidad científica.

- Seguir mejorando los sistemas taxonómicos para avanzar hacia un sistema global de clasificación de geoformas que garantice un marco comparativo común a partir de una taxonomía estandarizada y multiescalar, donde se sistematicen los tipos geomorfológicos y sus relaciones jerárquicas y genéticas.

Referencias

Aber JD. 1979. Foliage-height profiles and succession in northern hardwood forests. Ecology, 60(1), 18-23.

Acosta J, Uchupi E, Smith D, Muñoz A, Herranz P, Palomo C, Llanes P, Ballesteros M, ZEE Working Group. 2003. Comparison of volcanic rifts on La Palma and El Hierro, Canary Islands and the Island of Hawaii. Marine Geophysical Researches 24: 59–90.

Acosta J, Uchupi E, Smith D, Muñoz A, Herranz P, Palomo C, ZEE Working Group. 2005. Comparison of volcanic rifts on La Palma and El Hierro, Canary Islands and the island of Hawaii. In Geophysics of the Canary Islands. Springer: Dordrecht; 59–90.

Alexander CS. 1966. A method of descriptive shore classification and mapping as applied to the northeast coast of Tanganyika. Ann. Assoc. Am. Geogr. 56, 128–140.

Almeida-Neto M, Guimaraes P, Guimaraes Jr PR, Loyola RD, Ulrich W. 2008. A consistent metric for nestedness analysis in ecological systems: reconciling concept and measurement. Oikos, 117(8), 1227-1239.

Alonso I, Alcántara-Carrió J, Cabrera L, 2002. Tourist resorts and their impact on beach erosion at Sotavento beaches, Fuerteventura, Spain. J. Coast. Res. 36, 1–7.

Alonso I, Hernández L, Alcántara-Carrió J, Cabrera L, Yanes A. 2011. Los grandes campos de dunas actuales de Canarias. In: Sanjaume Saumell E, Gracía Prieto, FJ. (Eds.), Las dunas en España. Sociedad Española de Geomorfología, pp. 467–496.

Alonso I, Sánchez I, Cabrera L, Benavides A, Alcántara-Carrió J, Usera J. 2006. Decadal evolution of a coastal dune field and adjacent beaches at north of Fuerteventura (Canary Islands, Spain) J. Coast. Res. 39, 198–203.

Alveirinho Dias JM, Neal WJ. 1992. Sea cliff retreat in southern Portugal: profiles, processes, and problems. J. Coast. Res. 8 (3), 641–654.

Amante C, Eakins BW. 2009. ETOPO1 Global Relief Model converted to PanMap layer format. NOAA-National Geophysical Data Center, doi, 10.

Amin SMN, Davidson-Arnott RGD. 1997. A statistical analysis of the controls on shoreline erosion rates, Lake Ontario. J. Coast. Res. 13 (4), 1093–1101.

Ancochea E, Brändle JL, Cubas CR, Hernán F, Huertas MJ. 1996. Volcanic complexes in the eastern ridge of the Canary Islands: the Miocene activity of the island of Fuerteventura. Journal of Volcanology and Geothermal Research 70(3–4): 183–204.

Ancochea E, Huertas MJ, Hernán F, Brändle JL. 2010. Volcanic evolution of São Vicente, Cape Verde Islands: The Praia Grande landslide. Journal of Volcanology and Geothermal Research, 198(1), 143-157.

Andrle R. 1994. The angle measure technique: a new method for characterizing the complexity of geomorphic lines. Mathematical Geology, 26(1), 83-97.

Anguita F, Hernán F. 2000. The Canary Islands origin: a unifying model. J. Volcanol. Geotherm. Res. 103 (1–4), 1–26.

Anthony EJ, Marriner N, Morhange C. 2014. Human influence and the changing geomorphology of Mediterranean deltas and coasts over the last 6000 years: From progradation to destruction phase? Earth-Science Reviews, 139, 336-361.

Araña V, Carracedo J. 1980. Los volcanes de las islas canarias III. Gran Canaria. Ed. Rueda.

Argyriou AV, Sarris A, Teeuw RM. 2016. Using geoinformatics and geomorphometrics to quantify the geodiversity of Crete, Greece. International journal of applied earth observation and geoinformation, 51, 47-59.

Argyriou AV, Sarris A, Teeuw RM. 2016. Using geoinformatics and geomorphometrics to quantify the geodiversity of Crete, Greece. Int. J. Appl. Earth Obs. Geoinf. 51, 47–59.

Aubié S, Tastet JP. 2000. Coastal erosion, processes and rates: an historical study of the Gironde coastline, Southwestern France. J. Coast. Res. 16 (3), 756–767.
Baas AC. 2002. Chaos, fractals and self-organization in coastal geomorphology: simulating dune landscapes in vegetated environments. Geomorphology, 48(1-3), 309-328.
Bajocco S, De Angelis A, Perini L, Ferrara A, Salvati L. 2012. The impact of landuse/ land cover changes on land degradation dynamics: a Mediterranean case study. Environ. Manag. 49 (5), 980–989.
Bartley JD, Buddemeier RW, Bennett DA. 2001. Coastline complexity: a parameter for functional classification of coastal environments. Journal of Sea Research 46(2): 87–97.
Benito-Calvo A, Pérez-González A, Magri O, Meza P. 2009. Assessing regional geodiversity: the Iberian peninsula. Earth Surf. Process. Landf. 34 (10), 1433.
Benumof BT, Storlazzi CD, Seymour RJ, Griggs GB. 2000. The relationship between incident wave energy and seacliff erosion rates: San Diego County, California. Journal of Coastal Research, 1162-1178.
Biolchi S, Furlani S, Devoto S, Gauci R, Castaldini D, Soldati M. 2016. Geomorphological identification, classification and spatial distribution of coastal landforms of Malta (Mediterranean Sea). Journal of Maps, 12(1), 87-99.
Bird EC. 2008. Coastal Geomorphology: An Introduction. John Wiley & Sons.
Bodansky E, Gribov A, Pilouk, M. 2002. Smoothing and compression of lines obtained by raster-to-vector conversion. International Workshop on Graphics Recognition. Springer, Berlin, Heidelberg, pp. 256–265.
Brazier V, Bruneau PM, Gordon JE, Rennie AF. 2012. Making space for nature in a changing climate: the role of geodiversity in biodiversity conservation. Scottish Geographical Journal, 128(3-4), 211-233.
Brilha J. 2015. Inventory and quantitative assessment of geosites and geodiversity sites: a review. Geoheritage 8 (2), 119–134.
Brocx M, Semeniuk V, 2010. Coastal geoheritage: a hierarchical approach to classifying coastal types as a basis for identifying geodiversity and sites of significance in Western Australia. J. R. Soc. West. Aust. 93 (2), 81–113.
Brooke B. 2001. The distribution of carbonate eolianite. Earth Sci. Rev. 55 (1–2), 135–164.
Bruschi VM, Cendrero A. 2005. Geosite evaluation: can we measure intangible values. Il Quaternario 18 (1), 293–306.
Burnett MR, August PV, Brown JH, Killingbeck KT. 1998. The influence of geomorphological heterogeneity on biodiversity I. A patch-scale perspective. Conservation Biology, 12(2), 363-370.
Buscombe D, Masselink G. 2006. Concepts in gravel beach dynamics. Earth-Science Reviews 79(1–2): 33–52.
Cabrera-Vega LL, Cruz-Avero N, Hernández-Calvento L, Hernández-Cordero AI, Fernández-Cabrera E. 2013. Morphological changes in dunes as an indicator of anthropogenic interferences in arid dune fields. J. Coast. Res. 65, 1271–1276.
Carpenter NE, Dickson ME, Walkden MJA, Nicholls RJ, Powrie W. 2014. Effects of varied lithology on soft-cliff recession rates. Marine Geology, 354, 40-52.
Carracedo JC. 1999. Growth, structure, instability and collapse of Canarian volcanoes and comparisons with Hawaiian volcanoes. J. Volcanol. Geotherm. Res. 94, 1), 1–19.
Carracedo JC, Day S, Guillou H, Rodríguez Badiola E, Canas JA, Pérez Torrado FJ. 1998. Hotspot volcanism close to a passive continental margin: the Canary Islands. Geol. Mag. 135 (05), 591–604.
Carracedo JC, Day SJ, Guillou H, Torrado FJP. 1999. Giant quaternary landslides in the evolution of La Palma and El Hierro, Canary Islands. J. Volcanol. Geotherm. Res. 94 (1), 169–190.
Carracedo JC, Rodríguez Badiola E, Guillou H, Nuez Pestana JDL, Perez-Torrado FJ. 2001.

Geology and Volcanology of La Palma and El Hierro, Western Canaries.
Carter RWG. 1988. Coastal environments: an introduction to the physical, ecological and cultual systems of coastlines, 617.
Castedo R, Murphy W, Lawrence J, Paredes C. 2012. A new process–response coastal recession model of soft rock cliffs. Geomorphology, 177, 128-143.
Çetiner ZS, Ertekin C, Yiğitbaş E. 2018. Evaluating scientific value of geodiversity for natural protected sites: the Biga Peninsula, Northwestern Turkey. Geoheritage 10 (1), 49–65.
Clarke KR, Warwick RM. 2001. A further biodiversity index applicable to species lists: variation in taxonomic distinctness. Mar. Ecol. Prog. Ser. 216, 265–278.
Cody ML. 1975. Towards a theory of continental species diversities. Ecology and evolution of communities, 214-257.
Cotton CA. 1954. Deductive morphology and genetic classification of coasts. The Scientific Monthly 78(3): 163–181.
Criado C, Torres JM, Hansen A, Lillo P, Naranjo A. 2012. Intercalaciones de polvo sahariano en paleodunas bioclásticas de Fuerteventura (Islas Canarias). Cuaternario y Geomorfología 26 (1–2), 73–88.
Cui BL, Li XY. 2011. Coastline change of the Yellow River estuary and its response to the sediment and runoff (1976–2005). Geomorphology 127 (1), 32–40.
D'Alessandro L, De Pippo T, Donadio C, Mazzarella A, Miccadei E. 2006. Fractal dimension in Italy: a geomorphological key to interpretation. Zeit. Geom. NF, 50(4), 479-499.
Dai ZJ, Li CC, Zhang QL. 2004. Fractal analysis of shoreline patterns for crenulate-bay beaches, Southern China. Estuarine, Coastal and Shelf Science, 61(1), 65-71.
Dana JD. 1890. Characteristics of Volcanoes: With Contributions of Facts and Principles from the Hawaiian Islands, Including a Historical Review of Hawaiian Volcanic Action for the Past Sixty-seven Years, a Discussion of the Relations of Volcanic Islands to Deep-sea Topography, and a Chapter on Volcanic-island Denudation. Dodd, Mead.
Darwin CR. 1842. The structure and distribution of coral reefs. Being the first part of the geology of the voyage of the Beagle, under the command of Capt. Fitzroy, R.N. during the years 1832 to 1836. London: Smith Elder and Co.
Davidson-Arnott R. 2010. Introduction to Coastal Processes and Geomorphology. Cambridge University Press.
Davies JL. 1980. Geographical Variation in Coastal Development, Clayton KM (ed). Longman: London.
Davis WM. 1899. The geographical cycle. The Geographical Journal, 14(5), 481-504.
Dawson JL, Smithers SG. 2010. Shoreline and beach volume change between 1967 and 2007 at Raine Island, Great Barrier Reef, Australia. Glob. Planet. Chang. 72 (3), 141–154.
De Muro S, Di Grande A, Brambati A, Ibba A. 2015. Geomorphology map of the marine and transitional terraces and raised shorelines of the Península Juan Mazía, Tierra del Fuego. Straits of Magellan–Chile. Journal of Maps, 11(5), 698-710.
Dearing JA, Richmond N, Plater AJ, Wolf J, Prandle D, Coulthard TJ. 2006. Modelling approaches for coastal simulation based on cellular automata: the need and potential. Philosophical Transactions of the Royal Society of London A: Mathematical, Physical and Engineering Sciences, 364(1841), 1051-1071.
Del Arco MJ, Wildpret W, Pérez PL, Rodríguez O, Acebes JR, García A, Martín VE, Reyes JA, Salas M, Díaz MA, Bermejo JA, González R, Cabrera MV, García S. 2006. Mapa de vegetación de Canarias. GRAFCAN: Santa Cruz de Tenerife.
Delcourt HR, Delcourt PA. 1988. Quaternary landscape ecology: relevant scales in space and time. Landsc. Ecol. 2 (1), 23—44.
Dixon G. 1995. Aspects of Geoconservation in Tasmania: A Preliminary Review of Significant Earth Features. Report to the Australian Heritage Commission, Occasional Paper 32. Parks & Wildlife Service, Tasmania.

Dolan R, Trossbach S, Buckley M. 1990. New shoreline erosion data for the Mid-Atlantic Coast. J. Coast. Res. 471–477.
Dornbusch U, Robinson DA, Moses CA, Williams RBG. 2008. Temporal and spatial variations of chalk cliff retreat in East Sussex, 1873 to 2001. Mar. Geol. 249, 271–282.
Dyhr CT, Holm PM. 2010. A volcanological and geochemical investigation of Boa Vista, Cape Verde Islands; 40 Ar/39 Ar geochronology and field constraints. Journal of Volcanology and Geothermal Research, 189(1), 19-32.
Efron B, Tibshirani RJ. 1993. An introduction to the bootstrap. CRC press.
El Banna M, Frihy. 2009. Human-induced changes in the geomorphology of the north-eastern coast of the Nile delta, Egypt. Geomorphology 107, 72–78.
Emery KO, Kuhn GG. 1982. Sea cliffs: their processes, profiles, and classification. Geol. Soc. Am. Bull. 93 (7), 644–654.
Erdős L, Bátori Z, Tölgyesi C, Körmöczi L. 2014. The Moving Split Window (MSW) analysis in vegetation science–an overview. Appl. Ecol. Environ. Res. 12, 787–805.
Fagherazzi S, Palermo C, Rulli MC, Carniello L, Defina A. 2007. Wind waves in shallow microtidal basins and the dynamic equilibrium of tidal flats. Journal of Geophysical Research: Earth Surface, 112(F2).
Fairbridge RW. 2004. Classification of coasts. J. Coast. Res. 155–165.
Faith DP. 2002. Quantifying biodiversity: a phylogenetic perspective. Conserv. Biol. 16 (1), 248–252.
Farhan AR, Lim S. 2011. Resilience assessment on coastline changes and urban settlements: a case study in Seribu Islands, Indonesia. Ocean Coast. Manag. 54 (5), 391–400.
Ferrer-Valero N. 2018. Measuring geomorphological diversity on coastal environments: a new approach to geodiversity. Geomorphology 318: 217–229.
Ferrer-Valero N, Hernández-Calvento L, Hernández-Cordero AI. 2017. Human impacts quantification on the coastal landforms of Gran Canaria Island (Canary Islands). Geomorphology 286, 58–67.
Ferrer-Valero N, Hernández-Calvento L, Hernández-Cordero AI. 2018. Insights of long-term geomorphological evolution of coastal landscapes in hot-spot oceanic islands. Earth Surface Processes and Landforms. DOI: 10.1002/esp.4518.
Feuillet T, Sourp E. 2011. Geomorphological heritage of the Pyrenees National Park (France): assessment, clustering, and promotion of geomorphosites. Geoheritage 3 (3), 151–162.
Finkl CW. 2004. Coastal classification: systematic approaches to consider in the development of a comprehensive scheme. J. Coast. Res. 166–213.
Fletcher C, Rooney J, Barbee M, Lim SC, Richmond B. 2003. Mapping shoreline change using digital orthophotogrammetry on Maui, Hawaii. J. Coast. Res. 106–124.
Flor-Blanco G, Flor G, Pando L. 2013. Evolution of the Salinas-El Espartal and Xagó beach/dune systems in north-western Spain over recent decades: evidence for responses to natural processes and anthropogenic interventions. GeoMar. Lett. 33, 143–157.
Gallagher EL, Elgar S, Guza RT. 1998. Observations of sand bar evolution on a natural beach. Journal of Geophysical Research, Oceans 103: 3203–3215.
García-Romero L, Hernández-Cordero AI, Fernández-Cabrera E, Peña-Alonso C, Hernández-Calvento L, Pérez-Chacón E. 2016. Urban-touristic impacts on the aeolian sedimentary systems of the Canary Islands: conflict between development and conservation. Island Studies Journal 11 (1), 91–112.
Gordon JE, Barron HF, Hansom JD, Thomas MF. 2012. Engaging with geodiversity— why it matters. Proc. Geol. Assoc. 123 (1), 1–6.
Gray M. 2004. Geodiversity: valuing and conserving abiotic nature. John Wiley & Sons.
Gray M. 2005. Geodiversity and geoconservation: what, why, and how. The George Wright

Forum 22(3): 4–12.
Gray M. 2008. Geodiversity: developing the paradigm. Proceedings of the Geologists' Association 119(3–4): 287–298.
Grunewald R. 2006. Assessment of damages from recreational activities on coastal dunes of the southern Baltic Sea. J. Coast. Res. 22, 1145–1157.
Guo Y, Gong P, Amundson R. 2003. Pedodiversity in the United States of America. Geoderma 117 (1–2), 99–115.
Hall AM, Hansom JD, Williams DM, Jarvis J. 2006. Distribution, geomorphology and lithofacies of cliff-top storm deposits: examples from the high-energy coasts of Scotland and Ireland. Mar. Geol. 232 (3–4), 131–155.
Hapke CJ, Kratzmann MG, Himmelstoss EA. 2013. Geomorphic and human influence on large-scale coastal change. Geomorphology 199, 160–170.
Hay JE. 2013. Small island developing states: coastal systems, global change and sustainability. Sustain. Sci. 8 (3), 309–326.
Hernández-Calvento L, Jackson DWT, Medina R, Hernández-Cordero AI, Cruz N, Requejo S. 2014. Downwind effects on an arid dunefield from an evolving urbanised area. Aeolian Res. 15, 301–309.
Hernández-Calvento L, Jackson DW, Cooper A, Pérez-Chacón E. 2017. Island-Encapsulating Eolian Sedimentary Systems of the Canary and Cape Verde Archipelagos. Journal of Sedimentary Research, 87(2), 117-125.
Hernández-Cordero AI, Pérez-Chacón Espino E, Hernández-Calvento L. 2012. La investigación como soporte de la gestión: el ejemplo de la duna costera (foredune) de Maspalomas (Gran Canaria, Islas Canarias). La gestión integrada de playas y dunas: experiencias en Latinoamérica y Europa. Monografies de la Societat d'Història Natural de les Balears. 19, pp. 289–306.
Hernández-Cordero AI, Hernández-Calvento L, Espino EPC. 2017. Vegetation changes as an indicator of impact from tourist development in an arid transgressive coastal dune field. Land Use Policy 64: 479–491.
Hernández-Cordero AI, Hernández-Calvento L, Hesp PA, Pérez-Chacón, E. 2018. Geomorphological changes in an arid transgressive coastal dune field due to natural processes and human impacts. Earth Surface Processes and Landforms.
Hernández-Cordero AI, Peña-Alonso C, Hernández-Calvento L, Ferrer-Valero N, Santana-Cordero AM, García-Romero L, Espino EPC. 2019. Aeolian Sedimentary Systems of the Canary Islands. In The Spanish Coastal Systems (pp. 699-725). Springer, Cham.
Hesp P. 2002. Foredunes and blowouts: initiation, geomorphology and dynamics. Geomorphology 48(1–3): 245–268.
Hesp PA, Walker IJ. 2013. Coastal dunes. Treatise on Geomorphology. Elsevier Inc.
Hjort J, Luoto M. 2010. Geodiversity of high-latitude landscapes in northern Finland. Geomorphology 115 (1), 109–116.
Hjort J, Luoto M. 2012. Can geodiversity be predicted from space? Geomorphology 153, 74–80.
Hjort J, Heikkinen RK, Luoto M. 2012. Inclusion of explicit measures of geodiversity improve biodiversity models in a boreal landscape. Bio-diversity and Conservation 21: 3487–3506.
Hjort J, Gordon JE, Gray M, Hunter ML. 2015. Why geodiversity matters in valuing nature's stage. Conserv. Biol. 29 (3), 630–639.
Hoernle K, Carracedo JC. 2009. Canary Islands Geology. University of California Press: Berkeley, CA.
Holm PM, Grandvuinet T, Friis J, Wilson JR, Barker AK, Plesner S. 2008. An 40Ar-39Ar study of the Cape Verde hot spot: Temporal evolution in a semistationary plate environment. Journal of Geophysical Research: Solid Earth, 113(B8).
Houser, C., Hapke, C., Hamilton, S., 2008. Controls on coastal dune morphology, shoreline

erosion and barrier island response to extreme storms. Geomorphology 100 (3), 223–240.
Ibáñez JJ, Pérez-González A, Jiménez-Ballesta R, Saldaña A, Gallardo- Díaz J. 1994. Evolution of fluvial dissection landscapes in Mediterranean environments. Quantitative estimates and geomorphological, pedological and phytocenotic repercussions (with 3 figures and 2 tables). Zeitschrift für Geomorphologie 38(1): 105–120.
Ibáñez JJ, De-Alba S, Bermúdez FF, García-Álvarez A. 1995. Pedodiversity: concepts and measures. Catena 24 (3), 215–232.
Ibáñez JJ, De-Alba S, Lobo A, Zucarello V. 1998. Pedodiversity and global soil patterns at coarse scales (with discussion). Geoderma 83(3–4): 171–192.
Ibáñez JJ, Caniego J, San Jose F, Carrera C. 2005. Pedodiversity-area relationships for islands. Ecol. Model. 182 (3), 257–269.
Ibáñez JJ, Effland, WR. 2011. Toward a theory of island pedogeography: testing the driving forces for pedological assemblages in archipelagos of different origins. Geomorphology 135 (3), 215–223.
Ilić M, Stojković S, Rundić L, Ćalić J, Sandić D. 2016. Application of the geodiversity index for the assessment of geodiversity in urban areas: an example of the Belgrade city area, Serbia. Geologia Croatica 69 (3), 325–336.
Inman DL, Nordstrom CE. 1971. On the tectonic and morphologic classification of coasts. The Journal of Geology 79(1): 1–21.
Instituto Español de Oceanografía (IEO). 2006. Mapa topobatimétrico del Archipiélago Canario 1:700. IEO: Madrid; 000.
Isola I, Bini M, Ribolini A, Pappalardo M, Consoloni I, Fucks E, Boretto G, Ragaini L, Zanchetta G. 2011. Geomorphologic map of northeastern sector of San Jorge gulf (Chubut, Argentina). Journal of Maps, 7(1), 476-485.
ISTAC. 2009. Anuario Estadístico de Canarias 2008. Instituto Canario de Estadística, Gobierno de Canarias.
Izsák J, Papp L. 2000. A link between ecological diversity indices and measures of biodiversity. Ecological Modelling 130(1): 151–156.
Jackson NL, Nordstrom KF. 2011. Aeolian sediment transport and landforms in managed coastal systems: a review. Aeolian Res. 3, 181–196.
Jenks GF. 1967. The data model concept in statistical mapping. International Yearbook of Cartography vol. 7, pp. 186–190.
Jennings R, Shulmeister J. 2002. A field based classification scheme for gravel beaches. Mar. Geol. 186 (3–4), 211–228.
Jiang J, Plotnick RE. 1998. Fractal analysis of the complexity of United States coastlines. Mathematical Geology, 30(5), 535-546.
Jie C, Xue-lei Z, Zi-tong G, Jun W. 2001. Pedodiversity: a controversial concept. J. Geogr. Sci. 11 (1), 110–116.
Johnson DW. 1919. Shore Processes and Shoreline Development. John Wiley & Sons: Chichester.
Jones JR, Cameron B, Fisher JJ. 1993. Analysis of cliff retreat and shoreline erosion: Thompson Island, Massachusetts, USA. J. Coast. Res. 87–96.
Karátson D, Yepes J, Favalli M, Rodríguez-Peces MJ, Fornaciai A. 2016. Reconstructing eroded paleovolcanoes on Gran Canaria, Canary Islands, using advanced geomorphometry. Geomorphology 253: 123–134.
Kennedy DM. 2014. The rock coast of Australia. Geol. Soc. Lond. Mem. 40 (1), 235–245.
Kiernan K. 1994. The Geoconservation Significance of Lake Pedder and its Contribution to Geodiversity. Unpublished Report to the Lake Pedder Study Group.
King CA. 1972. Beaches and coasts. Arnold.
Kjerfve B. 1994. Coastal lagoons. Elsevier Oceanography Series vol. 60. Elsevier, pp. 1–8.
Kot R. 2017. A comparison of results from geomorphological diversity evaluation methods

in the Polish Lowland (Toruń Basin and Chełmno Lakeland). Geografisk Tidsskrift-Danish Journal of Geography 1–19.
Kurt S, Karaburun A, Demirci A. 2010. Coastline changes in Istanbul between 1987 and 2007. Sci. Res. Essays 5 (19), 3009–3017.
Lacey EM, Peck JA. 1998. Long-term beach profile varations along the south shore of Rhode Island, USA. J. Coast. Res. 1255–1264.
Langenheim VA, Clague DA. 1987. The Hawaiian-Emperor volcanic chain. Part 2, 55–84.
Lee EM. 2008. Coastal cliff behaviour: observations on the relationship between beach levels and recession rates. Geomorphology 101: 558–571.
Lim M, Petley DN, Rosser NJ, Allison RJ, Long AJ, Pybus D. 2005. Combined digital photogrammetry and time-of-flight laser scanning for monitoring cliff evolution. The Photogrammetric Record 20(110):109–129.
Lim M, Rosser NJ, Allison RJ, Petley DN. 2010. Erosional processes in the hard rock coastal cliffs at Staithes, North Yorkshire. Geomorphology 114(1–2): 12–21.
Limber PW, Patsch KB, Griggs GB. 2008. Coastal sediment budgets and the littoral cutoff diameter: a grain size threshold for quantifying active sediment inputs. Journal of Coastal Research, 24(sp2), 122-133.
Lira C, Silva A, Taborda R, Andrade C. 2016. Coastline evolution of Portuguese low- lying sandy coast in the last 50 years: an integrated approach. Earth System Science Data http://dx.doi.org/10.5194/essd-2016-5.
Machado F, de Assunção CFT. 1965. Carta geológica de Cabo Verde (na escala de 1/100,000): notícia explicativa da folha da ilha do Fogo-estudos petrográficos. Madrid 175 pp.
Magurran AE. 1988. Ecological Diversity and its Measurement. Croom Helm: London.
Magurran AE. 2004. Measuring biological diversity. John Wiley & Sons.
Malinowska E, Szumacher I. 2013. Application of landscape metrics in the evaluation of geodiversity. Miscellanea Geographica-Regional Studies on Development 17 (4), 28–33.
Mandelbrot BB. 1967. How long is the coast of Britain? Statistical self-similarity and fractional dimension. Science 156 (3775), 636–638.
Mandelbrot BB. 1982. The fractal geometry of nature (Vol. 1). New York: WH freeman.
Margalef R. 1958. Information theory in ecology. Gen. Syst. 3, 36–71.
Martínez ML, Intralawan A, Vázquez G, Pérez-Maqueo O, Sutton P, Landgrave R. 2007. The coasts of our world: ecological, economic and social importance. Ecol. Econ. 63, 254–272.
Marzol Jaén MV. 1987. El régimen anual de las lluvias en el archipiélago Canario. Ería: Revista cuatrimestral de geografía 14: 187–194.
Masson DG, Watts AB, Gee MJR, Urgeles R, Mitchell NC, Le Bas TP, Canals M. 2002. Slope failures on the flanks of the western Canary Islands. Earth-Science Reviews 57(1): 1–35.
Mattox TN, Mangan MT. 1997. Littoral hydrovolcanic explosions: a case study of lava–seawater interaction at Kilauea Volcano. J. Volcanol. Geotherm. Res. 75 (1–2), 1–17.
McBratney A, Minasny B. 2007. On measuring pedodiversity. Geoderma 141(1): 149–154.
McDonald DG, Dimmick J. 2003. The conceptualization and measurement of diversity. Communication Research, 30(1), 60-79.
McDougall I. 1964. Potassium-argon ages from lavas of the Hawaiian Islands. Geological Society of America Bulletin, 75(2), 107-128.
McDougall I. 1971. Volcanic island chains and seafloor spreading. Nature 231: 141–144.
McGill JT. 1958. Map of coastal landforms of the world. Geogr. Rev. 48 (3), 402–405.
Meco J, Scaillet S, Guillou H, Lomoschitz A, Carracedo JC, Ballester J, Cilleros A. 2007. Evidence for long-term uplift on the Canary Islands from emergent Mio–Pliocene littoral deposits. Global and Planetary Change 57(3): 222–234.

Melelli L, Vergari F, Liucci L, Del Monte M. 2017. Geomorphodiversity index: quantifying the diversity of landforms and physical landscape. Sci. Total Environ. 584, 701–714.
Menard HW. 1986. Islands. Scientific American Library: New York.
Miccadei E, Mascioli F, Piacentini T, Ricci F. 2011. Geomorphological features of coastal dunes along the Central Adriatic Coast (Abruzzo, Italy). J. Coast. Res. 27 (6), 1122–1136.
Mimura N, Nurse L, McLean RF, Agard J, Briguglio L, Lefale Payet P, Sem G. 2007. Small islands. Climate Change 687–716.
Minasny B, McBratney AB. 2007. Incorporating taxonomic distance into spatial prediction and digital mapping of soil classes. Geoderma 142 (3–4), 285–293.
Minasny B, McBratney AB, Hartemink AE. 2010. Global pedodiversity, taxonomic distance, and the World Reference Base. Geoderma 155 (3–4), 132–139.
Mitchell AH, Reading HG. 1969. Continental margins, geosynclines, and ocean floor spreading. The Journal of Geology 77(6): 629–646.
Moore JG. 1987. Subsidence of the Hawaiian Ridge. In Volcanism in Hawaii, Decker W, Wright TL, Stauffer PH (eds) , Vol. 1. US Geological Survey: Reston, VA; 85–107.US Geological Survey Professional Paper 1350
Moore JG, Normark WR, Holcomb RT. 1994. Giant hawaiian landslides. Annual Review of Earth and Planetary Sciences, 22(1), 119-144.
Morales Matos G, Santana Santana A. 1993. Proceso de construcción y transformación del espacio litoral grancanario inducidos por el fenómeno turístico. Ería: Revista cuatrimestral de geografía 32, 225–246.
Nagendra H. 2002. Opposite trends in response for the Shannon and Simpson indices of landscape diversity. Applied Geography 22(2): 175–186.
Narayana AC, Priju CP. 2006. Landform and shoreline changes inferred from satellite images along the Central Kerala coast. Journal of Gological Society of India 68 (1), 35–49.
Naylor LA, Stephenson WJ, Trenhaile AS. 2010. Rock coast geomorphology: recent advances and future research directions. Geomorphology 114 (1), 3–11.
Norcross ZM, Fletcher CH, Merrifield M. 2002. Annual and interannual changes on a reef-fringed pocket beach: Kailua Bay, Hawaii. Mar. Geol. 190 (3), 553–580.
Nordstrom KF. 1994. Beaches and dunes of human-altered coasts. Prog. Phys. Geogr. 18 (4), 497–516.
Nordstrom KF. 2000. Beaches and Dunes of Developed Coasts. Cambridge University Press, Cambridge.
Nunes M, Ferreira Ó, Schaefer M, Clifton J, Baily B, Moura D, Loureiro C. 2009. Hazard assessment in rock cliffs at Central Algarve (Portugal): a tool for coastal management. Ocean Coast. Manag. 52 (10), 506–515.
Ojeda Zújar J, Borgniet L, Pérez Romero AM, Loder JF. 2002. Monitoring morphological changes along the coast of Huelva (SW Spain) using soft-copy photogrammetry and GIS. J. Coast. Conserv. 8, 69–76.
Owens EH. 1994. Canadian coastal environments, shoreline processes, and oil spill cleanup. Environment Canada.
Owens IP, Bennett PM. 2000. Quantifying biodiversity: a phenotypic perspective. Conserv. Biol. 14 (4), 1014–1022.
Özşahin E. 2017. Geodiversity assessment in the Ganos (Isıklar) Mount (NW Turkey). Environ. Earth Sci. 76 (7), 271.
Panizza M, Piacente S. 2009. Cultural geomorphology and geodiversity. Geomorphosites. Pfeil Verlag, Munich, pp. 35–48.
Parks KE, Mulligan M. 2010. On the relationship between a resource based measure of geodiversity and broad scale biodiversity patterns. Biodiversity and Conservation, 19(9), 2751-2766.

Pellitero R, González-Amuchastegui MJ, Ruiz-Flaño P, Serrano E. 2011. Geodiversity and geomorphosite assessment applied to a natural protected area: the Ebro and Rudron Gorges Natural Park (Spain). Geoheritage 3 (3), 163–174.

Pereira DI, Pereira P, Brilha J, Santos L. 2013. Geodiversity assessment of Paraná State (Brazil): an innovative approach. Environ. Manag. 52 (3), 541–552.

Pérez-Chacón, E., Hernández Calvento, L., Yanes Luque, A., 2007. Transformaciones humanas y sus consecuencias sobre los litorales de las islas Canarias. In: Étienne, S., Paris, R. (Eds.), Les littoraux volcaniques – Une approche environnementale. Presses universitaires Blaise Pascal, Clermont-Ferrand (Francia), pp. 173–191.

Pérez-Torrado FJ, Mangas J. 1994. Origen y evolución geológica de la barra de Las Canteras (Las Palmas de Gran Canaria). Vector Plus 1, 4–14.

Pethick JS. 1984. An Introduction to Coastal Geomorphology. Dept. of Geography, Univ. of Hull.

Phillips JD. 2006. Evolutionary geomorphology: thresholds and nonlinearity in landform response to environmental change. Hydrology and Earth System Sciences Discussions, European Geosciences Union, 3 (2), pp.365-394.

Pickett ST. 1989. Space-for-time substitution as an alternative to long-term studies. In Long-term Studies in Ecology. Springer: New York; 110–135.

Pielou EC. 1975. Ecology diversity. New York: John.

Pierre G. 2006. Processes and rate of retreat of the clay and sandstone sea cliffs of the northern Boulonnais (France). Geomorphology 73 (1), 64–77.

Piña-García F, Pereda-García R, de Luis-Ruiz JM, Pérez-Álvarez R, Husillos-Rodríguez R. 2016. Determination of geometry and measurement of maritime–terrestrial lines by means of fractals: application to the Coast of Cantabria (Spain). J. Coast. Res. 32 (5), 1174–1183.

Porter-Smith R, McKinlay J. 2012. Mesoscale coastal complexity and its relationship to structure and forcing from marine processes. Marine Geology 323: 1–13.

Pye K, Blott SJ, Howe MA. 2014. Coastal dune stabilization in Wales and requirements for rejuvenation. J. Coast. Conserv. 18, 27–54.

Quartau R, Trenhaile AS, Mitchell NC, Tempera F. 2010. Development of volcanic insular shelves: insights from observations and modelling of Faial Island in the Azores archipelago. Marine Geology 275(1): 66–83.

Quartau R, Madeira J, Mitchell NC, Tempera F, Silva PF, Brandão F. 2016. Reply to comment by Marques et al. on "The insular shelves of the Faial Pico Ridge (Azores archipelago): a morphological record of its evolution". Geochemistry, Geophysics, Geosystems 17(2): 633–641.

Ramalho RA. 2011. Building the Cape Verde Islands. Springer Science & Business Media.

Ramalho RS, Quartau R, Trenhaile AS, Mitchell NC, Woodroffe CD, Ávila SP. 2013. Coastal evolution on volcanic oceanic islands: a complex interplay between volcanism, erosion, sedimentation, sea-level change and biogenic production. Earth-Science Reviews 127: 140–170.

Ramírez R, Tuya F, Tabraue RH. 2008. El intermareal Canario: poblaciones de lapas, burgados y canadillas. Cabildo de Fuerteventura, Medio Ambiente.

Rao CR. 1982. Diversity and dissimilarity coefficients: a unified approach. Theor. Popul. Biol. 21 (1), 24–43.

Ricotta C, Avena GC. 2005. A 'fast-food approach' to the standardization of quadratic diversity. Plant Biosyst. 139, 411–413.

Rodrigues SC, Silva TI. 2012. Dam construction and loss of geodiversity in the Araguari river basin, Brazil. Land Degradation & Development, 23(4), 419-426.

Routledge RD. 1977. On Whittaker's components of diversity. Ecology, 58(5), 1120-1127.

Rovere A, Casella E, Vacchi M, Parravicini V, Firpo M, Ferrari M, Bianchi CN. 2015. Coastal and marine geomorphology between Albenga and Savona (NW Mediterranean Sea,

Italy). Journal of Maps, 11(2), 278-286.
Ruban DA. 2010. Quantification of geodiversity and its loss. Proc. Geol. Assoc. 121 (3), 326–333.
Rumohr H, Karakassis I, Jensen JN. 2001. Estimating species richness, abundance and diversity with 70 macrobenthic replicates in the Western Baltic Sea. Marine Ecology Progress Series 214: 103–110.
Sallenger Jr AH, Krabill WB, Swift RN, Brock J, List J, Hansen M, Holman RA, Manizade S, Sontag J, Meredith A, Morgan K, Yunkel JK, Frederick EB, Stockdon H. 2003. Evaluation of airborne topographic lidar for quantifying beach changes. J. Coast. Res. 19 (1), 125–133.
Sander L, Fruergaard M, Pejrup M. 2016. Coastal landforms and the Holocene evolution of the Island of Samsø, Denmark. Journal of Maps, 12(2), 276-286.
Santana-Cordero A, Monteiro Quintana ML, Hernández Calvento L. 2014. Reconstructing the environmental conditions of extinct coastal dune systems using historical sources: the case of the Guanarteme dune field (Canary Islands, Spain). J. Coast. Conserv. 18, 323–337.
Santana-Cordero A, Monteiro-Quintana ML, Hernández-Calvento L. 2016. Reconstruction of the land uses that led to the termination of an arid coastal dune system: the case of the Guanarteme dune system (Canary Islands, Spain), 1834–2012. Land Use Policy 55, 73–85.
Schmincke HU, Sumita M. 1998. Volcanic evolution of Gran Canaria reconstructed from apron sediments: synthesis of vicap project drilling. In: Weaver, P.P.E., Schmincke, H.U., Firth, J.V., Duffield, W. (Eds.), Proceedings of the Ocean Drilling Program, Scientific Results vol. 157 (1998).
Schumm SA, Lichty RW. 1965. Time, space, and causality in geomorphology. American Journal of Science 263(2): 110–119.
Seijmonsbergen AC, Guldenaar J, Rijsdijk KF. 2017. Exploring Hawaiian long-term insular geodiversity dynamics. Landform Analysis, 35.
Serralheiro A. 1976. A Geologia da ilha de Santiago, Cabo Verde.
Serrano E, Ruiz-Flaño P. 2007. Geodiversity: a theoretical and applied concept. Geographica Helvetica 62(3): 140–147.
Serrano E, Ruiz-Flaño P, Arroyo P. 2009. Geodiversity assessment in a rural landscape: Tiermes-Caracena area (Soria, Spain). Memorie Descrittive Della Carta Geoligica d'Italia 87, 173–180.
Shannon C, Weaver W. 1949. The Mathematical Theory of Communication. University of Illinois Press: Urbana, IL 125 pp.
Sharples C. 1993. A Methodology for the Identification of Significant Landforms and Geological Sites for Geoconservation Purposes. Forestry Commission, Tasmania.
Shepard FP. 1937. Revised classification of marine shorelines. The Journal of Geology 45(6): 602–624.
Shepard FP. 1976. Coastal classification and changing coastlines. Geoscience and Man 14: 53–64.
Sherman DJ, Bauer BO. 1993. Dynamics of beach–dune systems. Progress in Physical Geography 17(4): 413–447.
Shipman H. 2008. A Geomorphic Classification of Puget Sound Nearshore Landforms. Puget Sound Nearshore Partnership.
Simpson EH. 1949. Measurement of diversity. Nature 163: 688.
Smirnova MA, Gerasimova MI. 2017. Orders in the soil classification system of Russia: taxonomic distance as a measure of their adequate identification. Eurasian Soil Sci. 50 (3), 263–275.
Smith SE, Abdel-Kader A. 1988. Coastal erosion along the Egyptian delta. J. Coast. Res. 245–255.

Spedding N. 1997. On growth and form in geomorphology. Earth Surface Processes and Landforms: The Journal of the British Geomorphological Group, 22(3), 261-265.
Spellerberg IF, Fedor PJ. 2003. A tribute to Claude Shannon (1916–2001) and a plea for more rigorous use of species richness, species diversity and the 'Shannon–Wiener' Index. Glob. Ecol. Biogeogr. 12 (3), 177–179.
Stephenson WJ. 2000. Shore platforms: a neglected coastal feature? Prog. Phys. Geogr. 24 (3), 311–327.
Stephenson WJ, Kirk RM. 2000. Development of shore platforms on Kaikoura Peninsula, South Island, New Zealand: part one: the role of waves. Geomorphology 32(1–2): 21–41.
Stepišnik U, Trenchovska A. 2018. A new quantitative model for comprehensive geodiversity evaluation: the Škocjan Caves Regional Park, Slovenia. Geoheritage 10 (1), 39–48.
Stillman CJ. 1999. Giant Miocene landslides and the evolution of Fuerteventura, Canary Islands. Journal of Volcanology and Geothermal Research 94(1): 89–104.
Storms JE, Weltje GJ, Van Dijke JJ, Geel CR, Kroonenberg SB. 2002. Process-response modeling of wave-dominated coastal systems: simulating evolution and stratigraphy on geological timescales. Journal of Sedimentary Research, 72(2), 226-239.
Sunamura T. 1992. Geomorphology of Rocky Coasts. John Wiley & Son Ltd.
Tanner BR, Perfect E, Kelley JT. 2006. Fractal analysis of Maine's glaciated shoreline tests established coastal classification scheme. Journal of coastal research, 1300-1304.
Teixeira SB. 2006. Slope mass movements on rocky sea-cliffs: a power-law distributed natural hazard on the Barlavento Coast, Algarve, Portugal. Cont. Shelf Res. 26 (9), 1077–1091.
Terich T, Levenseller T. 1986. The severe erosion of Cape Shoalwater, Washington. J. Coast. Res. 465–477.
Thomas M. 2012. A geomorphological approach to geodiversity - its applications to geoconservation and geotourism. Quaestiones Geographicae 31 (1), 81–89.
Travis SE, Hester MW. 2005. A space-for-time substitution reveals the long-term decline in genotypic diversity of a widespread salt marsh plant, Spartina alterniflora, over a span of 1500 years. Journal of Ecology, 93(2), 417-430.
Trenhaile AS. 2000. Modeling the development of wave-cut shore platforms. Marine Geology 166(1): 163–178.
Trenhaile AS. 2001a. Modelling the Quaternary evolution of shore platforms and erosional continental shelves. Earth Surface Processes and Landforms 26(10): 1103–1128.
Trenhaile AS. 2001b. Modeling the effect of late Quaternary interglacial sea levels on wave-cut shore platforms. Marine Geology 172(3): 205–223.
Trenhaile AS. 2002. Modeling the development of marine terraces on tectonically mobile rock coasts. Marine Geology 185(3): 341–361.
Trenhaile AS. 2005. Modelling the effect of waves, weathering and beach development on shore platform development. Earth Surface Processes and Landforms 30(5): 613–634.
Trenhaile AS, Pérez Alberti A, Martínez Cortizas A, Costa Casais M, Blanco Chao R. 1999. Rock coast inheritance: an example from Galicia, northwestern Spain. Earth Surface Processes and Landforms: The Journal of the British Geomorphological Research Group, 24(7), 605-621.
Tukiainen H, Bailey JJ, Field R, Kangas K, Hjort J. 2017. Combining geodiversity with climate and topography to account for threatened species richness. Conservation Biology 31: 364–375.
Tzatzanis M, Wrbka T, Sauberer N. 2003. Landscape and vegetation responses to human impact in sandy coasts of Western Crete, Greece. J. Nat. Conserv. 11, 187–195.
Uuemaa E, Roosaare J, Oja T, Mander U. 2011. Analysing the spatial structure of the Estonian landscapes: which landscape metrics are the most suitable for comparing

different landscapes? Estonian Journal of Ecology 60(1): 70–80.
Van Huyssteen CW, Michéli E, Fuchs M, Waltner I. 2014. Taxonomic distance between South African diagnostic horizons and the World Reference Base diagnostics. Catena 113, 276–280.
Walker IJ, Hesp PA. 2013. Fundamentals of aeolian sediment transport: airflow over dunes. In Treatise on Geomorphology. Elsevier: Amsterdam.
Walker IJ, Davidson-Arnott RG, Bauer BO, Hesp PA, Delgado-Fernandez I, Ollerhead J, Smyth TA. 2017. Scale-dependent perspectives on the geomorphology and evolution of beach–dune systems. Earth-Science Reviews 171: 220–253.
Wang Y, Dong P, Oguchi T, Chen S, Shen H. 2013. Long-term (1842–2006) morphological change and equilibrium state of the Changjiang (Yangtze) Estuary, China. Cont. Shelf Res. 56, 71–81.
Wegener A. 1966. The origin of continents and oceans. Courier Corporation.
Werner BT. 2003. Modeling landforms as self-organized, hierarchical dynamical systems. Prediction in geomorphology, 133-150.
White SA, Wang Y. 2003. Utilizing DEMs derived from LIDAR data to analyze morphologic change in the North Carolina coastline. Remote Sens. Environ. 85 (1), 39–47.
Whittaker RJ, Triantis KA, Ladle RJ. 2008. A general dynamic theory of oceanic island biogeography. Journal of Biogeography 35(6): 977–994. Wilson JT. 1963. A possible origin of the Hawaiian Islands. Canadian Journal of Physics 41(6): 863-870.
Whittaker RH. 1960. Vegetation of the Siskiyou mountains, Oregon and California. Ecological monographs, 30(3), 279-338.
Wilkerson F. 1997. In: Dikau, R., Brunsden, D., Schrott, L., Ibsen, M.L. (Eds.), Landslide Recognition: Identification, Movement, and Causes. J. Wiley and Sons, New York (1996, 210 pp.).
Wilson JT. 1963. A possible origin of the Hawaiian Islands. Can. J. Phys. 41 (6), 863–870.
Woodroffe CD. 2014. The rock coasts of oceanic islands. In Rock Coast Geomorphology: A Global Synthesis, Kennedy DM, Stephenson WJ, Naylor LA (eds). Geological Society of London: London.
Woolard JW, Colby JD. 2002. Spatial characterization, resolution, and volumetric change of coastal dunes using airborne LIDAR: Cape Hatteras, North Carolina. Geomorphology 48 (1), 269–287.
Wright LD, Short AD. 1984. Morphodynamic variability of surf zones and beaches: a synthesis. Marine Geology 56(1–4): 93–118.
Xiaohua Z, Yunlong C, Xiuchun Y. 2004. On fractal dimensions of China's coastlines. Math. Geol. 36 (4), 447–461.
Xu T, Moore ID, Gallant JC. 1993. Fractals, fractal dimensions and landscapes—a review. Geomorphology 8 (4), 245–262.
Yatsu E. 1962: Rock control in geomorphology. Tokyo: Sozosha, 135 pp.
Young A, Clayton KM. 1972. Slopes. Longman.
Zarnetske PL, Hacker SD, Seabloom EW, Ruggiero P, Killian JR, Maddux TB, Cox D. 2012. Biophysical feedback mediates effects of invasive grasses on coastal dune shape. Ecology, 93(6), 1439-1450.
Zazo C. 1999. Interglacial sea levels. Quat. Int. 55 (1), 101–113.
Zwoliński Z, Najwer A, Giardino M. 2018. Methods for assessing geodiversity. Geoheritage: Assessment, Protection, and Management. Elsevier, pp. 27–52.